26ª Reunião da Associação Brasileira de Cristalografia

Livro de Resumos

12 a 14 de novembro de 2023

Ribeirão Preto - SP

Universidade de São Paulo

COMITÊ ORGANIZADOR:

Cristina Nonato (FCFRP-USP, Ribeirão Preto SP)
Alejandro Ayala (DF-UFC, Fortaleza CE)
Beatriz Guimarães (ICC-FIOCRUZ, Curitiba PR)
Cláudia Gatto (UnB, Brasília DF)
Cristiano de Oliveira (IF-USP, São Paulo SP)
Eduardo Granado Monteiro da Silva (UNICAMP, Campinas SP)
Fábio Furlan Ferreira (UFABC, Santo André SP)
Javier Ellena (IFSC-USP, São Carlos SP)
João Alexandre Barbosa (UnB, Brasília DF)
Márcia Fantini (IF-USP, São Paulo SP)
Narcizo Marques de Souza Neto (LNLS-CNPEM, Campinas SP)
Sandra Pulcinelli (UNESP, Araraquara SP)

PATROCINADORES:

CAPES

IUCr

Anton Paar

Essencis TECHNOLOGIES

Malvern Panalytical a spectris company

Rigaku Leading With Innovation

DAIRIX

Plenárias

The nanoscience revolution: upgrades to the high-throughput SAXS beamline B21 to support measurement of nanoparticles and advanced materials

N.P. Cowieson[a], N. Khunti[a], K. Inoue[a], M. B. Cardoso[b], R. Rambo[a]

[a]*Diamond Light Source, Harwell Science and Innovation Campus, Didcot, Oxforshire, UK, OX11 0DE.*

[b]*Brazilian Synchrotron Light Laboratory (LNLS), Brazilian Center for Research in Energy & Materials (CNPEM), Campinas, Sao Paulo, 13083-970, Brazil.* .

nathan.cowieson@diamond.ac.uk

B21 is a solution state SAXS beamline at the Diamond Light Source synchrotron in the UK that has traditionally specialised in structural biology applications. During the past five years we noticed an increasing number of our users measuring nanoparticles and other advanced materials on the beamline. Synthetic nanoparticles are strikingly more like naturally occurring molecular machines (proteins!) than they are to more traditional manufactured materials; particularly in their mono-dispersity and complex mechanisms of action. It has been enjoyable and instructive to compare the structural properties of proteins and nanoparticles.

I will give several examples of how SAXS can be used to measure structure and dynamics of protein systems including the activation of the anti-clotting protein plasminogen followed by several examples of the characterisation of nanoparticles including measuring protein corona formation on silica nanoparticles.

We are making several upgrades to the beamline with the specific aim of improving our ability to characterise synthetic particles: extending our Q range via a WAXS detector, increasing the speed and range of temperature ramping of the sample, improving automated handling of viscous and solid samples and developing a facility for illuminating samples with UV-VIS light in situ during SAXS data collection. I will discuss these upgrades and make some closing comments on the scope for characterising proteins and nanoparticles via SAXS.

References:

Cowieson, Nathan P et al. “Beamline B21: high-throughput small-angle X-ray scattering at Diamond Light Source.” Journal of synchrotron radiation vol. 27,Pt 5 (2020): 1438-1446. doi:10.1107/S1600577520009960

Structural effects on oxygen incorporation and oxygen transport in perovskites for IT-SOFC cathodes.

L. Suescun, J. Grassi, M. Macías, S. Vázquez, N. Di Benedetto, S. Pioli

Cryssmat-Lab/DETEMA, Facultad de Química, Universidad de la República, Montevideo 11800, Uruguay.

Solid oxide cells (SOCs) are considered the best alternative for future large-scale production and utilization of green hydrogen. In particular solid oxide fuel cells (SOFCs) are considered the best alternative for large-scale or continuous electric energy generation, since they are fuel-flexible (they can use hydrogen or carbon-containing fuels), tolerant to impurities, simple to produce, durable and cheaper than currently used low-temperature cells. The main disadvantage of these cells is the required high-temperature operation (>800 °C), due to the required ionic conductivity and catalytic properties of the solid components.

Cobalt-containing perovskite oxides have demonstrated the best mixed ionic-electronic conductivity and catalytic activity for the cathodic oxygen-reduction reaction (ORR). However, Co is expensive, its use is limited by socio-political issues and cobaltites suffer from chemical and mechanical incompatibilities with standard electrolytes.

In the last 10 years we have developed a cheap and efficient preparation technique of nano/micro-structured Cu-containing perovskites by autocombustion synthesis that have been shown to be efficient SOFC cathodes in the intermediate-temperature range (600-800 °C). $(RE/A)_{0.6}Sr_{0.4}Fe_{0.8}Cu_{0.2}O_{3-\delta}$ [1], $La_4ACu_5O_{13-\delta}$ [2] and $REBa_2Cu_3O_{6+\delta}$ [3] (RE=lanthanoids, A=Sr, Ba) have been prepared and characterized and the electrochemical behavior has been correlated to the structure and microstructure of the cathodes using in-situ X-ray powder diffraction. The case of $REBa_2Cu_3O_{6+\delta}$ with YBCO-123 high-TC superconductor structure is particularly interesting since oxygen incorporation and transport only occur at Cu^+ planes surrounded by Ba^{2+} cations but the limiting step in the ORR of the electrodes depends on RE^{3+} ionic radii. This dependence is in opposite directions so the limiting step for the ORR could be tweaked with the ionic radii of RE^{3+}, demonstrating a very strong structure-property coupling.

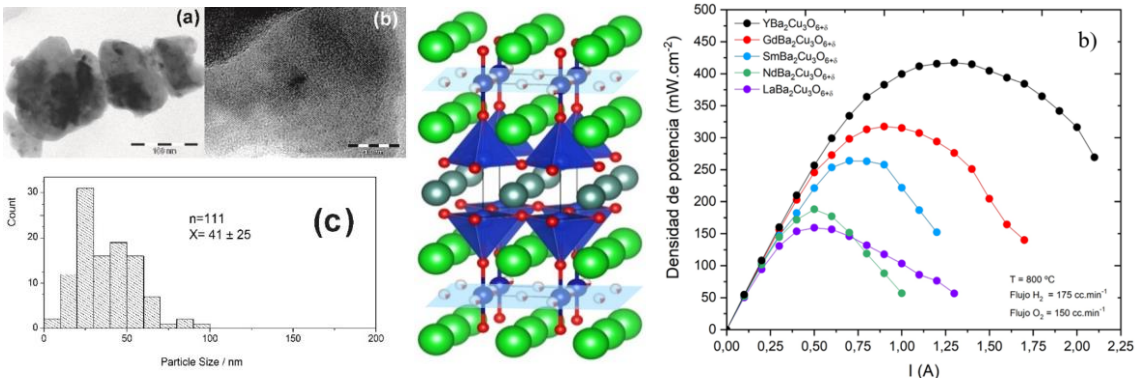

The microstructure of as-prepared $La_{0.6}Sr_{0.4}Fe_{0.8}Cu_{0.2}O_{3-\delta}$ [1] (left). The crystal structure (center) and power density of SOFC at 800 °C for different $REBa_2Cu_3O_{6+\delta}$ [3] cathodes (right).

References:

1- Vázquez S. et al, J. Solid State Chem. 228 (2015) 208. DOI: 10.1016/j.jssc.2015.04.044.

2- Macías M. A. et al, Solid State Ionics 288 (2016) 68–75. DOI: 10.1016/j.ssi.2016.02.010

3- Grassi, J. et al, Electrochim Acta (2023) 464, 142931. DOI: 10.1016/j.electacta.2023.142931.

Acknowlegments: The authors are indebted to ANII and PEDECIBA (Financial support and bursaries), CAP-UdelaR (bursaries) and CNPEM for the use of LNLS D10B-XPD powder diffraction beamline.

Accelerating crystallographic and cryo-EM structure solution with predicted structures

P. Adams

Lawrence Berkeley Laboratory, 1 Cyclotron Road, BLDG 33R0345, Berkeley, CA

The large number of protein structures available in the Protein Data Bank (PDB) have enabled new structure prediction algorithms, such as AlphaFold, RosettaFold and OpenFold. The ability to rapidly predict accurate atomic models of proteins from their sequence is an amazing development for the field of biology, and structural biology in particular. However, structure prediction methods do not fundamentally change the importance of experiments because protein conformations depend on conditions and the presence of other macromolecules and small molecules, and because even high-confidence regions of predictions can contain errors. Excitingly, these new algorithms can greatly accelerate the analysis of experimental data, making the determination of protein crystal structures a molecular replacement problem and protein cryo-EM structure determination a docking problem. We have therefore developed new methods in the Phenix software to exploit structure prediction methods to improve crystallographic and cryo-EM structure determination. Most recently this includes iteratively improving AlphaFold modeling by docking an AlphaFold model into density, rebuilding it, and using the rebuilt model as a template for further AlphaFold model generation.

Sessão Temática:

Novas Técnicas de Imagem por Difração de Feixe Coerente de Raios-X

The Sirius fourth-generation synchrotron source: opportunities using the X-ray coherence properties with nanoprobes

H. C. N. Tolentino[a],

[a]*Laboratório Nacional de Luz Síncrotron – LNLS, Centro Nacional de Pesquisa em Energia e Materiais - CNPEM, Ccampinas, SP, Brazil.*

In this presentation, I will introduce Sirius, a fourth-generation synchrotron radiation source, and briefly discuss its X-ray coherence properties and associated techniques. I will focus on the scanning X-ray nanoprobe and its available multiple and correlated techniques. Multispectral studies in diverse materials will be presented using simultaneous X-ray ptychography, fluorescence, diffraction, absorption, and excited optical luminescence experiments.

Figure 1: Overview of the Sirius synchrotron radiation source at LNLS-CNPEM.

References:

[1] L. Liu, R.T. Neuenschwander, A.R.D. Rodrigues, Synchrotron radiation sources in Brazil, Philos. Trans. R. Soc. A: Math. Phys. Eng. Sci. 377 (2019), 20180235, https://doi.org/10.1098/rsta.2018.0235.

[2] A.R.D. Rodrigues, others, Sirius Status Report, in: Proc. of International Particle Accelerator Conference (IPAC'16), Busan, Korea, May 8–13, 2016, JACoW, Geneva, Switzerland, 2016: pp. 2811–2814. https://doi.org/10.18429/JACoWIPAC2016-WEPOW001.

[3] H. Westfahl, S.A. Lordano Luiz, B.C. Meyer, F. Meneau, The coherent radiation fraction of low-emittance synchrotrons, J. Synchrotron Radiat. 24 (2017) 566–575, https://doi.org/10.1107/S1600577517003058.

[4] H. Westfahl, H.C.N. Tolentino, F. Meneau, N. Archilha, N.M. de, S. Neto, L. Lin, L. Sanfelici, B.C. Meyer, J.M. Polli, E. Miqueles, X-ray microscopy at Sirius, the New Brazilian synchrotron light source, Microsc. Microanal. 24 (2018) 176–179, https://doi.org/10.1017/S1431927618013235.

[5] H.C.N. Tolentino, R. R. Geraldes, F. M.C. da Silva, M. G. D. Guaita, C. M. Camarda, R. Szostak, I. T. Neckel, V. C. Teixeira, D. Hesterberg, C. A. Perez, D. Galante, F. Callefo, A. C.P. Neto, L. M. Kofukuda, A.P.S. Sotero, G.B.Z.L. Moreno, S. A.L. Luiz, C.S.N.C. Bueno, F.R. Lena, H. Westfahl Jr, The CARNAÚBA X-ray nanospectroscopy beamline at the Sirius-LNLS synchrotron light source: Developments, commissioning, and first Science at the TARUMÃ station, Journal of Electron Spectroscopy and Related Phenomena 266 (2023) 147340.

Acknowlegments: This research used facilities of the Brazilian Synchrotron Light Laboratory (LNLS), part of the Brazilian Center for Research in Energy and Materials (CNPEM), a private non-profit organization under the supervision of the Brazilian Ministry for Science, Technology, and Innovations (MCTI).

Coherent Diffractive Imaging for Biological and Physical Sciences: Reaching Unprecedented Spatio-Temporal Resolutions

F. Meneau[a,b]

[a]*Brazilian Synchrotron Light Laboratory (LNLS), Brazilian Center for Research in Energy and Materials (CNPEM), 13083-970, Campinas-SP, Brazil.*
[b]*Physics Institute of Chemistry, University of Campinas (UNICAMP), 13083-970 Campinas-SP, Brazil..*

Novel 4th generation synchrotron facilities and X-ray free-electron lasers are leading to the development of new X-ray methods of microscopy. Among these techniques, coherent diffractive imaging (CDI) is one of the most promising, enabling nanometre-scale imaging of non-crystallographic samples. It is a lensless imaging technique where phase iterative algorithms replace conventional lenses, to reconstruct the three-dimensional (3D) sample structure from the 2D coherent diffraction patterns collected in the far-field. Indeed, new visualisation methods can be used to resolve structures at resolutions that were previously unachievable. Here, I will present the application of ptychographic X-ray computed tomography for the visualisation of soft matter with a resolution of ~26 nm over large fields of view. Thanks to the high-penetration depth of the X-ray beam, we visualised the 3D complex porous structure of polymer hollow fibers in a non-destructive manner and obtain quantitative information about pore size distribution and pore network interconnectivity across the whole membrane wall. The non-destructive nature of this method, coupled with its ability to image samples without requiring modification or a high vacuum environment, makes it valuable in the fields of porous- and nano-material sciences enabling imaging under different environmental conditions [1]. Moreover, the recent implementation of single-shot large field of view CDI (*lfov*CDI) enabled to image three-dimensionally 10s of micron-size zeolite crystals and an entire vero cells in cryogenic environment. With *lfov*CDI, a full tomogram can be acquired in less than 2 hours with resolutions < 50 nm. The temporal resolution of CDI will pave the way to novel *in situ* time-resolved and *in operando* nanotomography studies exploring real-time phenomena, spanning chemistry, biology, catalysis and materials research fields. These methods are implemented at the Cateretê beamline [2] at the SIRIUS 4th generation synchrotron source.

References:

1- Górecki, R, Polo C. C, Kalile A. K, Miqueles E, Tonin Y, Upadhyaya L, Meneau F, Nunes S.P, Ptychographic X-ray computed tomography of porous membranes with nanoscale resolution**,** ***Communications Materials***, 4, 68 (2023). https://doi.org/10.1038/s43246-023-00396-x.

2- Meneau, F.; Passos, A. R.; Garcia, P. R. A. F.; Vinaches, P.; Manoel, L.; Kalile, T.; Zerba, J.P.; Rodrigues, G. L. M. P.; Miqueles, E.; Baraldi, G.; Polli, J.; Meyer, B. C.; Luiz, S. A. L.; Polo C. C. Cateretê: the coherent x-ray scattering beamline at the 4th generation synchrotron facility SIRIUS. ***Foundations of Crystallography***, 77, C283, 2021.

Acknowlegments: *Financial support from the King Abdullah University of Science and Technology - KAUST (#CRG8-4040.2) and the São Paulo Research Foundation - FAPESP (#2021/06876-1) are gratefully acknowledged*.

Sessões Temáticas Paralelas

Biologia Estrutural

Designing catalytic and non-catalytic septins and their relationship to specific filament assembly

D. A. Leonardo[a], S. A. Sculaccio[a], A. Pinto[a], H. Ciol[a], T. Watanabe[a], R. C. Garratt[a]

[a]*Instituto de Física de São Carlos, Universidade de São Paulo, São Carlos, São Paulo, Brasil*

Septins are GTPases considered to be the fourth component of the cytoskeleton. They form heterofilaments with a specific order for each subunit[1]. Due to their ability to form heteropolymers, they are related to a diversity of biological processes such as cytokinesis, exocytosis, scaffolding, etc[2]. Likewise, an alteration in the order of the subunits or miss-folding can cause several diseases. Despite our extensive physiological and structural knowledge, there is a lack of information regarding the importance of GTPase inactive septins as a fundamental component of the heterofilament[3]. Here, using structural analysis-based mutagenesis, we transformed an inactive septin (SEPT6) and an active septin (SEPT9) into their functional counterparts (active and inactive respectively) to test their ability to form complexes with their physiological partners. The co-expression of SEPT6mut with SEPT2 and SEPT9mut with SEPT7 (the physiological partners) shows a destabilization in the formation of heterodimers, recovering monomeric proteins after purification by SEC. This demonstrates that both GTP hydrolysis and the nature of the nucleotide bound influence in the specificity and stabilization of heterodimeric complexes via the G-interface between septins.

References:

1- Sirajuddin, M., Farkasovsky, M., Hauer, F., Kühlmann, D., Macara, I.G., Weyand, M., Stark, H., Wittinghofer, A., 2007. Structural insight into filament formation by mammalian septins. Nature 449, 311–317

2- Mostowy, S., Cossart, P., 2012. Septins: the fourth component of the cytoskeleton. Nat Rev Mol Cell Biol 13, 183–94

3- Cavini, I.A., Leonardo, D.A., Rosa, H. V.D., Castro, D.K.S.V., D'Muniz Pereira, H., Valadares, N.F., Araujo, A.P.U., Garratt, R.C., 2021. The Structural Biology of Septins and Their Filaments: An Update. Front Cell Dev Biol.

Acknowlegments: Fundação de Amparo à Pesquisa do Estado de São Paulo (FAPESP) - 2021/08158-9.

Structural biology in the bacteria-phage interface

Germán G. Sgro

Faculdade de Ciências Farmacêuticas de Ribeirão Preto, Universidade de São Paulo, Ribeirão Preto, Brazil.

Bacteriophages (phages) are viruses that infect bacteria and are the smallest and most abundant biological entities on Earth. To replicate, they use the bacterial host machinery to either i) immediately produce new progeny after infection which leads to the death of the infected cell (lytic pathway), or ii) integrate into the bacterial chromosome as a prophage which allows establish a symbiotic relationship between the parties (lysogenic pathway). The interaction begins with the recognition and adsorption of the phage on the surface of the bacterium, which determines the specificity and host range. Most known phages have a narrow host range, usually infecting specific strains or isolates of a particular bacterial species. For such recognition, virions have specific proteins that bind to receptors located on the bacterial surface, such as LPS, EPS, outer membrane proteins, fimbriae, pili and flagella. In recent decades, the interest in the use of phages as therapeutic agents (phage therapy) in the biological control of infections by multidrug-resistant bacteria has increased, as well as in the development of strategies for the biocontrol of pathogenic species in agricultural crops. In this context, understanding the molecular mechanisms underlying phage-bacteria interactions is crucial to obtain information on how phages affect microbial populations and how they can be used in clinical and biotechnological applications. Here, we present our results about the high-resolution molecular structures involved in the infectious process of lytic bacteriophages that interact and infect bacterial strains of relevance in medicine and agriculture.

Unveiling molecular mechanisms of substrate-specificity in dehydrogenases active on lignin-related compounds

A.J.V.C Brilhante[a,b], L.D. Wolf[a], D.B. Martim[a,b], P.O. Giuseppe[a]

[a] *Brazilian Biorenewables National Laboratory (LNBR), Brazilian Center for Research in Energy and Materials (CNPEM), Campinas, Brazil.*

[b] *Graduate Program in Genetics and Molecular Biology, Biology Institute, UNICAMP, Campinas, Brazil.*

The heterogeneity of lignin depolymerization products is one of the major challenges for using this abundant and renewable material as a feedstock for chemicals production. In this context, microbial convergent biocatalysis has emerged as a promising approach to funneling lignin derived compounds into target molecules[1]. Biological pathways and enzymes for the catabolism of aromatic compounds derived from the syringyl (S), guaiacyl (G), and *p*-hydroxyphenyl (H) subunits of lignin (e.g. syringate, vanilate, and *p*-coumarate, respectively) have been described for some bacterial species[2]. Despite these advances, there is still little information regarding the enzymatic strategies for the catabolism of the monolignols coniferyl alcohol (G), *p*-coumaryl alcohol (H) and sinapyl alcohol (S). In this work, we identified an aryl-alcohol dehydrogenase (XarA, *XAC0353*) from *Xanthomonas citri* subsp. *citri* 306 that belongs to the short-chain dehydrogenase/reductases (SDR) superfamily and has about 60% sequence identity with CalA from *Pseudomonas* sp. HR199, the only bacterial SDR active on coniferyl alcohol with experimental data available so far[3]. Gene knockout studies showed that XarA plays an important role in the first step of monolignols catabolism in *X. citri*. Biochemical assays demonstrated that XarA is a NAD^+-dependent dehydrogenase, with optimal activity at 30 °C (pH 10). XarA showed the following relative activity profile: *p*-coumaryl alcohol (100%) > cinnamyl alcohol (83%) > coniferyl alcohol (48%) > sinapyl alcohol (34%) > 4-hydroxybenzyl alcohol (10%) > vanillyl alcohol (3%) > benzyl alcohol (2%), indicating that XarA has greater activity on aryl alcohols containing longer (propenol) side chains, with a decrease in specific activity as the degree of methoxylation in the aromatic ring increases, and only a residual activity on aryl alcohols with shorter (methanol) side chains. The crystal structures of XarA in complex with NAD^+ and coniferyl alcohol or with NAD^+ and vanillin were solved by molecular replacement at 2.8 Å and 2.7 Å resolution, respectively. Comparative analysis indicated that the aryl group of coniferyl alcohol and vanillin shares the same binding site, leading to a favorable positioning of the alcohol group from coniferyl alcohol in the active site, but maintaining further away the aldehyde group of vanillin (equivalent to the alcohol group of shorter aryl substrates), explaining the higher activity of XarA in monolignols compared to benzyl alcohol analogues. Analysis of the NAD^+ binding site showed that residue side chains from the 2'-phosphate-binging loop influences co-substrate specificity by modulating spatial and electrostatic constraints. In summary, here we presented the first crystal structures of a bacterial SDR able to convert the three main lignin precursors (G, H and S monolignols) into their respective aldehydes, the first step required for their entry into catabolic funneling pathways. By combining structural analyses, molecular dynamics simulations and kinetic studies, we expect to provide a deeper understanding on the substrate recognition mechanisms that determine the substrate preference of XarA, thus contributing to the knowledge regarding the structure-function relationship of SDRs active on monolignols and supporting the development of biotechnologies for the sustainable production of industrially relevant bioproducts.

References:

1- Beckham GT, *et al.* Curr Opin Biotechnol. 2016 ;42:40-53.
2- Brink DP, *et al.* Appl Microbiol Biotechnol. 2019;103(10):3979-4002.
3- Patent EP0845532A2

Acknowlegments: FAPESP 2022/01070-1, 2019/08590-8, 2019/06921-7, CAPES, CNPq.

Fármacos e Produtos Naturais

Structure and application relationship of Zn-based nanoparticles in antimicrobial and theranostic systems

Leila A. Chiavacci[a], ,*Bruna Lallo da Silva*[a], *Thulio W. Lemos*[a], *Mariana Picchi Salto*[a], *Rafael Fulindi*[a], *Laurent Lemaire*[b]

[a]*Department of Drugs and Medicines, São Paulo State University (UNESP), School of Pharmaceutical Sciences,Araraquara, São Paulo, Brazil*

[b]MINT, INSERM, CNRS, SFR-ICAT, UNIV Angers, 49000 Angers, France

In the health area, many advances are associated to the development of new materials or the modification of the existing ones. The final properties and consequently application of nanostructured materials in this area are closely related to their chemical composition and structural characteristics. Thus, the purpose of this work is to present and to discuss the correlation between physical-chemical and structural characteristics of zinc based inorganic nanoparticles and the possibility of applying these materials as antimicrobial, antibiofilm or theragnostic agents. In this way zinc-based nanoparticles (ZnO, ZnS, GdZnCuInS/ZnO/ZnS and Fe doped ZnO) and iron oxide nanoparticles with modified size and surfaces were prepared and characterized to evaluate de relationship between structural properties and antimicrobial, antibiofilm activity and theragnostic application. The Figure 1 (a) shows emissions of gadolinium doped ZnO (ZnOGd) nanoparticles under ultraviolet (UV) lamp at 254 nm and emissions of GdZnCuIn (GCIS/ZnS) and conjugated ZnOGd-GCIS/ZnS (75% of ZnOGd and 25% of GCIS/ZnS) using different wavelengths of excitation revealing that the conjugation od two different nanoparticles resulted in a new one with modulated emission and able to be use as contrast agent[1]. The Figure 1 (c) and (d) shows the scanning electron microscopy (SEM) of S. aureus bacteria before and after treatment with modified surface and controlled size ZnO nanoparticles[2]. The results revealed that the modification of the surface of the zinc-based nanoparticles evaluated in this work, their size and their chemical composition strongly affect their efficiency as antimicrobial, antibiofilm or theragnostic agents and determine their possibility of application in biological medium. Regardless of the type of nanomaterial studied, the results presented confirm the importance of modifying structural parameters to obtain more efficient and more stable materials for the desired applications in healthy.

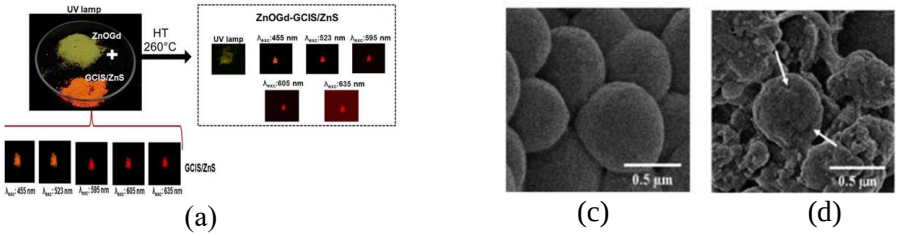

(a) (c) (d)

Figure 1.Emissions of ZnOGd under ultraviolet (UV) lamp at 254 nm and emissions of GCIS/ZnS and conjugated ZnOGd-GCIS/ZnS (75% of ZnOGd and 25% of GCIS/ZnS) using different wavelengths of excitation (a) and Scanning electron microscopy (SEM)of S. aureus(c) and S. aureus treated with GPTMS-ZnO-24 h(d).

References:

1- LALLO DA SILVA, B. et al. Nanomaterials 2021, 11(7), 1817; https://doi.org/10.3390/nano11071817

2- LALLO DA SILVA, B. et al. Colloids and Surfaces B: Biointerfaces 2019, 177, 440; https://doi.org/10.1016/j.colsurfb.2019.02.013

Acknowlegments: FAPESP, CAPES, CNPq and the PPG-CF Postgraduate Program in Pharmaceutical Sciences.

Nanostructure Arrangements of pharmaceutical forms based on ureasil-polyether materials containing dexamethasone acetate

J. A. Oshiro-Junior

Departamento Ciências Farmacêuticas, Universdade Estadual da Paraíba, Campina Grande, Brasil.

Ureasil-polyether materials have been employed in the production of various pharmaceutical forms such as solid films, membranes for guided bone regeneration, rings, and vaginal suppositories[1-3] containing different active substances, whether hydrophilic or hydrophobic in nature. In these materials, siloxane nanoparticles serve as cross-linking points between polymeric chains, resulting in a three-dimensional network. However, molecular weight significantly influences encapsulation efficiency and release profile. Therefore, Ureasil-Poly(ethylene oxide) (u-PEO) and Ureasil-Poly(propylene oxide) (u-PPO), loaded and unloaded with dexamethasone acetate, were investigated through atomic force microscopy (AFM), contact angle measurements, and release experiments. Additionally, X-ray diffraction, small-angle X-ray scattering, and infrared spectroscopy were also employed to provide essential information for understanding the structural organization of the films. Our results reveal that, while in u-PEO, DMA (dexamethasone acetate) occupies sites near the ether oxygen and remains absent from the film surface, in u-PPO, new crystalline phases are formed when DMA is loaded. These phases appear as rounded clusters with diameters of approximately 30-100 nm aligned along a well-defined direction, presumably related to the characteristic polymer ropes discernible on the surface of the unloaded u-PPO film. Occasionally, larger needle-shaped DMA crystals are also observed. UFM reveals that in the unloaded u-PPO matrix, the polymer ropes consist of filaments, which, in turn, consist of aligned clusters with a diameter of approximately 180 nm that are stiffer and possibly formed by siloxane node aggregates. The new crystalline phases may grow between the filaments when the drug is loaded. These results highlight the importance of combining physicochemical techniques, to visualize the nanostructural arrangements in polymeric matrices intended for drug delivery.

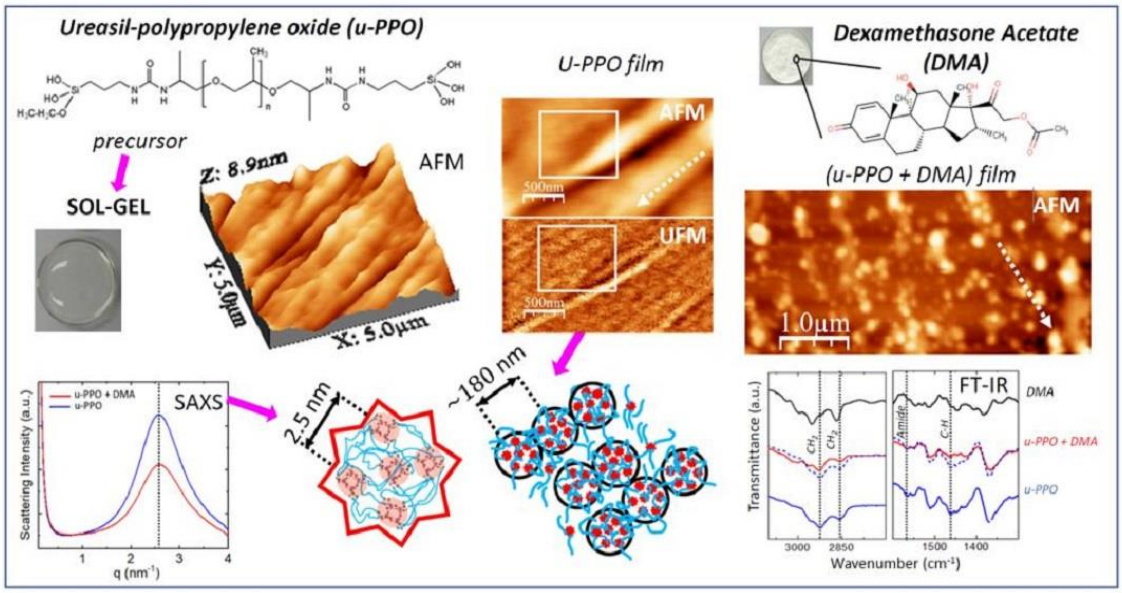

Figure 1: Representação visual dos Arranjos de Ureasil-Poliéter com Dexametasona, acompanhados de Gráficos AFM, SAXS e DRX para análise estrutural.

References:
1- Oshiro-Junior, J.A.; Lusuardi, A.; Beamud, E.M.; Chiavacci, L.A.; Cuberes, M.T. Nanostructural Arrangements and Surface Morphology on Ureasil-Polyether Films Loaded with Dexamethasone Acetate. Nanomaterials 2021, 11, 1362. https://doi.org/10.3390/nano11061362
2- Nicolau Costa, K.M.; Sato, M.R.; Barbosa, T.L.A.; Rodrigues, M.G.F.; Medeiros, A.C.D.; Damasceno, B.P.G.d.L.; Oshiro-Júnior, J.A. Curcumin-Loaded Micelles Dispersed in Ureasil-Polyether Materials for a Novel Sustained-Release Formulation. Pharmaceutics 2021, 13, 675. https://doi.org/10.3390/pharmaceutics13050675
3- Barros, R.M.; Da Silva, C.G.; Nicolau Costa, K.M.; Da Silva-Junior, A.A.; Scardueli, C.R.; Marcantonio, R.A.C.; Chiavacci, L.A.; Oshiro-Junior, J.A. Dexamethasone-Loaded Ureasil Hydrophobic Membrane for Bone Guided Regeneration. Pharmaceutics 2022, 14, 1027. https://doi.org/10.3390/pharmaceutics14051027

Acknowlegments: This study was financed in part by the Coordenação de Aperfeiçoamento Pessoal de Nível Superior, Brasil (CAPES), Finance Code 001 and CNPq called MCTIC/CNPq 28/2018 Universal A, process 422231/2018-5.

Influência de manteigas obtidas de plantas amazônicas na estrutura de sistemas líquido cristalinos aplicados a protetores solares inorgânicos

Renata C. K. Kaminski[a], Ane Karoline Silva Andrade[a], Barbara Vasconcelos Santana[a], Eloísa Berbel Manaia[a]

[a]*Departamento de Química (DQCI), Universidade Federal de Sergipe, campus Prof. Alberto Carvalho, Av. Vereador Olímpio Grande, s/n, Itabaiana, SE, Brasil.*

[b]*Institut Galien Paris-Sud, Univ. Paris-Sud, CNRS, Université Paris-Saclay, 92290 Châtenay-Malabry, France*

Filtros solares baseados em ativos inorgânicos a base de nanopartículas de dióxido de titânio (TiO_2), oferecem vantagens como fotoestabilidade, amplo espectro de proteção e baixo potencial de causar alergias. Com o intuito de produzir protetores solares que além de fornecer fotoproteção, também proporcionem benefícios à pele, alguns óleos ou manteigas vegetais podem ser incorporados na formulação cosmética, como a manteiga de ucuúba (*Virola Surinamensis*), pois possui efeitos antifúngicos, antibacterianos e anti-inflamatórios. Essas propriedades se devem ao elevado teor de ácidos graxos saturados, com destaque para o ácido mirístico ($C_{14:0}$) (cerca de 77%), sendo este alto valor pouco encontrado em outras oleaginosas. Dessa forma, o presente trabalho visa preparar formulações de protetores solares a base de nanopartículas de TiO_2 e avaliar os efeitos da manteiga de ucuúba e a influência do tensoativo na estrutura líquido cristalino dos sistemas nanoestruturados. As formulações foram preparadas a partir de misturas ternárias de água, manteiga de ucuúba (fase oleosa) e Tween 80 (tensoativo), contendo 30 e 40% de tensoativo, variando-se fase oleosa em 10, 20, 30 e 40% para cada percentagem de Tween 80. A caracterização das amostras foi realizada através de Espalhamento de Raios X a baixo ângulo (SAXS), reologia de fluxo e teste oclusivo *in vitro*. As análises de SAXS demostraram a formação de vários picos estreitos, característicos de estruturas líquido cristalinas, com razões das distâncias dos objetos espalhadores indicativas de mesofase hexagonal para a formulação com 30% de tensoativo e 20% de manteiga, enquanto as demais formulações apresentaram razões de mesofases cúbicas micelares e bicontínuas, as quais possuem maior estruturação segundo a ordem: cúbica bicontínua > hexagonal > cúbica micelar. Por meio das análises reológicas foi observado que o aumento da quantidade de tensoativo no sistema proporciona maior caráter pseudoplástico, sendo esta uma característica desejável em formulações cosméticas tópicas, uma vez que evita que o produto escorra durante a aplicação. O estudo de oclusividade mostrou que o aumento da quantidade de manteiga no sistema proporciona maior efeito oclusivo, comportamento este esperado, visto que o aumento da fase oleosa resulta em maiores quantidades de compostos hidrofóbicos na formulação, o que resulta na diminuição da perda de água. Sendo assim, as formulações são promissoras para protetores solares, uma vez que apresentam sistemas líquido cristalinos com caráter pseudoplástico, além de bom fator de oclusão.

.

Acknowlegments: CNPq/CAPES/FAPITEC/LNLS

Materiais em Condições Extremas

Structure and Properties of Advanced Perovskites at Extreme Conditions

A. P. Ayala

Departamento de Física, Universdade Federal do Ceará, Fortaleza, Brazil.

Perovskites are a versatile class of materials with exceptional properties and wide-ranging applications. This talk will explore the structure and properties of advanced perovskites under extreme conditions, revealing novel phases and emergent properties with potential for innovative applications in high-performance electronics and solar cells.

Under high pressure, perovskites can undergo dramatic structural transformations, leading to the emergence of novel phases with exotic properties. These discoveries offer exciting new possibilities for developing next-generation materials with unprecedented functionalities.

On the other hand, temperature can also have a profound impact on perovskite stability and functionality. For example, some perovskite halides have been shown to exhibit enhanced light absorption/emission properties at low temperatures, making them promising candidates for next-generation solar cell materials.

Using state-of-the-art experimental techniques, including high-pressure diamond anvil cells, synchrotron X-ray diffraction, and advanced spectroscopic methods, we have investigated a diverse range of perovskite compositions, encompassing oxides [1,2], halides[3], and hybrid organic-inorganic materials[4,5]. Our research aims to elucidate the intricate interplay between structure and properties under extreme conditions, providing insights into the fundamental mechanisms that underlie perovskite behavior.

References:

1 - B. S. Araújo, A. M. Arévalo-López, C. C. Santos, J. P. Attfield, C. W. A. Paschoal and A. P. Ayala, *Journal of Physics and Chemistry of Solids*, 2021, **154**, 110044.
2 - W. C. Ferreira, G. L. C. Rodrigues, B. S. Araújo, F. A. A. de Aguiar, A. N. A. de Abreu Silva, P. B. A. Fechine, C. W. de Araujo Paschoal and A. P. Ayala, *Ceram Int*, 2020, **46**, 18056–18062.
3 - W. Castro Ferreira, B. S. Araújo, M. A. P. P. Gómez, F. E. O. O. Medeiros, C. W. de Araujo Paschoal, C. B. da Silva, P. T. C. C. Freire, U. F. Kaneko, F. M. Ardito, N. M. Souza-Neto and A. P. Ayala, *The Journal of Physical Chemistry C*, 2022, **126**, 541–550.
4 - R. X. Silva, R. R. Hora, A. Nonato, A. García-Fernández, J. Salgado-Beceiro, M. A. Señarís-Rodríguez, M. S. Andújar, A. P. Ayala and C. W. A. Paschoal, *Spectrochim Acta A Mol Biomol Spectrosc*, 2023, **289**, 122198.
5 - N. Vasconcelos, B. S. Araújo, D. S. Abreu, M. A. P. Gómez, A. P. Ayala and C. W. A. Paschoal, *Mater Adv*, 2022, **3**, 8597–8607.

Acknowlegments: This study was partly financed by the CAPES, CNPq, FINEP, and CNPEM

Search for the Kitaev quantum spin liquid state in honeycomb iridates at high pressures

Gilberto Fabbris[a]

[a]*Advanced Photon Source, Argonne National Laboratory, Lemont-IL, USA*

Compounds with 5*d* transition metal ions have attracted recent attention due to the prediction and observation of novel forms of topological magnetic and electronic states. Among these, particular attention has been given to the Kitaev quantum spin liquid state that is expected to occur in honeycomb iridates, and which is a potential candidate for topologically protected quantum computing. However, the presence of a spin liquid in these materials rely on the delicate balance between Kitaev and Heisenberg exchange interactions; such balance is very sensitive to structural deviations away from a perfect honeycomb motif. In this talk I will present our efforts in the study of honeycomb iridates using several x-ray techniques at high pressure to control and probe their structure, as well as electronic and magnetic ground states. Particular focus will be given to our recent results on Cu_2IrO_3 and Na_2IrO_3, highlighting their distinct and complex phase diagram.

Acknowlegments: *This research used resources of the Advanced Photon Source, a U.S. Department of Energy (DOE) Office of Science user facility operated for the DOE Office of Science by Argonne National Laboratory under Contract No. DE-AC02-06CH11357.*

X-ray techniques under extreme conditions at Sirius

Ricardo D. dos Reis and Narcizo M. Souza Neto

Laboratório Nacional de Luz Síncrotron – LNLS, Centro Nacional de Pesquisa em Energia e Materiais - CNPEM, Ccampinas, SP, Brazil.

The research exploring the limits of thermodynamical parameters, such as pressure, temperature, and magnetic field, is a fast-growing and fascinating discipline of science and technology that unravel many truths and facts of nature, which are not possible in ambient conditions. However, improving the quality of the experimental data obtained at extreme thermodynamical remains challenging. To understand the implication of such huge contraction, small focused X-ray beams, smaller than 1 micrometer, is essential to allow in-situ investigations of the crystalline and electronic structure of materials under high pressure. The Extreme condition Methods of Analysis beamline (EMA), of the new Brazilian light source, was designed to overcome this challenge by having both ~0.5x1 μm2 focused beam size with high photon flux (1013 photons/s @ 10 keV) and ~100x100 nm2 focused beam size (with ~1011 photons/s @ 10 keV), both with well-defined gaussian beam shape, which will allow the realization of X-ray absorption (XAS), X-ray diffraction (XRD), coherent diffraction image (CDI) and X-ray Raman experiments at extreme pressure with good spatial selectivity and also to avoid pressure gradients. As most complex scientific problems do need a combination of conditions to explore yet unreached points of the phase diagram, we aim at coupling the high-pressure capabilities to low and high temperatures (as low as 300 mK, as high as 8000 K) and high magnetic fields (up to 11T).

Materiais Inorgânicos

Recent advances in perovskite solar cells and supercapacitors

Gabriel L. Nogueira[a], Hugo G. Lemos[a], Jessica H. H. Rossato[a], Silvia L. Fernandes[b], João Pedro F. Assunção[a], João V. M. Lima[a], Carlos F.O. Graeff [a].

[a] *São Paulo State University (Unesp), School of Sciences, Department of Physics and Meteorology, Bauru, SP, 17033-360, Brazil*

[b] *Oninn, Belo Horizonte, MG, 31035-536, Brazil*

Email: carlos.graeff@unesp.br

The growing demand for energy in modern society has driven the development of alternative energy conversion and storage technologies. Our research group is interested in solar energy, with a focus on perovskite solar cells (PSCs), as well supercapacitors. In this review, we will discuss our ongoing research on the development of materials for improving PSCs and supercapacitors. Specifically, the incorporation of two-dimensional (2D) materials and/or oxide semiconductor layers has been shown to enhance the performance of these devices. Our work on PCSs involves the development of ETLs that are suitable for the double-cation mixes halide perovskite film ($Cs_{0.17}FA_{0.83}Pb(I_{0.83}Br_{0.17})_3$). For example, we developed Nb_2O_5 layers to act as ETL that resulted in power conversion efficiency (PCE) of approximately 17% and 18% when deposited via sputtering or spin-coating deposition, respectively. We achieved enhanced performance and stability after adding $Ti_3C_2T_x$ MXene into a solution-processable ETL [1]. The addition of MXene increased the PCE (19.46% for the champion device) and the stability (96% of its original PCE after 500 hours) compared to pristine devices. The improved performance of the Nb_2O_5–Ti_3C_2 devices is attributed to the alignment of the energy bands between perovskite and the ETL layer. We investigated also the use of a $Ti_3C_2T_x$ MXene dispersion containing water dispersible PANI and PPy conducting polymers (CPs) as active electrodes for symmetric supercapacitors [4]. The $Ti_3C_2T_x$@CPs electrodes demonstrated a 32% increase in specific capacitance with the presence of PANI and a 22% increase with PPy, compared to $Ti_3C_2T_x$ pristine. Cycling stability measurements revealed that the addition of PANI and PPy resulted in outstanding capacitance retention (>98%) after 5000 cycles, compared to only 88% of the $Ti_3C_2T_x$ pristine device.

References

[1] H.G. Lemos et al., *J. Mater. Chem. C*, 2023,11, 3571-3580 (DOI: 10.1039/d3tc00022b).
[2] Silvia: The role of Nb2O5 deposition process on perovskite solar cells (DOI: 10.1063/5.0083073).
[3] João Pedro: Self-suspended Nb2O5 nanoparticles for efficient and printable mesoscopic perovskite solar cells (in writing).
[4] João Morais: Long-cycle-life supercapacitors based on water-dispersible Ti3C2Tx MXene@conducting polymer electrodes (submitted for publication).

The authors acknowledge FAPESP (Projects: 2020/12356-8 and 2013/07296-2), FINEP, CAPES and CNPq for financial support.

Materiais Magnéticos Moleculares Multifuncionais

Cynthia L.M.Pereira[a], Cleber R. Araújo Júnior[a], Cleverton O.C. da Silveira[a], Willian X.C. Oliveira[a], Carlos B. Pinheiro[b], Felipe T. Martins[c], Emerson F. Pedroso[d].

[a]*Departamento de Química, Universidade Federal de Minas Gerais, Belo Horizonte, Brasil.*
[b]*Departamento de Física, Universidade Federal de Minas Gerais, Belo Horizonte, Brasil.*
[c]*Instituto de Química, Universidade Federal de Goiás, Goiânia, Brasil.*
[d]*Departamento de Química, Centro Federal de Educação Tecnológica de Minas Gerais, Belo Horizonte, Brasil.*

Os materiais magnéticos podem ser obtidos em laboratório através de síntese química, em condições brandas, tais como temperatura e pressões ambientes, e baixas concentrações, e utilizando-se solventes verdes como a água, por exemplo. Esses materiais podem ser construídos quimicamente através da automontagem, átomo a átomo, formando moléculas ou íons. Portanto, utilizando-se estratégias de síntese próprias da química de coordenação, são obtidos sistemas com diferentes dimensionalidades de rede e propriedades, onde os ligantes orgânicos e os íons metálicos podem atuar como moduladores destas propriedades, principalmente no que se refere ao magnetismo observado. Além disso, é importante ressaltar que pequenas modificações durante o processo de síntese podem levar a diferentes produtos, com estruturas cristalinas distintas, o que é próprio das interações supramoleculares que ocorrem nestes compostos.[2] Desta forma, variando-se as estratégias de síntese pode-se levar à obtenção de materiais multifuncionais, que apresentam propriedades magnéticas, fotoluminescentes[3] ou atividade catalítica para descontaminação ambiental, por exemplo, partindo-se de uma estratégia racional para a obtenção de tais compostos.

Neste trabalho, serão apresentados alguns exemplos dos últimos resultados obtidos, envolvendo ligantes do tipo oxamato, íons de metais de transição, e íons de terras raras. Importante mencionar que os materiais magnéticos moleculares que apresentam relaxação da magnetização possuem potencial aplicação na área da computação quântica.

Referências:

1- R. Jankowski, M. Wyczesany, S. Chorazy, *Chem. Comm.* **2023**, *59*, 5961.
2- T.T. da Cunha, C.O.C. da Silveira, V.M.M. Barbosa, W.X.C. Oliveira, E.N. da Silva Júnior, F.F. Ferreira, E.F. Pedroso, C.L.M. Pereira, *CrystEngComm* **2021**, *23*, 1885.
3- R.C.A. Vaz, I.O. Esteves, W.X.C. Oliveira, J. Honorato, F.T. Martins, L.F Marques, G.L. dos Santos, R.O. Freire, L.T. Jesus, E.F. Pedroso, W.C. Nunes, M. Julve, C.L.M. Pereira, *Dalton Trans.* **2020**, *49*, 1606.

Agradecimentos: Núcleo de Extensão do Departamento de Química (NEPS-DQ-UFMG), CAPES, CNPq, FAPEMIG.

Importância da DRXP para o desenvolvimento de novos materiais para impressão 3D

V. D. N. Bezzon[a]

[a]*Departamento de Física, Universidade Federal de Ouro Preto, Ouro Preto, Minas Gerais, Brasil.*

A técnica de difração de raios X por policristais (DRXP) desde o início de sua utilização favoreceu o desenvolvimento de novos materiais inorgânicos, fossem eles de natureza cerâmica, metálica, até materiais compósitos. Por meio da técnica juntamente com métodos correlacionados, como os métodos de Rietveld e *Pair Distribution Function*, é possível realizar diversos tipos de análise como identificação e quantificação de fases, caracterização de estruturas de longo e curto ordenamento, avaliação de tensão, defeitos, coordenação, dentro outras possibilidades. Dada essa versatilidade de análise, se tornou imprescindível em diversas áreas, como por exemplo no desenvolvimento de materiais para aplicação em impressão 3D.

Nessa palestra irei apresentar alguns exemplos de biomateriais compósitos com fosfatos de cálcio utilizados em impressão 3D além de outros compostos de interesse para estudos de ambientes biológicos controlados e que tiveram a DRXP e métodos correlacionados como ferramenta fundamental para sua obtenção e caracterização [1,2].

References:

1- Lopera, A. A., Bezzon, V. D. N., Ospina, V., Higuita-Castro, J. L., Ramirez, F. J., Ferraz, H. G., Orlando, M. T. A., Paucar, C. G., Robledo, S. M. & Garcia, C. P. (2023). Journal of the Korean Ceramic Society 60, 169–182.

2 -Lopera, A., Chavarriaga, E. A., Bezzon, V. D. N., Zutta, M., Gómez, A., Puerta, J., Robledo, S. M., Ospina, V. E., Paucar, C. & Garcia, C. (2021). Boletín de La Sociedad Española de Cerámica y Vidrio 61, 5, 487-497.

Acknowlegments: Laboratório de Crescimento e Caracterização de Materiais Cristalinos (UFOP), Grupo de Física Aplicada (UFES) e Prof. Dr. Alex Lopera (Unal – Colômbia).

Organometálicos e MOFs

Semiquantitative analysis of intermolecular interactions in the development of potential metallopharmaceuticals

N. Alvarez[a], J. Ellena[b], A. J. Costa-Filho[c], G. Facchin[a].

[a]*Química Inorgánica, Departamento Estrella Campos, Facultad de Química, Universidad de la República, Montevideo, Uruguay*

[b]*São Carlos Institute of Physics, University of São Paulo, São Carlos, Brazil*

[c]*Physics Department, Ribeirão Preto School of Philosophy, Science and Literature, University of São Paulo, Ribeirão Preto, Brazil*

Inorganic Medicinal Chemistry is a research area dedicated to the development and study of inorganic compounds, in the broader sense, for chemotherapy. Inorganic compounds have been used to treat several diseases for centuries. However, the study of metal complexes to cure diseases grew exponentially after the fortuitous discovery of the cytotoxic activity of cisplatin. The use of metal complexes in the design of novel pharmaceutical agents carries many advantages. The selection of the metal center, for instance, will determine the geometry, charge, redox behavior, among others. Ligands may be chosen for their own biological activity looking to enhance it through coordination, to tune the physicochemical activities of the complex, to increase their stability, to name a few options. In the study of new compounds for biological applications, it is essential to gather knowledge on the chemical identity, atom connectivity, aqueous solution behavior of the new molecular moieties.

Our group has been working for some time on the development of novel copper(II) compounds in the search of new drugs to treat cancer. Our latest efforts include complexes that combine the copper(II)-phenanthroline pharmacophore with a divalent anionic coligand, such as dipeptides [1-5], iminodiacetic acid [6] and dipicolinic acid [7]. This strategy yielded more than 30 complexes which classify as potent anticancer agents with IC50 values in the micromolar range. For some time now, we have focused on trying to rationalize the observed activities, the studies on biomolecular targets, such as DNA, and physicochemical properties, like lipophilicity. Since most of the complexes give single crystals suitable for X-ray diffraction experiments, capitalizing on the accumulated structural data became relevant.

Crystal Explorer [8] is a readily available software that through low computational cost quantum mechanical approximations allows the user to process molecule-molecule interactions semi quantitatively. We applied Hirshfeld surface analysis and surface percentage contributions of contacts to the surface to different series of the studied complexes in pursuit of relationships with DNA binding and lipophilicity. We were able to confirm that C-C interactions may be used as a predictor on the binding strength of [Cu(dipeptide)(neocurpoine)] partial intercalators and O-H interactions may be utilized as lipophilicity descriptors in the [Cu(dipicolinate)(diimine)] system. However, there is still a long way to go to be able to use structural parameters in QSAR studies due to the intrinsic versatility of coordination compounds.

1- S. Iglesias, et. al, Journal of Inorganic Biochemistry, vol. 139, 2014, pp. 117-123.
2- S. Iglesias, et. al, Structural Chemistry and Cryst. Communication, vol. 1, 2015, pp. 1-7.
3- N. Alvarez, et. al, Journal of Inorganic Biochemistry, vol. 203, 2020, pp. 110930.
4- N. Alvarez, et. al, Journal of Biological Inorganic Chemistry, vol. 27, 2022, pp. 431-441.
5- C.Y. Fernández, et. al, Molecules, vol. 28, 2023, pp. 896.
6- N. Alvarez, et. al, Inorganica Chimica Acta, vol. 483, 2018, pp. 61-70.
7- N. Alvarez, et. al, Pharmaceutics, vol. 15, 2023, pp. 1345.
8- P.R. Spackman, et. al, Journal of Applied Crystallography, vol. 54, 2021, pp. 1006-1011.

Acknowlegments: Programa de Desarrollo de las Ciencias Básicas (PEDECIBA-UY), Comisión Sectorial de Investigación Científica (UdelaR-UY, grants to G.F. and N.A.), Fundação de Amparo à Pesquisa do Estado de São Paulo (FAPESP, grants to A.C.F. and J.E.) and Conselho Nacional de Desenvolvimento Científico e Tecnológico (CNPq, grants to A.C.F. and J.E.).

Avaliação estrutural de complexos de Cu(II) com hidrazidas e derivados

P. H. O. Santiago[a], C. C. Gatto[b] , J. Ellena[a].

[a] *Instituto de Física de São Carlos, Universidade de São Paulo, São Carlos-SP, Brasil.*

[b]*Instituto de Química, Universidade de Brasília, Brasília-DF, Brasil.*

O cobre é um elemento traço essencial à vida, estando presente em diferentes proteínas envolvidas em processos biológicos de oxirredução, transporte de oxigênio e de sinalização celular.[1,2] Devido à relevância biológica do cobre para diversos organismos vivos, complexos de cobre(II) vêm atraindo grande interesse de estudo para obtenção de novos agentes quimioterápicos para o tratamento de câncer e de doenças infecciosas.[2,3] Dentro dos complexos de cobre(II) que vêm sendo estudados, destacam-se aqueles que são obtidos a partir de ligantes hidrazidas e seus derivados, os quais demonstraram apresentar amplo perfil farmacológico com pronunciadas atividades antitumoral, antitubercular e antimicrobiana.[4-6]

Nesse sentido, o presente trabalho abordará o desenvolvimento de complexos de cobre(II) sintetizados a partir de hidrazidas e seus derivados, com uma abordagem estrutural relacionando algumas propriedades físico-químicas e biológicas destes compostos com suas estruturas cristalinas e moleculares.

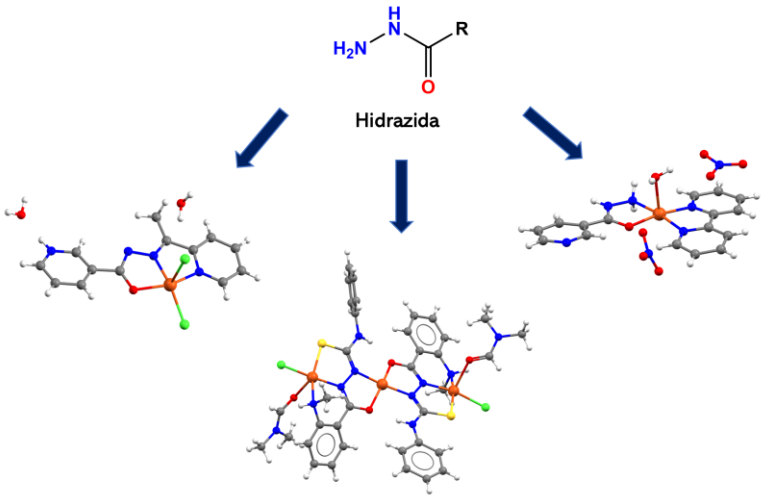

Figura 1: Exemplos de complexos de cobre(II) derivados de hidrazidas.

Referências:

1- Conry, R. R. *Encyclopedia of Inorganic Chemistry*, **2006**, 1st edition, 940.

2- Duncan, C.; White, A. R., *Metallomics* **2012**, 4(2), 127.

3- Zalevskaya, O. A.; Gur'eva, Y. A., *Russian Journal of Coordination Chemistry* **2021**, 47, 861.

4- Nguyen, H. H.; Pham, T. T.; Pham-Thi, N. O. , Tran, V. H.; Le, C. D.; Hoy, B. V.; Trieu, T. N.; Pham, C. T., *Journal of Molecular Structure* **2022**, 1249, 131680

5- Santiago, P. H. O.; Santiago, M. B.; Martins, C. H. G.; Gatto, C. C., *Inorganica Chimica Acta* **2020**, 508, 119632.

6- Hamzi, I., *Mini-Reviews in Organic Chemistry* **2022**, 19, 968.

Agradecimentos: FAPESP, CAPES e CNPq.

Aspectos estruturais como ferramenta para o desenho de complexos de Ru(II) bioativos

R. S. Corrêa[a]

[a]*Departamento de Química, Universdade Federal de Ouro Preto, Ouro Preto, Brasil*

A busca por fármacos mais eficientes é atualmente um dos maiores desafios da ciência. Compostos de coordenação derivados de rutênio, com ligantes de interesse biológico estão se mostrando promissores como agentes quimioterápicos para o tratamento do câncer. Sendo assim, a síntese de complexos de rutênio(II) tem si mostrado uma estratégia interessante. Destacam-se os derivados fosfínicos que vêm merecendo atenção especial, devido suas características biológicas, quanto sua parte química. Neste sentido, a ideia central de nosso trabalho é a inserção de moléculas com interesse biológico (bioligantes) em complexos fosfínicos de rutênio, com o intuito de potencializar suas propriedades biológicas. A estrutura de três complexos ativos contendo como bioligantes o fármaco anticâncer 5FU, a base nitrogenada timina e o nucleosídeo citidina estão representados na Figura 1. Além do bioligante, estão covalentemente ligados ao rutênio dois ligantes trifenilfosfina e uma bipiridina.

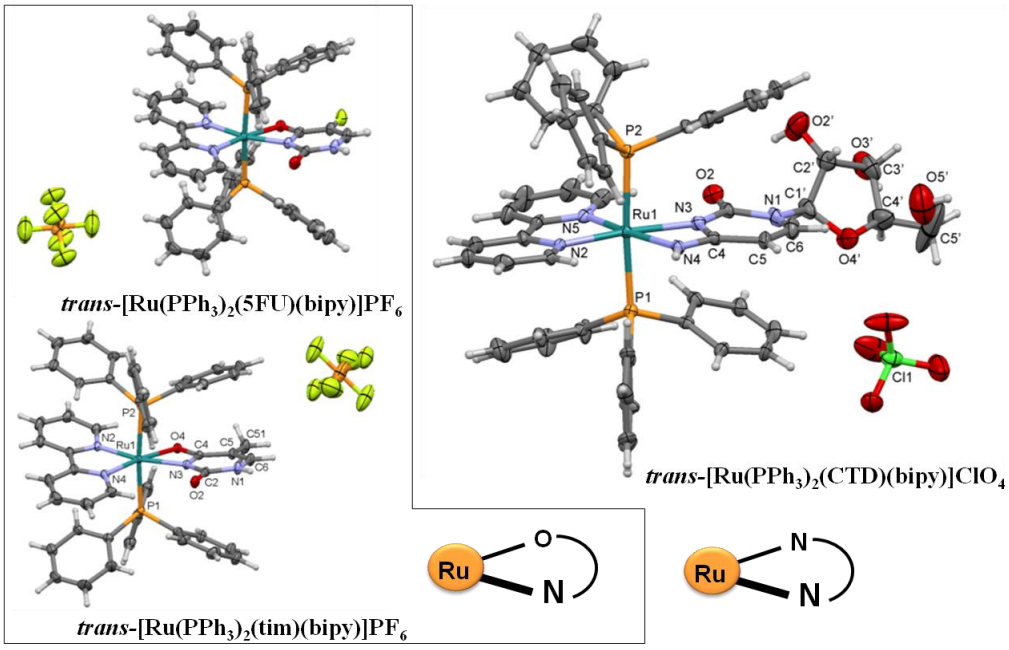

Figura 1. Estrutura cristalina dos complexos trans-$[Ru(PPh_3)_2(5FU)(bipy)]PF_6$, trans-$[Ru(PPh_3)_2(tim)(bipy)]PF_6$ e trans-$[Ru(PPh_3)_2(CTD)(bipy)]ClO_4$.

Estes compostos foram avaliados contra células de câncer de mama (MCF-7) e células sadias L-929. Os complexos que com os ligantes 5FU e timina apresentaram valores de IC_{50}, em MCF-7, próximo ao encontrado para o fármaco de referência, 5-fluorouracil. Dentre os três complexos, o com a citidina foi o complexo menos ativo em MCF-7. No entanto, quando testado em linhagem de célula sadia (L-929) este foi o menos citotóxico, sendo o mais seletivo para células tumorais do que os demais complexos e, também em relação à cisplatina. O complexo $[Ru(PPh_3)_2(5FU)(bipy)]PF_6$ é seletivo para câncer de mama, mas mostram-se menos seletivos do que o ligante 5FU livre, que já é um fármaco disponível no mercado. Um ponto positivo é que todos os complexos apresentaram seletividade maior do que 1, o que significa que todos apresentam citotoxicidade mais pronunciada em células tumorais (MCF-7) do que em células sadias (L-929). Portanto, estes compostos são promissores como agentes anticancerígenos e com maior seletividade dos novos complexos para as linhagens de células tumorais sob estudo. O intuito de utilizar diferentes bioligantes é uma estratégia interessante para desenhar complexos com um maior reconhecimento do alvo macromolecular.

Agradecimentos: FAPEMIG, CNPq, PROPPi-UFOP.

Comunicações Orais

Advancing Antiviral Therapies: A Comprehensive Study of Human DHODH Inhibitors Through Fragment Screening

A. D. Purificação[a], M. M. Vaidergorn[a,b]; T. dos Santos[b]; P. I. Palacio[a,b]; F. S. Emery[a,b]; L. S. Benz[c,d], M. S. Weiss[c]; M. C. Nonato[a,b]

[a]*School of Pharmaceutical Sciences, University of São Paulo, Ribeirão Preto, Brazil*
[b]*Center for the Research and Advancement in Fragments and molecular Targets (CRAFT), University of São Paulo, Ribeirão Preto, Brazil*
[c]*Helmholtz-Zentrum Berlin, Berlin, Germany*
[d]*Freie Universität Berlin, Institute for Chemistry and Biochemistry, Berlin, Germany*

The human enzyme DHODH (Dihydroorotate Dehydrogenase) plays a pivotal role in pyrimidine synthesis, which serves as the fundamental building blocks for DNA and RNA. Given its crucial role in cellular metabolism, DHODH has been extensively researched, particularly as a potential drug target for broad-spectrum antiviral therapies. Viruses are obligate intracellular parasites that heavily depend on the host's cellular machinery and nucleotide supply, among other resources. Moreover, inhibitors of human DHODH have the added benefit of stimulating the immune system, resulting in a dual antiviral mechanism.

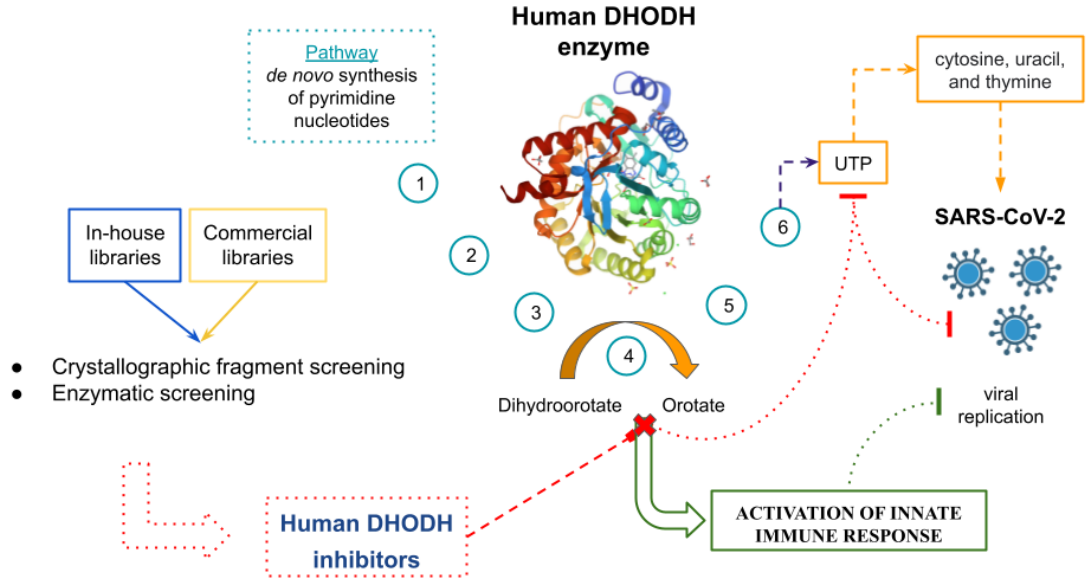

Figure 1: Human DHODH as a Target for Antiviral Therapies. Schematic figure illustrating the overall concept of the study, which explores various techniques to discover new inhibitors for the enzyme for use as an antiviral approach.

In this study, we employed a range of techniques to screen fragments for their potential as DHODH inhibitors and assessed their antiviral activity using SARS-CoV-2 as a model virus. Through extensive enzymatic inhibition assays using our in-house library, we successfully identified a novel chemical class with robust enzymatic inhibition properties and significant anti-SARS-CoV-2 activity. Subsequent to the identification of these fragments, we synthesized derivatives and conducted thorough enzymatic testing. Additionally, we performed crystallographic structure analysis of the enzyme in complex with these fragments. In another facet of our research, we employed crystallographic fragment screening, which unveiled the interaction pattern of fragments from an array of chemical cores, each binding to distinct regions on the enzyme. These findings provide valuable insights into potential druggable sites on DHODH, which can guide the development of new inhibitors with enhanced physicochemical properties and heightened potential as drug candidates. The core strategy here revolves around fragment merging to optimize compound design.

Acknowlegments: This work has been funded by CNPq BRICS STI COVID-19 (441038/2020-4), FAPEG (202010267000272), FAPESP (2020/06190-0, 2021/10084-3, 2021/13237-5 and 2020/05369-6) and iNEXT discovery.

Structural characterization and assessment of cytotoxicity of Ru(II) nitrosyl complexes with pyridines as ligands

C. C. Candido[a], H.V.R. Silva[a] , J. H. A. Neto[b,c] , J. A. Ellena[c] , G. A. F. Silva[d] , M. Ionta[d] , M. I. F. Barbosa[a] , A. C. Doriguetto[a]

[a]*Institute of Chemistry, Federal University of Alfenas, Alfenas-MG, Brazil.*
[b]*Institute of Chemistry, University of São Paulo, São Paulo-SP, Brazil.*
[c]*São Carlos Institute of Physics, University of São Paulo, São Carlos-SP, Brazil.*
[d]*Institute of Biomedical Sciences, Federal University of Alfenas, Alfenas-MG, Brazil.*

Ruthenium compounds can be an excellent alternative to platinum-based complexes, since they offer reduced toxicity potential, making them suitable for biological applications [1]. The nitric oxide can act in various biological activities and/or functions, in addition, NO has a high cytotoxic capacity [2]. So, nitrosyl complexes of ruthenium (II) with derivatives pyridines ligands were obtained of the type $[RuCl_2(NO)(dppb)(L)]PF_6$ (Figure 1) where: dppb = 1,4-bis(diphenylphosphino)butane, NO = nitric oxide, L = derivatives pyridines (L_1 = pyridine (**C1**), L_2 = 4-methyl-pyridine (**C2**), or L_3 = 4-vinyl-pyridine (**C3**)). The complexes were characterized by $^{31}P\{^1H\}$ NMR, molar conductivity, infrared and UV–vis spectroscopy, and the structure of $[RuCl_2(NO)(dppb)(L_2)]PF_6$ was confirmed by single crystal X-ray diffraction (Figure 1).

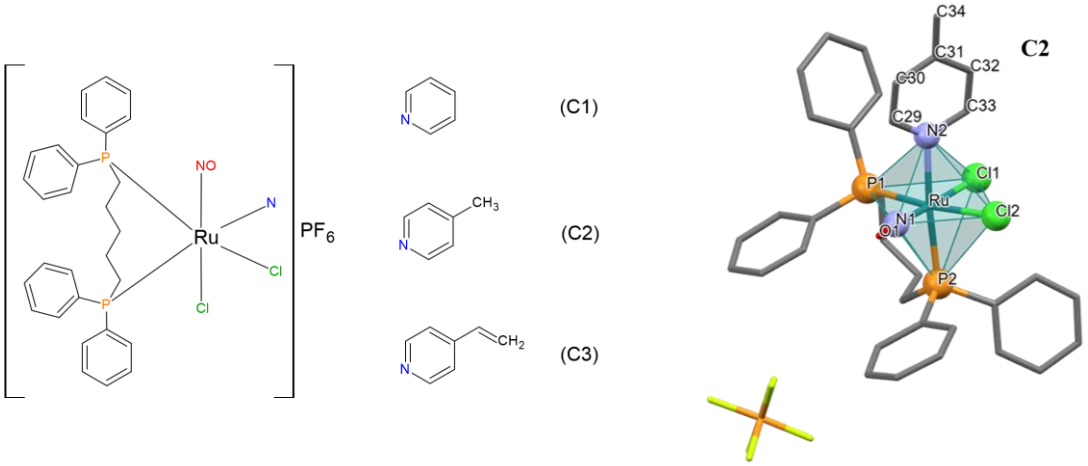

*Figure 1: General Structure of the complexes **C1-C3** and Capped stick/polyhedral complex crystal structure representation of **C2***

In addition, the X-ray powder diffraction method shows that the complex $[RuCl_2(NO)(L_3)(dppb)]PF_6$ (**C3**) has a diffractogram very similar to the **C2** complex, suggesting that the **C3** complex is isostructural of the **C2** complex. The evaluation of the cytotoxicity activity *in vitro* of the (**C1-C3**) complexes revealed that all tested complexes reduced the viability of tumor cells against MCF-7, HepG2, A549, and SK-MEL-147.

References:

1- S. Thota, *et al.*, J. Med. Chem., 61 (2018) 5805-5821.
2- J. A. McCleverty, Chem. Rev., 104 (2004) 403-418.

Acknowlegments: CAPES; CNPq; FAPEMIG; FINEP; UNIFAL-MG

Advanced Structural Investigation of Human Hair

C. L. P. Oliveira[a], C. R. R. C. Lima[a], A. C. C. Bandeira[a], C. Alves[b]

[a]*Physics Institute, University of São Paulo, São Paulo - Brazil* .

[b]*Course of Exact Sciences, Federal University of Paraná, Pontal do Paraná, Paraná - Brazil*

Human hair has two major morphological regions well distinct: the cuticle and cortex. Between the cells of the cuticle and cortex, cell membrane complexes (CMCs) are present, consisted of proteins and lipid bilayers. The main function of the cuticle, the outer structure, is to provide mechanical protection for the cortex, which contains a helical fraction comprising a crystalline phase (intermediate filaments - IFs) embedded in amorphous matrix that is sensible to water, largely influenced by the relative humidity. Hair treatments with chemical products and the use of thermal devices, can promote important structural changes like protein denaturation, water removal and surface damages on the cuticle. We combined a number of techniques, Small-Angle X-ray Scattering (SAXS) *in situ* measurements (varying the temperature), thermogravimetry coupled to mass spectrometry (TG/MS), optical microscopy (OP), X-Ray computer tomography (XRCT) and differential scanning calorimetry (DSC) to obtain structural details on the human hair and structural changes upon chemical and thermal treatments [1,2]. Caucasian virgin hair, Caucasian bleached hair, Caucasian straightened hair and Caucasian bleached and straightened hair were investigated. As will be shown, several results could be obtained providing important structural details as changes on porosity of the inner structure of hair, changes on the CMC structure and hair surface characterization. These results are very important for the basic knowledge on hair structure but also for the cosmetic companies and professionals on hair styling to understand the implications of their products and treatments.

References:

1- Lima, C. R. R. C. & Oliveira C. L. P. et al. 2023. "Alterations promoted by acid straightening and/or bleaching in hair microstructures." J. Appl. Cryst. 56:1002-1014. doi: 10.1107/S1600576723005599.

2- Lima, C. R. R. C. & Oliveira C. L. P. et al. 2020. "Human hair: subtle change in the thioester groups dynamics observed by combining neutron scattering, X-ray diffraction and thermal analysis." European Physical Journal-Special Topics 229 (17-18):2825-2832. doi: 10.1140/epjst/e2020-900217-4.

Acknowlegments: We thank IFUSP, USP, FAPESP, CNPq, CAPES and INCT-FCx for the support on our research.

Spin-State Ordering and Intermediate States in a Mixed-Valence Cobalt Oxyborate with Spin Crossover

Eduardo Granado[a], Carlos W. Galdino[a], Beatriz D. Moreno[b], Graham King[b], Daniele C. Freitas[c].

[a]*Instituto de Física Gleb Wataghin, Universidade Estadual de Campinas, Campinas, Brasil.*
[b]*Canadian Light Source Inc, Saskatoon, Canadá.*
[c]*Instituto de Física, Universidade Estadual Fluminense, Niterói, Brasil.*

Spin-state ordering - a periodic pattern of ions with different spin-state configurations along a crystal lattice - is a rare phenomenon, and its possible interrelation with other electronic degrees of freedom remains little explored. Here we perform a structural investigation of the mixed-valence Co homometallic ludwigite $Co_2^{2+}Co^{3+}O_2BO_3$. A superstructure consistent with a long-range Co^{3+} spin-state ordering is observed between T_4=580 K and T_3=510 K (see Fig. 1). Intermediate states with mesoscopic correlations are detected below T_3 down to T_1=480 K with a change of dimensionality at T_2=495 K. The spin-state correlations are connected to the charge sector as revealed by the abrupt changes in the electrical resistance at T_1 and T_2. The evolution of the structural parameters below T_1 indicate that the spin crossover is ignited by a moderate degree of thermally-induced Co^{2+}/Co^{3+} charge disorder. Charge and spin-state degrees of freedom can be interrelated in mixed-valence spin-crossover materials, leading to sharp transitions involving intermediate spin-state/charge correlated states at the mesoscale.

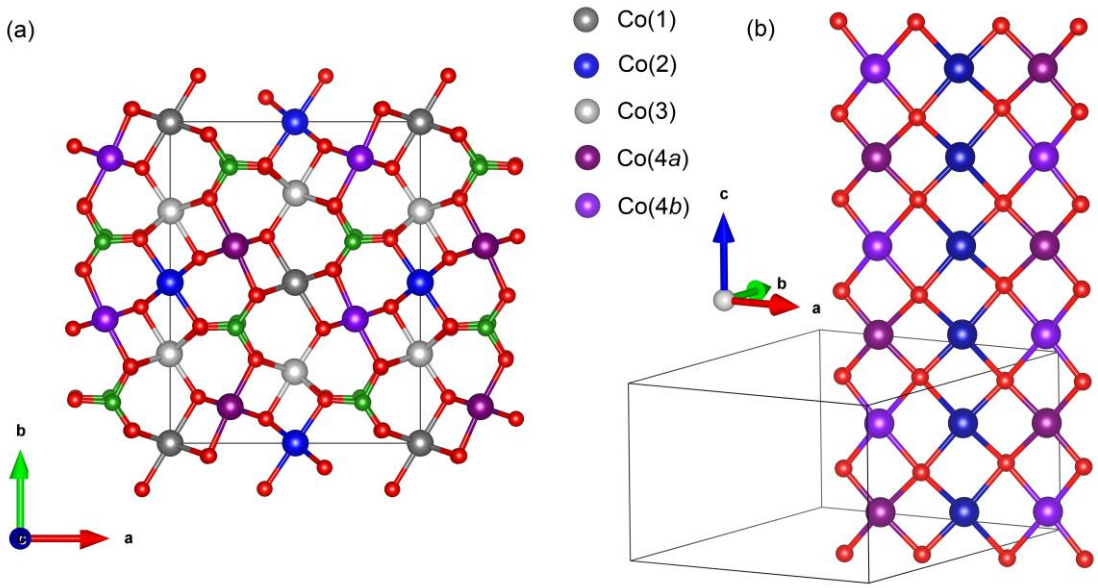

Figure 1: (a) ab-plane projection of the ludwigite superstructure of $Co_3O_2BO_3$ at T=525 K (Pbnm space group). (b) Detailed view of the Co(4a)-Co(2)-Co(4b) (424) three-legged ladders. The main difference of the superstructure with respect to the regular ludwigite (Pbam space group) is the splitting of the Co(4) site of the latter into inequivalent Co(4a) and Co(4b) sites that are alternately stacked along **c**, *leading to a doubled unit cell [thin black lines in (a) and (b)]. The various oxygen (red) and boron (green) sites are drawn with the same colors for simplicity.*

Acknowlegments: This work was supported by Fapesp, proc. 2022/03539-7. Canadian Light Source is acknowledged for concession of beamtime.

High quality data obtained on Laboratory SAXS equipment

Teobaldo, G. B. M. [a], Martins, I. G. V. [a], Reis, D. [a], Oliveira, C. L. P. [a]

[a]*Physics Institute, University of São Paulo, São Paulo, Brazil.*

X-ray scattering is a very versatile method for obtaining structural information on a given system. The X-ray photons interacts with the electron clouds of the sample and scatters. From the analysis of the obtained intensity it is possible to retrieve details on the particles shape, polydispersity, contrasts, interactions and overall supramolecular arrangements.

Recent advances on laboratory based equipment as optimized sources, optics, collimation, sample environment and detectors leveled up the quality of the obtained scattering/diffraction data. As a result a number of cutting edge applications are shown in the literature (1-4). The usual flux on laboratory based equipment (10^7-10^9 photons/mm^2) is several orders of magnitude lower than nowadays Synchrotrons (10^{12}-10^{14} photons/mm^2). However, if the investigation does not requires short measurements, laboratory systems can give data with reasonable quality. Also, since the incoming power in laboratory systems is reasonably smaller than larger facilities, one can have longer exposition times without any radiation damage on the sample.

At the Institute of Physics of University of São Paulo we have the Multiuser Center for Small Angle X-Ray Scattering, EMUSAXS (http://portal.if.usp.br/emu/). In this center we have three SAXS equipments (Nanostar with Xenocs upgrade, SAXS-LCr; Xenocs-Xeuss 1.0 and Xenocs-Xeuss 2.0). All equipment have microfocus source, optimized focusing mirrors and scatterless slits, providing high flux and low background, which is crucial for investigating weak scattering systems.

In this work several features of these equipment will be shown, with a number of applications and in-house developments for the investigation of different types of systems...

References:

1- Lima, C. R. R. C.; Lima, R. J. S.; Bandeira, A. C. C.; Couto, R. A. A.; Bordallo, H. N.; Oliveira, C. L. P. Alterations promoted by acid straightening and/or bleaching in hair microstructures. J. Appl. Cryst. 2023, 56, 1002-1014. DOI: 10.1107/S1600576723005599.

2- Tchakalova, V.; Oliveira, C. L. P.; Figueiredo Neto, A. M. New lyotropic complex fluid structured in sheets of ellipsoidal micelles solubilizing fragrance oils. ACS Omega 2023, 8, 29568−29584. DOI: 10.1021/acsomega.3c03500.

3- Garcia, P. R. A. F. R.; Araujo, W. W. R.; Teobaldo, G. B. M.; de Menezes, A. S.; Otubo, L.; Oliveira, C. L. P. Synthesis and structural characterization of gold nanorods. International Nano Letters 2021. DOI: 10.1007/s40089-020-00322-w.

4- Oliveira, C. L. P.; Lopes, J. L. S.; Sant'Anna, O. A.; Botosso, V. F.; Bordallo, H. N.; Fantini, M. C. A. The development of new oral vaccines using porous silica. Journal of Physics-Condensed Matter 2022, 34 (26). DOI: 10.1088/1361-648X/ac6559.

Acknowlegments: The authors are grateful to IFUSP, USP, FAPESP, CNPQ, CAPES, and National Institute of Complex Fluids, INCT-FCx.

Experimental charge density of tetraaquabis(hydrogenmaleato)iron(II)

H. F. Guimarães[a], B. L. Rodrigues[a].

[a]*Departament of Chemistry, Federal University of Minas Gerais, Belo Horizonte, Brazil.*

In order to obtain more information about the electron density distribution when chemical bonds are formed, it is necessary to consider atoms as aspherical constituents, modeling not only the core electrons but also the valence electrons. The most used approach to achieve this is the Hansen-Coppens multipole formalism[1]. Within this formalism, the electron density in the crystal is a superposition of atomic electron densities which are further expanded as the sum of the spherical core, the spherical valence, and the aspherical valence deformation density.

In this study, we propose a model for electron density deformation of tetraaquabis(hydrogenmaleato)iron(II) ($[Fe(C_4H_3O_4)_2(H_2O)_4]$), which is a coordination compound featuring a short intramolecular hydrogen bond.

The single crystal X-ray diffraction experiment was performed in an XtaLAB Synergy diffractometer equipped with a HyPix detector, using MoKα radiation. The data collection took place at a temperature of 100 K and resolution of d=0.36 Å. The multipole refinement was performed utilizing the XD2016[2] program, using the Hansen-Coppens formalism, and employing least squares refinement techniques. Residual and deformation maps, in addition to statistical parameters, were used to determine the optimal refinement.

Local symmetries were considered to choose the appropriate multipole functions for each atom. All atoms but hydrogen were anisotropically refined. Hydrogen atoms were isotropically refined. In the herein presented multipole model (MM), it is possible to observe a substantial decrease of residues in the regions of chemical bonds in comparison to the isolated atom model (Figure 1) and to detect electron density corresponding to the hydrogen atoms involved in the hydrogen bonds. As can be shown in the residual maps, this preliminary model may be improved, especially in the region of the short hydrogen bond. The statistical parameters of the refinement were: R(F)=0.0199, wR(F)=0.0212 and 329 parameters refined using 13370 independent reflections (I>3σ(I)).

Considering the Quantum Theory of Atoms in Molecules (QTAIM)[3], critical points related to nuclear positions, beyond the bond and ring-critical points of the electron density distribution were identified using the XDPROP module of XD2016.

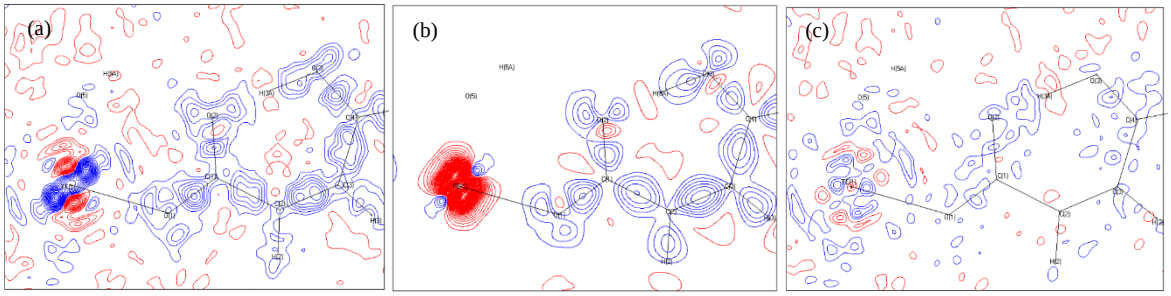

Figure 1: maps on the hydrogen maleate plane: (a) residual map for the isolated atom model, (b) deformation map for the multipole model, and (c) the residual map for the multipole model. Contours at 0.1 eÅ^{-3}. Blue contours are positive, and red contours are negative.

References:

1- Hansen, N. K. & Coppens, P. (1978). Acta Cryst. A34, 909921.

2- Volkov, A., Macchi, P., Farrugia, L. J., Gatti, C., Mallinson, P., Richer, T. & Koritsanszky, T. (2016). XD2016. http://www.chem.gla.ac.uk/ ~louis/xd-home/.

3- Bader, R. F. W. (1990). Atoms in Molecules. A Quantum Theory. Oxford: Oxford University Press.

Acknowlegments: CNPq, LabCri, FINEP.

Predicting and obtaining new solvates of curcumin, demethoxycurcumin and bisdemethoxycurcumin based on the CCDC statistical tools and Hansen Solubility Parameters

Julian Ticona Chambi[a], Edvaldo A. De Almeida[a], Ana Maria Do Espírito Santo[a], Lourdes Infantes[b], Silvia Lucia Cuffini[a].

[a]*Instituto de Ciência e Tecnologia (ICT), Universidade Federal de São Paulo (UNIFESP), 12331-280, São José dos Campos, Brazil.*

[b]*Instituto de Química Física Blas Cabrera (IQF), Consejo Superior de Investigaciones Científicas (CSIC), 28006, Madrid, Spain.*

The new multicomponent crystalline forms as cocrystal and solvates present an opportunity to improve the solubility of APIs. Commonly, the procedure to obtain multicomponent crystalline forms of a drug starts by screening the drug molecule with the different coformers/solvents. However, it is necessary to develop methods to obtain multicomponent forms in an efficient way and with the least possible environmental impact. The Hansen Solubility Parameters (HSPs) is considered a tool to obtain theoretical knowledge of the solubility of the target compound in the chosen solvent[1]. H-Bond Propensity (HBP), Molecular Complementarity (MC), Coordination Values (CV) are tools used for statistical prediction of cocrystals developed by the Cambridge Crystallographic Data Center (CCDC)[2]. The curcumin (Cur), target molecule, is commonly used as an anti-inflammatory. The demethoxycurcumin (Demcur) and bisdemethoxycurcumin (Bisdcur) are natural analogues of Cur from turmeric. Those target molecules have differences in their solubilities. In this way, the work aimed to analyze and compare different tools for prediction solvates of Cur, Demcur and Biscur. The HSP values were calculated for Cur, Demcur, and Biscur using HSPmol software[3]. From the HSPs of the target molecules and fifty organic solvents (listed in the HSP books), the relative energy difference (RED) was determined. The statistical probability of the target molecules would be interacting with the solvent molecule was determined using the CCDC tools. A dataset of the fifty molecules of organic solvents was ranked for each prediction method and by a consensus ranking of different combinations: HSP, CV, HBP and MC values. Based on the prediction, 15 solvents were selected. In a starting analysis, the slow evaporation technique was used to obtain solvates. The single crystals were collected by using a Bruker D8 Venture diffractometer, detector Photon100. The data processing and crystal structure determination were performed using APEX3 and Olex2-1.5 software. According to the results, the HSPs for Cur, Demcur and Biscur were obtained. With respect to prediction analyses, a way to evaluate the predicting method was through the ranking and the consensus ranking position of solvates already reported in the literature. It was observed that the combination of HSP-CV obtained the best results when compared to the other methods. Furthermore, seven new solvates were found up to now (four solvates with crystal structures and three with unit-cell parameter information). The preliminary results showed that the prediction method is showing a promising strategy to evaluate the possibility of forming multicomponent. It is currently working on obtaining single crystals.

References:

1- Peña, M. Á. & Martínez, F. Drugs . *Pharm. Sci.* **29**, 133–134 (2023).

2- Nunes Costa, R., Choquesillo-Lazarte, D., Cuffini, S. L., Pidcock, E. & Infantes, L. *CrystEngComm* **22**, 7460–7474 (2020).

3- Ed Trawtmam. HSPmol. (2022) doi:https://zenodo.org/record/7060000.

Acknowlegments: CAPES, IQF, CSIC - i-COOP+2020.

Isomorphous Coordination Polymers: Design and Building with mixed Ligands.

Luckerman D.G. Botelho[a], Rafaela M.R. da Silva[a], Guilherme P. Guedes,[b] Maria V. Marinho[a].

[a]*Instituto de Química, Universidade Federal de Alfenas, Alfenas-MG, Brasil.*
[b]*Instituto de Química, Universidade Federal Fluminense, Niterói-RJ, Brasil.*

A química de coordenação moderna começa no final do século XIX com o trabalho fundamental de Werner, fornecendo as noções básicas sobre geometria e estereoquímica da coordenação de ligantes ao centro metálico, definindo a estrutura molecular de um complexo[1]. A interação metal-ligante foi primeiramente atribuída como sendo principalmente de natureza eletrostática, mas com o conhecimento das propriedades eletrônicas dos complexos de metais de transição no início do século XX, tem-se estabelecido, desde então, que a interação metal-ligante pode ser melhor definida como fraca interação covalente[1]. Assim, novos compostos como as redes de coordenação (polímeros de coordenação (PC's) e redes metal-orgânicas (MOF's)) têm sido construídas[2] com importantes aplicações[3]. Neste trabalho, apresentamos resultados inéditos do processo de auto-organização entre os íons Co(II) e Cu(II) com dois ligantes orgânicos, um na forma de sal "1,3-fenilenobis(oxamato) de potássio" e outro neutro, contendo sítios N,O-doadores, disulfeto de 4,4'-dipiridila (dpss). A reação, por difusão, levou a obtenção de monocristais (Figura 1a) susceptíveis para DRXM, cujos dados revelam a formação de polímeros de coordenação de fórmula [M(H_2mpba)dps].2dmso (M= Co(II) **(1)** e Cu(II) **(2)**), contendo o ligante sulfeto de 4,4'-dipiridila (dps), obtido a partir da transformação *in situ* do ligante dpss. As curvas termogravimétricas (TG) de **1-2** mostram o mesmo perfil com estabilidade térmica até 160°C, com início da decomposição da parte orgânica a partir dessa temperatura. Os espectros de infravermelho mostram bandas de absorção características do ligante H_2mpba^{2-}, com estiramento $\nu_{(NH)}$ de amida (3179 **(1)**, 3220 **(2)** cm^{-1}) e estiramento $\nu_{(CO)}$ em 1666, 1615 cm^{-1}. Bandas em 1587 cm^{-1} indicam a presença do ligante dps coordenado ao centro metálico ($\nu_{(CC/CN)}$). Os dados de DRXP mostram que ambos os compostos são isomorfos (Figura 1b) e as estruturas determinadas por DRXM confirmam a coordenação de ambos os ligantes ao centro metálico, gerando um polímero de coordenação bidimensional de Co(II) **(1)** e Cu(II) **(2)**) (Figura 1c), com moléculas de dmso nas cavidades do polímero.

Figura 1a- Cristais de **(1)**.

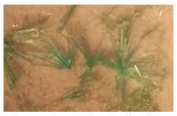

Figura 1a- Cristais de **(2)**.

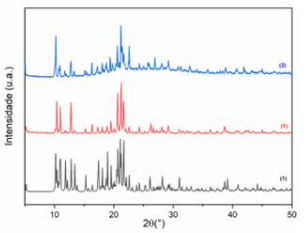

Figura 1 b- Difratogramas de raios X por policristal experimentais (**1**-**2**) (vermelho/azul) e o calculdo (cif) de **1** (preto).

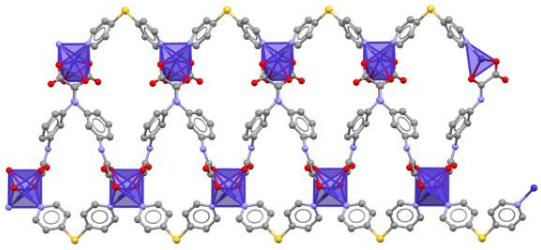

Figura 1c- Visão do polímero de coordenação {[Co(H_2mpba)dps].2dmso}$_n$. Átomos de hidrogênio e moléculas de dmso foram omitidas por claridade.

Referências:

1- Ferrando-Soria, J., Vallejo, J., *et al*. *Coord.Chem.Reviews*, 2017, 339, 17–103.; 2- Batten, S. R., Champness N. R., *et al*. *CrystEngComm*., 2012, 14, 3001–3004.; 3- Do Pim, W. D. *et al*. *Inorg. Chem*. 2022, 30, 11695–11701.

Agradecimentos: FAPEMIG (Projeto CEX - APQ-01597-17); CAPES- código 001, PIBICT-FAPEMIG (via Edital PRPPG-UNIFAL-MG), Laboratório multiusuário de difração de raios X por policristal (UNIFAL-MG) e monocristal (UFF-RJ), Central analítica II-UNIFAL-MG pelas medidas de TG/DSC (modelo TA 2910).

PyDDT: Structural refinement of single crystals via X-ray phase measurements

R. F. S. Penacchio[a], S. L. Morelhão[a], S. W. Kycia[b], C. M. R. Remédios[c], G. C. Andrade[d]

[a]*Institute of Physics, University of São Paulo, 05508-090 São Paulo, SP, Brazil.*
[b]*Department of Physics, University of Guelph, Guelph, ON, Canada.*
[c]*Physics Department, Federal University of Pará, Belém, Brazil.*
[d]*Brazilian Synchrotron Light Laboratory, Campinas, Brazil*

The development of fundamental areas of human knowledge, such as structural biology and materials engineering, relies heavily on structural analysis with atomic resolution. Every year, billions of dollars are invested globally in equipment and facilities intended for structural analysis. Nevertheless, solid limitations exist for resolving specific structural details, such as charge or orbital ordering. One way to gain more detailed structural information beyond that accessible by conventional crystallography is to exploit the X-ray dynamical diffraction (XRDD) phenomenon. XRDD allows direct measurements of diffracted wavefield phases, providing extra information on top of the diffracted intensities. Although many works exploit phase measurements [1-4, and references therein], a few steps may be challenging for inexperienced users, such as determining the structural details of a given system accessible only by phase measurements and performing data acquisition and analysis.

This work presents a general approach for exploiting XRDD as implemented into PyDDT - Python Dynamical Diffraction Toolkit, an open-source Python package for exploiting XRDD in nearly any crystalline system. It allows experiment planning based on a Crystallographic Information File (CIF) by providing insights on the susceptibility of XRDD to structural details such as valence of chemical species, vacancies, anti-site occupation, internal strain due to foreign atoms, and relative differences in atomic displacement. Optimum resonant diffraction conditions may also be identified before the actual experiment. After a successful data collection, a fast semi-automatic data analysis carried out by PyDDT extracts all structure factor phase information available in the data set. Graphic tools are also provided for comparing experimental and theoretical phases, stating feasible model structures that explain the XRDD data. Here, PyDDT usage is demonstrated in a few emblematic cases: probing electron charges in silicon covalent bonds and amino acid var der Waals bonds [3], as well as using resonant diffraction to elucidate vibrational atomic displacements in a thermoelectric crystal [4].

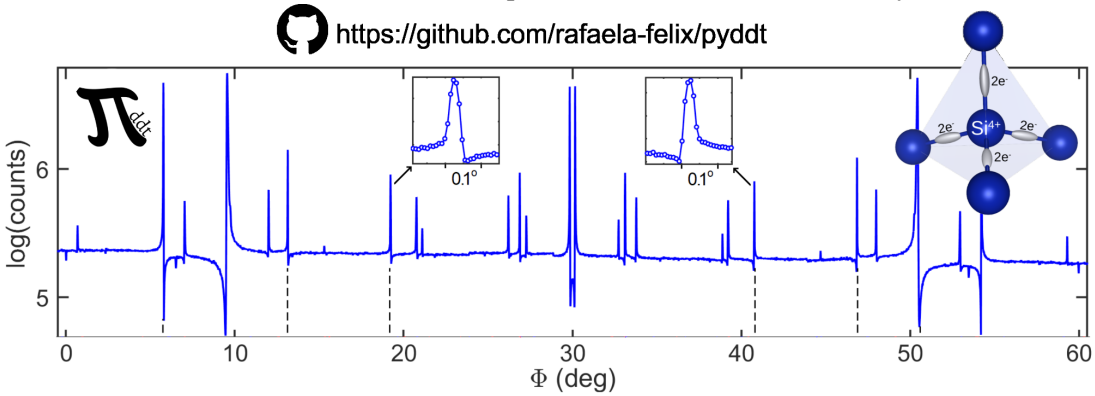

Figure 1: Φ-scan of silicon 222 reflection used for probing bonding charges through PyDDT.

References:
1- Q. Shen and K. D. Finkelstein. Phys. Rev. Lett. 65, 3337 (1990).
2- S. L. Morelhão and S. Kycia. Phys. Rev. Lett. 89, 015501 (2002).
3- S. L. Morelhão et al. J. Appl. Cryst. 50, 689–700 (2017).
4-A. Valério et al. MRS Communications 10, 265-271 (2020).

Acknowledgments: grant 2021/01004-6, São Paulo Research Foundation (FAPESP).

Linha do Tempo da Formação de Recursos Humanos em Cristalografia no Brasil

Yvonne P. Mascarenhas

Departamento de Física e Ciências Interdisciplinares, Instituto *de Física de São Carlos, Universidade de São Paulo, São Carlos, SP, Brasil.*

Tradicionalmente, a cristalografia foi definida como o estudo de cristais, que são sólidos homogêneos com uma ordem interna tridimensional. Essa ordem, sob condições favoráveis, pode se manifestar externamente através de superfícies planas e lisas. Até 1913, esse estudo era principalmente conduzido por técnicas goniométricas macroscópicas ou ópticas, que permitiam a classificação dos cristais em sete sistemas cristalinos, 32 grupos pontuais e, por fim, em 230 grupos espaciais. Esse campo foi então denominado de "Cristalografia Óptica".

Foi somente em 1913 que a experiência de difração de raios X, devidamente interpretada por W.L. Bragg, abriu a possibilidade de compreender a organização periódica dos átomos e moléculas que compõem o cristal. Isso, por sua vez, permitiu a determinação da estrutura molecular da substância cristalizada, um fator fundamental que influencia muitas de suas propriedades.

Logo se constatou que a difração de raios X aplicada a amostras policristalinas gerava padrões característicos que podiam ser utilizados como índices analíticos para identificar diversas substâncias. No Brasil, os primeiros trabalhos de Cristalografia de Raios X surgiram na sessão de Mineralogia do Instituto de Geociências da USP e, posteriormente, com o retorno do mineralogista Elisiário Távora da FNFi (Faculdade de Filosofia) da então Universidade do Brasil, atual UFRJ, após obter seu doutorado no MIT, EUA, em 1953, a pesquisa nesse campo ganhou impulso. Assim, a linha do tempo da formação de cristalógrafos no Brasil começa com esses dois eventos.

Dado o caráter intrinsecamente interdisciplinar da Cristalografia, incluímos na Linha de Cristalografia pesquisadores de diferentes formações, como químicos, físicos, bioquímicos, etc., com base no ano de conclusão de seus doutorados e com o critério de terem orientado pelo menos um doutorando. Para fornecer mais informações aos usuários da linha, também incluímos os endereços dos Currículos Lattes de todos os membros.

Até o momento, agosto de 2023, nossa Linha de Formação de Recursos Humanos em Cristalografia conta com 93 membros, sendo 66 do sexo masculino e 27 do sexo feminino. Agradecemos qualquer informação ou crítica que possa contribuir para o aprimoramento deste trabalho.

Painéis

The MANACÁ beamline at Sirius: structural biology and chemical crystallography

A.F.Z. Nascimento, E.A. Araujo, J.R.S. Rodriguez, F.C. Ramos, P. Benetton
Brazilian Synchrotron Light Laboratory – LNLS/CNPEM, Campinas, Brazil.

MANACÁ (**MA**cromolecular micro and **Na**no Serial **C**rystA**A**llography) is the macromolecular crystallography beamline at Sirius, optimised for high flux, with micro-size and small beam divergence (0.44 mrad). The focus is optimized to 10 x 7 μm (H x V) at sample position, but the beam size can be adjusted from 100 x 80 μm to 10 x 7 μm, allowing to adjust the beam to the crystal size. The current standard beam size and photon flux at sample position is 20 x 20 μm and 5×10^{11} ph/s/100mA at 12.7 keV, respectively. The energy can be adjusted from 5.6 to 20 keV without significative changes in the photon flux [1]. The experimental station has a mini-kappa [2] goniometer that allows the optimal alignment of crystals with long cell axes and the data collection from multiple orientations for small molecules crystals. Setups for serial crystallography data collection and analyses, as well as automation procedures, are being prepared.

The excellent beam characteristics provided by the Sirius source [3], coupled with the high stability and precision of the beamline optics and experimental setup, contribute together to make possible the diffraction of tiny crystals. The energy range and beamline setup allow native SAD phasing, reducing the necessity of additional experiments to solve new structures. The experiment control is performed using a user-friendly graphical interface (MXCuBE) [4], and automatic data processing (from data reduction to initial modelling) is also available.

Recently, MANACÁ has been officially opened for chemical (small molecule) crystallography community, which can take advantage of high-flux and small beam size to solve the structure of very small crystals, that usually do not diffract at home sources. This can be a great tool for natural product chemistry and any other low yield or difficult-to-crystallize systems.

We have also developed and validated an *in-house* crystal-to-structure pipeline tailored for *in situ* crystallography analysis at room temperature. This approach integrates the steps of protein sample crystallization, data collection and processing, while reducing the necessity for crystal manipulation, such as mounting or transfer. It has the potential to significantly enhance both the quality of acquired data and the subsequent structural elucidation.

References:

[1] Nascimento, A.F.Z., Araujo, E.A. *et al.* Launch of the Manacá Beamline at Sirius: First Protein Crystallography Structures and New Opportunities for Pharmaceutical Development Using Synchrotrons. *Synch Rad News* ***34***, 3–10 (2021).

[2] Brockhauser, S., Ravelli, R. B. G. & McCarthy, A. A. The use of a mini-κ goniometer head in macromolecular crystallography diffraction experiments. *Acta Cryst D* **69**, 1241–1251 (2013).

[3] Liu, L., Milas, N., Mukai, A. H. C., Resende, X. R. & Sá, F. H. de. The Sirius project. *J Synchrotron Rad* **21**, 904–911 (2014).

[4] Oscarsson, M. *et al.* MXCuBE2: the dawn of MXCuBE Collaboration. *J Synchrotron Rad* **26**, 393–405 (2019).

Acknowlegments: Ministry of Science, Technology and Innovation (Brazil), CNPEM/LNLS and the MANACÁ's users.

Distinctive Features of Trypanosomatid Translation Initiation Factors EIF4E Mediating the Interaction with hypermethylated mRNA 5'-end

B. M. S. Pereira[a,b], R.F.Penteado[a], N.I.T.Zanchin[a], B. G. Guimarães[a]

[a]*Laboratory of Structural Biology and Protein Engineering, Carlos Chagas Institute, FIOCRUZ-Paraná, Brazil*

[b]*Biochemistry Departament, Federal University of Paraná, Brazil*

Translation initiation in eukaryotes is a complex process that involves several protein factors to assemble the ribosomal subunits with an initiator methionyl-tRNA positioned at the start codon of the mRNA. Association of the initiation complex eIF4F with the cap structure on the 5′-end of the mRNA, mediated by its eIF4E subunit, is a key step for translation. In addition to eIF4E, eIF4F comprises the eIF4A helicase and eIF4G, a scaffolding protein that mediates association of the polyadenylate binding protein (PABP) and other regulatory factors. As compared to mammalian cells, trypanosomatid translation initiation presents several key differences, including a hypermethylated cap structure found in the 5'-end of mRNAs (called cap-4) and a higher number of genes encoding the eIF4E (EIF4E1-6), eIF4G (EIF4G1-5) and PABP (PABP1-2) translation factor homologues, giving rise to alternative eIF4F complexes (reviewed in 1).

In this work, we present the crystal structure of the initiation factor EIF4E5 from *Trypanosoma brucei* in complex with cap-4 determined at 1.35 Å resolution. Comparison with the structures of the *T. cruzi* and *Leishmania major* EIF4E5 homologs previously determined by our group (2, 3) revealed distinctive features in the cap-4 binding pocket, suggesting species-specific mechanisms for mRNA recognition. While the aromatic residues which form the stacking interaction with the m^7G moiety of the cap structure are conserved as observed in all eukaryotes, the interaction with the additional methylated nucleotides of cap-4 differs between the *T. brucei* and *T. cruzi* homologs.

Furthermore, we generated molecular models for all six EIF4E homologs from *T. cruzi*, *T. brucei* and *L. major*, using the Alphafold2 program. Comparative analysis revealed striking differences in the cap-4-interacting surfaces among the EIF4E homologs. This indicates distinct binding mechanisms that could account for variation in the eIF4E-mRNA 5'-end affinities and potentially impact the roles of alternative eIF4F complexes in promoting or regulating translation.

References:

1. Freire ER *et al*., Pathogens 6(4):55 (2017).
2. Reolon LW *et al.*, Nucleic Acids Res. 47(11):5973-5987 (2019).
3. de Lima GB *et al.*, RNA Biol. 18 (12): 2433-2449 (2021).

Support: CNPq, FIOCRUZ, Institut Pasteur (PTR-ACIP)

Clonagem, Expressão e Purificação do Macrodomain (MD) do vírus Chikungunya

I. Dolci[a], A.S. de Godoy[a], G. D. Noske[a], L. Cipriano[a], G. Oliva[a], R. S. Fernandes[a]

[a]*Instituto de Física de São Carlos, Universidade de São Paulo, São Carlos, Brasil*

Introdução: A febre chikungunya é causada pelo vírus Chikungunya (CHIKV – gênero *Alphavirus*), que é transmitido pela picada de mosquitos do gênero *Aedes.* A doença abrange uma variedade de sintomas que podem incluir artralgia severa, debilitação crônica e, em casos graves, levar à morte. Em 2014, um grande surto de febre CHIKV atingiu as Américas, resultando em uma epidemia no Brasil com 280.000 casos notificados em 2016, tornando o país o centro de infecções de CHIKV no mundo. Em 2020-2021, 106 mil casos de infecção por CHIKV foram sorologicamente confirmados no Brasil, mostrando que o vírus continua ativamente em circulação e tem potencial para causar novos surtos de febre Chikungunya no país [1]. Entretanto, ainda não existem fármacos ou vacinas disponíveis contra o CHIKV. Assim, é fundamental o desenvolvimento de um antiviral específico para um tratamento seguro e eficaz das infecções por CHIKV. O domínio N-terminal Macrodomain (MD), da proteína nsP3 de CHIKV, se liga a ADP-ribose e possui atividade hidrolase, e, apesar de ter poucos estudos na literatura sobre o mecanismo exato de ação deste domínio, o MD parece desempenhar um papel importante na replicação viral, representando assim, um alvo interessante na busca por inibidores específicos. **Objetivo:** O objetivo deste trabalho foi obter o MD recombinante da nsP3 de CHIKV para posteriores triagens de antivirais. **Metodologia:** A sequência codificante do MD de CHIKV (PDB: 3GPG_A: aminoácidos 1 a 160) foi clonada no vetor pET M11 pelo método *Gibson Assembly*. Em seguida, células de *E. coli* Rosetta 2 foram transformadas com o plasmídeo recombinante e a proteína foi expressa em 4 L de meio Terrific Broth. Após a expressão, o MD foi purificado por cromatografia de afinidade ao níquel, seguida por uma cromatografia de exclusão molecular e o resultado foi analisado por SDS-PAGE. **Resultados**: Como resultado, foi possível obter a proteína pura após as duas etapas de purificação, com rendimento final de 7 mg por litro de cultivo. **Perspectivas**: Os próximos passos serão cristalizar o macrodomínio para que possamos realizar triagens de fragmentos, buscando inibidores específicos.

References:

1- Yakob L. (2022). Predictable Chikungunya Infection Dynamics in Brazil. Viruses, 14(9), 1889. https://doi.org/10.3390/v14091889

2- Abraham R, Hauer D, McPherson RL, et al. ADP-ribosyl-binding and hydrolase activities of the alphavirus nsP3 macrodomain are critical for initiation of virus replication. Proc Natl Acad Sci U S A. 2018;115(44):E10457-E10466. doi:10.1073/pnas.1812130115

Acknowlegments: FAPESP (Processo: 2022/16111-5).

The heterodimeric septin coiled coil: structure and interaction with BORG3-BD3

Cavini I.A.[a], Castro D.K.S.V.[a], Winter A.J.[b], Pereira H.M.[a], Araujo A.P.U.[a], Woolfson D.N.[b], Crump M.P.[b], Garratt R.C.[a]

[a]*Physics Institute of São Carlos, University of São Paulo, Brazil.*
[b]*School of Chemistry,University of Bristol, United Kingdom.*

Septins are cytoskeletal proteins that serve as important scaffold components within cells. In humans, there are 13 different septins, some of which possess a C-terminal domain (CTD) containing coiled-coil (CC) repeats. Filament formation happens by the end-to-end association of heterooctamers and/or heterohexamers, such as SEPT2-6-7-(9-9)-7-6-2. Notably, it is postulated that closely related septins can substitute for one another in the same relative position within filaments; for instance, SEPT8/10/11/14 might replace SEPT6. Despite considerable advancements in understanding septin structure [1], certain aspects remain uncharacterized. Specifically, the structural properties of the heterodimeric coiled coil, along with its long known interaction with the BORG's BD3 (BORG homology domain) motif [2], have yet to be fully elucidated. In this study, we present the X-ray structure of the SEPT14-SEPT7 heterodimeric CC (Figure 1) [3]. Additionally, we investigate the interaction between the SEPT6-SEPT7 CC and a BD3 peptide of BORG3 [4]. Remarkably, the structure of the SEPT14-SEPT7 CC exhibits a distinctive parallel arrangement, featuring two distinct CC periodicities: heptads and hendecads. The N-terminal portion of the hendecad region proves crucial for heterodimerization, suggesting a potential role in septin molecular recognition. Furthermore, supported by AlphaFold modeling predictions, we establish that this region within the heterodimeric CC serves as the binding site for BD3. These versatile CTDs facilitate the formation of both parallel-heterodimer and antiparallel-homodimer CC arrangements and represent a hotspot for interaction with partners.

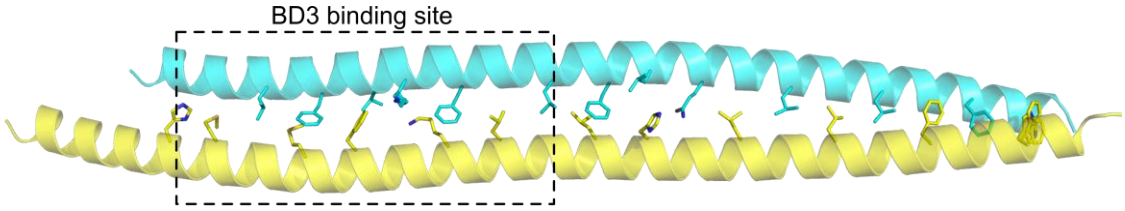

Figure 1: SEPT14 (cyan) - SEPT7 (yellow) heterodimeric coiled coil (PDB 8SJJ). N-termini are shown in the left and only core side chains are depicted. BD3 of BORG3 is modelled by AlphaFold to interact at the N-terminal hendecad-containing half of the structure.

References:

[1] CAVINI, Italo A. et al. The structural biology of septins and their filaments: an update. **Frontiers in Cell and Developmental Biology**, v. 9, p. 765085, 2021.

[2] SHEFFIELD, Peter J. et al. Borg/septin interactions and the assembly of mammalian septin heterodimers, trimers, and filaments. **Journal of Biological Chemistry**, v. 278, n. 5, p. 3483-3488, 2003.

[3] CAVINI, Italo A. et al. X-ray structure of the metastable SEPT14–SEPT7 coiled coil reveals a hendecad region crucial for heterodimerization. **Acta Crystallographica Section D**, v. D79, 2023.

[4] CASTRO, Danielle KSV et al. Dissecting the binding interface of the septin polymerization enhancer Borg BD3. **Journal of Molecular Biology**, v. 435, n. 13, p. 168132, 2023.

Acknowlegments: FAPESP (grants 2014/15546-1, 2018/19992-7, 2020/02897-1 and 2022/00262-4) and CNPq (grant 142394/2018-1).

Keywords: septin, heterodimeric coiled coil, protein-protein interaction.

Kinetic and structural characterization of the endoxylanase HXYN2 from *Humicola grisea* var. *thermoidea* in complex with ferulic acid

I.C. M. Oliveira[a], A. V. Garay[a] , A. A. Souza[a], N. F. Valadares[a], J. A. R. G. Barbosa[a], F. P. Faria[b], S. M. Freitas[a]

[a]*Biology Institute, Department of Cell Biology, Laboratory of Biophysics, University of Brasília (UnB), Brasília, Brazil.*

[b]*Biological Sciences Institute, Department of Biochemistry and Molecular Biology, Federal University of Goiás, Goiânia, Brazil*

An endo-1,4-beta-xylanase from *Humicola grisea* var. *thermoidea* belonging to the GH11 family was obtained by expression in *Pichia pastoris* and named HXYN2. Endoxylanases are the main commercialized hemicellulases because they are applied in several industrial sectors. Studies that search to understand the relationship between structure and function of these enzymes are fundamental for increasing catalytic efficiency under different conditions, aiming at rational biotechnological application.

The effect of eight phenolic compounds on HXYN2 activity was evaluated and, among these, ferulic acid (FA) increased enzymatic activity by 75%. Kinetic parameters indicated that FA did not alter the enzyme's affinity for the beechwood xylan substrate, but increased the Vmax of the reaction, the catalytic efficiency and the enzyme turnover number. Data from isothermal titration calorimetry (ITC), fluorescence quenching and molecular docking showed that FA forms a complex with HXYN2 in the aglycone region, interacting with solvent-exposed tryptophan residues and other residues in this vicinity, through hydrogen bonds, hydrophobic and ionic interactions. Binding constant values for the HXYN2:FA complex are pH dependent and indicated moderate (at pH 7.0 and 9.0) to strong (at pH 4.0) affinity. In the presence of FA, the fluorescence spectra of HXYN2 showed pH-dependent changes in the position and intensity of the emission bands.

The secondary structure of HXYN2 in the presence of FA was altered with a decrease in the α-helix and an increase in the β-turn and disordered structures. The thermal denaturation curve in the presence of AF showed a Tm of 54 °C, indicating lower structural stability of HXYN2 in the presence of this compound. HXYN2 crystals were obtained under different crystallization conditions in the screening step. The refinement of these conditions resulted in crystals of different shapes and sizes. Two of these crystals were taken to the National Laboratory of Synchrotron Light – Sirius for the collection of X-ray diffraction data. The diffraction data were processed, and the results indicated the space group $P2_12_12_1$ (orthorhombic), the presence of two molecules in the asymmetric unit and resolution of 1.6 Å. The crystallographic structure of HXYN2 was obtained by molecular replacement, using the atomic coordinates of the structure of endoxylanase from Thermomyces lanuginosus (PDB 1YNA) as a model, and refinement is in progress.

Acknowlegments: I would like to thank the National Synchroton Light Laboratory for all the support in carrying out the X-ray diffraction experiments.

Clonagem, expressão e purificação da protease (nsP2pro) do vírus Chikungunya

CIPRIANO[a], Lavinia, DOLCI[a], Isabela, NOSKE[a], Gabriela, FERNANDES[a], Rafaela, GODOY[a], André, OLIVA[a], Glaucius

[a] *Instituto de Física de Sâo Carlos - USP*

Introdução: O vírus Chinkunguya (CHIKV) é um arbovírus da família *Togaviridae*, transmitido pela picada de mosquitos do gênero *Aedes* (1). Infecções causadas pelo CHIKV foram registradas pela primeira vez na Tanzânia, em 1952, e na última década o vírus se espalhou por mais de 100 países nas Américas, África, Europa e Ásia, afetando inclusive o Brasil, onde o número de casos vem aumentando desde o primeiro surto em 2014. Até o presente momento, não existe nenhum antiviral e não há uma vacina disponível, tornando a necessidade por um tratamento específico contra o CHIKV cada vez mais urgente. A nsP2pro do vírus, uma cisteinoprotease, é responsável por processar a poliproteína nsP1234, nas quatro proteínas não-estruturais (nsPs) individuais (nsP1 a 4), que formam o complexo de replicação viral, sendo assim um alvo promissor para o desenvolvimento de drogas (2, 3). **Objetivos:** Os objetivos deste trabalho foram clonar, expressar e purificar a protease nSP2pro recombinante de CHIKV para a identificação de antivirais. **Metodologia:** A clonagem do fragmento codificante da nsP2 domínio protease (GenBank KY703894.1 – nucleotídeos 43 a 175) foi realizada utilizando o método Gibson Assembly e diferentes vetores: pET-M11, pET-sumo e pET-TRX. Os plasmídeos contendo os fragmentos de interesse foram transformados em células de *E. coli* e purificados utilizando o kit PureYield™ Plasmid Miniprep System (PROMEGA®). Em seguida, linhagens de *E. coli* Rosetta 2 (DE3) e BL21 foram transformadas com os plasmídeos recombinantes e foram realizados testes de expressão da proteína nos meios TB, LB e Zym. A nsP2pro foi purificada através de duas etapas: primeiro, uma cromatografia de afinidade ao níquel e, segundo, uma cromatografia de exclusão molecular. A pureza das amostras foi verificada por SDS-PAGE. **Resultados e perpesctivas:** A partir dos testes de expressão, concluiu-se que a condição que resultou em um maior rendimento da nsP2pro foi em meio LB induzido com 0,4 mM de IPTG, utilizando a linhagem BL21 contendo a construção em vetor pET-Sumo. A partir deste resultado, a obtenção da proteína será otimizada em maior volume de meio (4L) e a atividade enzimática será validada para posteriores ensaios de triagem de antivirais.

References:

1 - AN AALST, Mariëlle; NELEN, Charlotte Marieke; GOORHUIS, Abraham; STIJNIS, Cornelis; GROBUSCH, Martin Peter. Long-term sequelae of chikungunya virus disease: A systematic review. **Travel Medicine and Infectious Disease**, [S. l.], v. 15, p. 8–22, 2017. DOI: 10.1016/j.tmaid.2017.01.004.

2 - NARWAL, Manju; SINGH, Harvijay; PRATAP, Shivendra; MALIK, Anjali; KUHN, Richard J.; KUMAR, Pravindra; TOMAR, Shailly. International Journal of Biological Macromolecules Crystal structure of chikungunya virus nsP2 cysteine protease reveals a putative flexible loop blocking its active site. **International Journal of Biological Macromolecules**, [S. l.], v. 116, p. 451–462, 2018. DOI: 10.1016/j.ijbiomac.2018.05.007.

3 - DAS, Pratyush Kumar; PUUSEPP, Laura; VARGHESE, Finny S.; UTT, Age; AHOLA, Tero; KANANOVICH, Dzmitry G.; LOPP, Margus; MERITS, Andres; KARELSON, Mati. Design and validation of novel chikungunya virus protease inhibitors. **Antimicrobial Agents and Chemotherapy**, [S. l.], v. 60, n. 12, p. 7382–7395, 2016. DOI: 10.1128/AAC.01421-16.

Acknowlegments: FAPESP (Processo 01266-3).

Discovery and Characterization of novel human kynurenine 3-monooxygenase inhibitors for the treatment of Neuropathic Pain

A.A. Souza[a,b,d], A.A. Oliveira[a,b], A.T. Cordeiro[a], J.N.F. Souza[a], R.R. Oliveira[a], M. Bruder[a], J.K.R. Bonalumi[a], R. Meneghello[a], P. Jardim[a], R. Felício[a], M.L. Sforca[a], A. Cassago[d], R.V. Portugal[d], J.C. Farias Alves-Filho[b], F. Q. Cunha[b], T.M. Cunha[b] and D.B.B. Trivella[a].

[a]*Brazilian Biosciences National Laboratory, CNPEM, Campinas, SP, Brazil.*

[b]*Center of Research in Inflammatory Diseases (CRID), Department of Pharmacology, Ribeirao Preto Medical School, University of Sao Paulo, Ribeirao Preto, SP, Brazil.*

[c]*Brazilian Nanotechnology National Laboratory, CNPEM, Campinas, SP, Brazil.*

[d]*Biology Institute, Laboratory of Biophysics, University of Brasília (UNB), Brasília, Brazil.*

The kynurenine 3-monooxygenase (KMO) is an important protein branching of the kynurenine pathway, catalyzing the hydroxylation of L-kynurenine to form 3-hydroxykynurenine (3-HK), a neurotoxic compound. The 3-HK induces apoptosis and injurious to different cell types[1]. This enzyme is an attractive therapeutical target for several neurodegenerative and neuroinflammatory diseases and is the target of our project which intends to discover and develop novel KMO inhibitors in the context of neuropathic pain. We aim to find new inhibitors for KMO coupling screening of innovative chemical libraries (from both synthetic and natural origins) with integrative structural biology. The first step was to purify the KMO for both inhibition and structural biology assays. A robust high-throughput screening (HTS) assay (Z'>0.8, I/noisy> 6) was developed for screening hKMO inhibitors[2]. About 13 thousand compounds were tested, and the hits found were further validated using orthogonal assays, combining concentration-response curves and LC-MS/MS direct detection of the KMO enzyme reaction components. Six hits were selected for structural analysis in complexes with KMOs. For structural studies, the complexity of full-length hKMO, a membrane protein, and the crystallization is challenging, being so far unsuccessful. In our project, hKMO-FL was produced for HTS campaigns, as well as for STD-NMR fast and cryo-EM studies to assess protein−ligand interaction and structural elucidation. We produced a homologous PfKMO for high-throughput crystallography approaches. This KMO variant was crystallized and diffracted at the MANACA beamline (Sirius, Brazil) [3], with structures determined to up to 1.7 Å. The STD-NMR results confirmed that five hits out of the six selected were ligands of hKMO and PfKMO. The soak protocols were established, and the X-ray protein crystallography strategy demonstrates that PfKMO was successfully selected for crystallization with KMO commercial inhibitors and three hits found in our HTS. The data collected and processed using the HT crystallography pipeline (XDS and PanDDA pipelines) showed a clear density of ligands in complexes with PfKMO. The next step will be the determination of the structure PfKMO-ligand complexes and in vitro/in vivo assay to inhibitory confirmation using neural cells and Intrathecal PoE strategy. In parallel, electron microscopy routines are being established to determine the hKMO-FL structure and its complexes with the hits found by HTS. It is expected that the strategy of using the different structural approaches will help us to obtain KMO complexes with hits that will be used to guide lead molecules for neuropathic pain targeting KMO.

References:

1- Kim HT et al. (2018). Cell Chemical Biology. doi: 10.1016/j.chembiol.2018.01.008.
2- Jacobs KR et al. (2018). SLAS Discovery. doi: 10.1177/2472555218757180.
3-Nascimento A et al. (2021). Synchrotron Radiation News. doi: 10.1080/08940886.2021.1994310.

Acknowlegments:
National Center for Research in Energy and Materials (CNPEM)
Center of Research in Inflammatory Diseases (CRID)
The São Paulo Research Foundation (FAPESP)

Unveiling Advanced Efavirenz Cocrystal Systems: A Leap in Drug Solubility Enhancement.

M. A. S. Chagas[a], M. A. M. Luz[a], J. A. L. C. Resende[a].

[a]*Universidade Federal de Mato Grosso – Campus do Araguaia, Barra do Garças, Brazil.*

The solubility and dissolution of drugs with low water solubility are influenced by particle size, crystalline structure, and physical form, adversely impacting formulation processes regarding bioavailability and effectiveness. Among all possible modifications, multi-component crystals, such as cocrystals and eutectic compositions, have been successfully utilized to enhance drug solubility. This study aimed to prepare and characterize multi-component systems of efavirenz (EFV), a low-solubility non-nucleoside reverse transcriptase inhibitor antiretroviral drug used to treat Acquired Immunodeficiency Syndrome (AIDS). Seven potential coformers were evaluated in these multi-component tests: L-valine (VAL) and 3-aminobenzoic acid (3AB). The results suggest two potential new multi-component systems, notably the EFV/VAL and EFV/3AB systems, with possible cocrystal formation. Two cocrystals were produced by synthesizing EFV and each coformer in appropriate proportions using fusion and reflux methods. The materials were identified as EFV/VAL and EFV/3AB, showing possible molecular interactions for EFV/VAL and EFV/3AB. When compared to the EFV/VAL cocrystal, the X-ray patterns of VAL exhibited characteristic peaks at 7.3°, 14.7°, and 29.6°. Meanwhile, the EFV/VAL cocrystal revealed new characteristic peaks at 10.2°, 11.7°, and 28.3°, indicating the formation of a new phase. The X-ray patterns for 3AB, compared to the EFV/3AB cocrystal, showed characteristic peaks at 16.73°, 17.48°, 27.24°, and 28.50°. The EFV/VAL cocrystal displayed new characteristic peaks at 8.43°, 10.44°, 11.30°, 11.85°, 12.45°, and 21.56°, indicating the formation of another new phase. Thus, the new cocrystals exhibited a PXRD pattern with different peak positions than EFV and the coformer. Based on the results, it can be inferred that both EFV/3AB and EFV/VAL have distinct internal crystalline structures compared to their initial components.

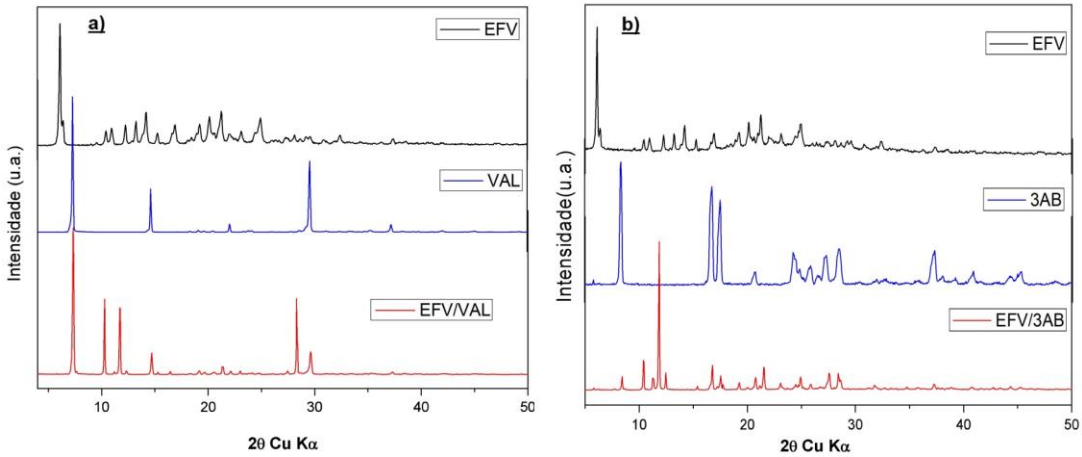

Figure 1: a) X-ray diffraction patterns: EFV, VAL and EFV/VAL and b) X-ray diffraction patterns: EFV, 3AB and EFV/3AB

References:

1- Marques, M. M.; Rezende, C. A.; Lima, G. C.; Marques, A. C. S.; Prado, L. D.; Leal, K. Z.; Rocha, H. V. A.; Ferreira, G. B.; Resende, J. A. L. C. J. Mol. Struct. 2017, 1137, 476–484.

2- Goud, N. R.; Suresh, K.; Sanphui, P.; Nangia, A. Int. J. Pharm. 2012, 439 (1-2), 63–72.

3- Hiendrawan, S.; Veriansyah, B.; Widjojokusumo, E.; Soewandhi, S. N.; Wikarsa, S.; Tjandrawinata, R. R. Int. J. Pharm. 2016, 497, 106–113.

Acknowlegments: CNPq, CAPES, FAPEMAT and UFMT.

Desenvolvimento, caracterização e avaliação da função antimicrobiana de sulfadiazina de prata com superfície modificada

M.P. Salto[a], B.V. Silva[b], J.L. Santos[b], R.C L.R. Pietro[c], L.A.C. Favorin[a]

[a]*Laboratório de Ciências dos Materiais aplicada à Farmácia, Faculdade de Ciências Farmacêuticas, Universidade Estadual Paulista, Araraquara/SP, Brasil.*
[b]*Laboratório de Pesquisa e Desenvolvimento de Fármacos, Faculdade de Ciências Farmacêuticas, Universidade Estadual Paulista, Araraquara/SP, Brasil.*
[c]*Laboratório de Biotecnologia, Faculdade de Ciências Farmacêuticas, Universidade Estadual Paulista, Araraquara/SP, Brasil.*

A descoberta de antibióticos foi um marco para a medicina moderna, entretanto, seu uso contínuo promoveu o desenvolvimento de cepas bacterianas multirresistentes [(3)]. Dessa forma, há uma necessidade de descobrir novos agentes antimicrobianos. Pesquisas evidenciam que alguns compostos inorgânicos são promissores como novos produtos com função antimicrobiana, como as nanopartículas metálicas, que apresentam tamanhos semelhantes aos dos microrganismos, promovendo diferentes meios de ação celular que levam à destruição destes. Além disso, impossibilitam a adaptação de estatégias das cepas bacterianas para sua própria sobrevivência, fator primordial para impedir a resistência bacteriana [(1)]. Visando aumentar a eficácia antimicrobiana das nanopartículas metálicas, é possível realizar a modificação de sua superfície com produtos que são utilizados em tratamentos infecciosos, como a sulfadiazina de prata. Sobre seu potencial antimicrobiano, uma pesquisa evidenciou que a utilização de sulfadiazina de prata na concentração de 1% já se mostrou eficaz para o tratamento de queimaduras, impedindo o crescimento bacteriano e promovendo melhor cicatrização [(2)]. Diante do exposto, o objetivo deste trabalho foi modificar a superfície da sulfadiazina de prata com um organosilano, 3-glicidiloxipropiltrimetoxissilano (GPTMS). A sulfadiazina modificada foi caracterizada por difração de raios X e ressonância magnética nuclear e comparada à sulfadiazina de prata comercial. Também foram realizadas análises para investigar a atividade antimicrobiana frente a uma cepa bacteriana gram positiva, *Staphylococcus aureus*, tanto para a sulfadiazina modificada quanto para a comercial. Os resultados de difração de raios X revelaram que a modificação da superfície não alterou a estrutura cristalina dos compostos. Os espectros de ressonância magnética nuclear revelaram a formação de ligações entre a sulfadizina e o GPTMS. As análises de atividade antimicrobiana realizadas através da verificação do halo de inibição em cepas de *S. aureus* revelaram que a atividade da sulfadiazina modificada é similar à da comercial. Espera-se, como perspectiva futura, modificar a superfície de nanopartículas de óxido de zinco com o composto sulfadizina-GPTMS obtido neste trabalho.

Referências:

1- ALMEIDA, C.I. *et al.* A utilização de nanopartículas no combate à resistência bacteriana. **Brazilian Journal of Surgery and Clinical Research – BJSCR**, v.19, n.2, 2017. ISSN online: 2317-4404.
2- RAGONHA, A.C.O. *et al.* Avaliação microbiológica de coberturas com sulfadiazina de prata a 1% utilizada em queimaduras. **Rev Latino-am Enfermagem**, v.13, n.4, 2005. https://doi.org/10.1590/S0104-11692005000400009.
3- ROCHA, D.P. *et al.* Coordenação de metais a antibióticos como uma estratégia de combate à resistência bacteriana. **Química nova**, v.34, n.1, 2011.

Human indoleamine-2,3-dioxygenase 1 (IDO1) modulation towards neuropathic pain treatment: screening and orthogonal assays, structural investigations, and preliminary hit characterization.

Jardim, P. (1) e 2; Souza, A. A. (1-2) e 2; Oliveira, A. A.; Oliveira R. R. (2); Bruder M.C.P (2); Cunha, T.M. (1); Trivella, D. B. B. (2).

(1) Universidade de São Paulo, Faculdade de Medicina de Ribeirão preto (FMRP USP)- Ribeirão Preto, SP;

(2) Centro Nacional de Pesquisa em Energia e Materiais (CNPEM)-Campinas, SP.

Neuropathic pain represents one of the most important types of chronic pain, affecting about 10% of the global population. That condition could be triggered by pathology affecting the somatosensorial nervous system and damage caused directly to the central or peripherical nervous system. Known treatments for neuropathic pain are limited and scarce, therefore new pharmacological approaches are required. Preliminary results obtained by our research group demonstrated that neuropathic pain could be ablated or reduced by tryptophan catabolic pathway inhibition, particularly the kynurenine pathway (kynpath). The first enzyme in kynpath, indoleamine-2,3-dioxygenase 1 (IDO1), compromises the substrate tryptophan into the pathway and is considered a key enzyme to be targeted in the kynpath. We aimed to develop in vitro assays to search for new IDO1 inhibitors, then characterize and improve the molecules, and finally test the selected inhibitors in pre-clinical in vivo models of neuropathic pain. As a result, firstly, IDO1 expression and purification procedures were implemented and validated to obtain the enzyme in the required quantities and high purity. An IDO1 high throughput screening assay was then developed to screen 14k chemical samples. Hits were selected and evaluated in concentration-response curves to extract their IC_{50} values. Forty-five IDO1 inhibitors showed IC_{50} values below 10 µM. These were further subjected to orthogonal assays, returning 33 confirmed IDO1 inhibitors, 5 have already been confirmed as IDO1 ligands by STD-fast. The confirmed molecules belong to five different chemical classes, 2 of which represent novel classes of IDO1 inhibitors. About half of the selected IDO1 inhibitors have already been tested in humans for other applications, and 9 are approved drugs. These IDO1 inhibitors represent opportunities for drug repurposing for chronic pain. In addition, about 35% of the IDO1 inhibitors found are novel bioactive molecules that can be used as a basis for innovative drug discovery. IDO1 apo crystals under different crystallization conditions were acquired at up to 2.1 Å resolution by x-ray diffraction. The project's next steps consist of obtaining IDO1 crystallographic complexes with the selected inhibitors by establishing soaking and co-crystallization protocols. In parallel, the hit series are being expanded and evaluated in structure-activity relationship models along with ADME-Tox evaluation, aiming to select the best hits to progress or to be optimized, in the pipeline of discovering IDO1 inhibitors for neuropathic pain.

References:

1-LUO, Shukun et al. High-resolution structures of inhibitor complexes of human indoleamine 2, 3-dioxygenase 1 in a new crystal form. Acta Crystallographica Section F: Structural Biology Communications, v. 74, n. 11, p. 717-724, 2018.

2-MAGANIN, Alexandre GM et al. Meningeal dendritic cells drive neuropathic pain through elevation of the kynurenine metabolic pathway in mice. The Journal of Clinical Investigation, 2022.

Acknowlegments: CNPEM, LNBio, CRID, USP, FAPESP e CAPES.

DESENVOLVIMENTO DE NOVAS FORMAS SÓLIDAS DE ACICLOVIR COM ÁCIDOS DICARBOXÍLICOS: UMA ESTRATÉGIA PARA REPOSICIONAMENTO FARMACÊUTICO

Souza, P. N.[a], Santiago, P. H. O. [a]Ellena, J. [a].

[a]*Instituto de Física de São Carlos, Universidade de São Paulo, São Carlos, Brasil.*

O cenário pandêmico ocasionado pelo Coronavírus (COVID-19) evidenciou a necessidade de desenvolver agentes terapêuticos capazes de prevenir e controlar surtos virais. O reposicionamento farmacêutico oferece diversas vantagens sobre o desenvolvimento tradicional de fármacos como ser mais barato, consumir menos tempo e ser menos arriscado.[1] Nesse cenário, insumos farmacêuticos ativos (IFAs) que agem e interferem com a replicação viral foram selecionados para terem sua atividade antiviral investigada contra a COVID-19. Dentre eles podemos destacar o Aciclovir (Acv), um antiviral barato e de fácil acesso ao redor do mundo usado para tratar o vírus herpes simples (HSV) e o vírus varicela zoster (VZV), o qual mostrou capacidade de inibir proteases virais e múltiplas expressões gênicas virais, ajudando na terapia de pacientes com COVID-19.[2] Os IFAs geralmente se encontram em estado cristalino ou amorfo, disponibilizados por várias formulações farmacêuticas como cápsulas, pós, suspensões ou géis, sendo administrados em grande parte por via oral na forma de comprimidos. Além disso, quando encontrados no estado cristalino, podem existir em várias formas sólidas distintas que influenciam diretamente em suas propriedades físico-químicas, tais como sais, co-cristais, hidratos e solvatos. Atualmente, mais de 40% dos IFAs disponíveis comercialmente apresentam problemas de biodisponibilidade, com o Aciclovir se enquadrando na classe III/IV da BCS, caracterizado por sua baixa permeabilidade e, em alguns casos, discreta solubilidade em água (dependendo da concentração). Considerando que o desenvolvimento de novas formas sólidas cristalinas de IFAs se apresenta como uma estratégia eficaz para melhorar suas propriedades farmacocinéticas e farmacodinâmicas, este trabalho relata a obtenção de duas novas formas sólidas de Acv com os ácidos oxálico e málico, racionalmente planejadas utilizando a base de dados Cambridge Structural Database (CSD) que foram obtidas por meio de síntese mecanoquímica de quantidades equimolares dos compostos utilizando pequenas quantidades (20ul) de solvente, visando melhorar suas propriedades farmacocinéticas. Estas novas formas sólidas foram avaliadas por difração de raios X de pó (DRXP), calorimetria exploratória diferencial (DSC), infravermelho com transformada de Fourier (FTIR), espectroscopia Raman e análise termogravimétrica (TGA).

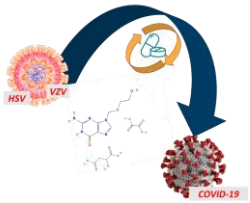

Figura 1 - Reposicionamento Farmacêutico do fármaco Aciclovir

Referências:

1- Borcherding, N.; Jethava, Y.; Vikas, P. Repurposing Anti-Cancer Drugs for COVID-19 Treatment. Drug Des. Dev. Ther. 2020, 14, 5045–5058. https://doi.org/10.2147/DDDT.S282252L.

2- Guo, D. Old Weapon for New Enemy: Drug Repurposing for Treatment of Newly Emerging Viral Diseases. Virol. Sin. 2020, 35, 253–255. https://doi.org/10.1007/S12250-020-00204-7.

Acknowlegments: IFSC/USP, CNPQ

Análise Avançada da Cristalografia em Superfícies de Baterias de Chumbo-Ácido por Meio de Técnicas de Raios-X In-Operando

D.O. G. Espinola[a,b], F. P. Fernandes[c], J.R.C. Salgado[a], F. S. Da Silva[d], R.L.O. Basso[a], and M.G. Hönnicke[a]

[a]*Universidade Federal da Integração Latino-Americana, Foz do Iguaçu, Paraná, Brazil*
[b]*Universidad Católica Nuestra Señora de la Asunción, Hernandarias, Alto Paraná, Paraguay.*
[c]*Instituto de Tecnologia Aplicada e Inovação (ITAI) , Foz do Iguaçu, Paraná, Brazil.*
[d]*Empresa Brasileira de Aeronáutica S.A (EMBRAER), São José dos Campos, São Paulo, Brazil.*

Neste estudo, é proposta uma análise in-operando da cristalografia da superfície de chumbo (Pb) em baterias de chumbo-ácido, fazendo uso de técnicas de difração de raios-X (XRD) e reflectometria de raios-X (XRR). O experimento é conduzido com uma célula eletroquímica de baixo custo e simplicidade, conforme delineado por Espinola et al. (em revisão), compreendendo uma estrutura impressa em 3D. Essa célula é constituída por um eletrodo retangular de chumbo, um eletrodo de platina como contador, um eletrodo de referência de mercúrio/sulfato mercuroso (Hg/Hg2SO4) e janelas de polipropileno. Uma corrente galvanostática é aplicada, e as respostas de potencial são monitoradas por meio de um potenciostato acessível. Concomitantemente, as técnicas de XRD e XRR rastreiam a evolução dos produtos de corrosão e descarga, abrangendo desde películas extremamente finas até o crescimento de cristais de PbSO4. O procedimento experimental tem início com uma etapa de limpeza eletroquímica para eliminar resíduos provenientes do polimento mecânico na superfície de Pb. O estudo apresenta associações entre os processos eletroquímicos galvanostáticos e os resultados de raios-X na interface Pb/PbSO4/H2SO4, fornecendo valiosas perspectivas sobre os mecanismos subjacentes às baterias de chumbo-ácido. Esta pesquisa contribui para uma compreensão mais profunda dos fenômenos cristalográficos nesses sistemas eletroquímicos.

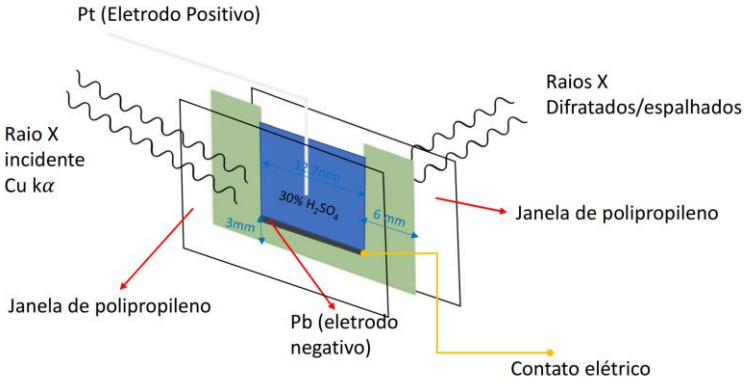

Figure 1: Diagrama esquemático da célula proposta para as medidas in situ.

References:

1- Angerer, P., Mann, R., Gavrilovic-Wohlmuther, A., & Nauer, G. E. (2009). In-situ X-ray diffraction study of the electrochemical reaction on lead electrodes in sulphate electrolytes. *Materials Chemistry and Physics*, *114*, 983–989. https://doi.org/10.1016/j.matchemphys.2008.11.006

2- Chladil, L., Cech, O., & Vanýsek, P. (2016). XRD Study of Lead Sulphate Crystal Growth in a Sulphuric Acid Solution. *ECS Transactions*, *74*(1), 147. https://doi.org/10.1149/07401.0147ecst

3- D´alkaine, C., Berton, M., & Tulio, P. (2003). Galvanostatic Growth of Passivating Films Under Transient Conditions. I. Model and Quantitative Analysis for the Zn/ZnO System. *Portugaliae Electrochimica Acta*, *21*, 15–32. https://doi.org/10.4152/pea.200301015

4- Espinola, D. O. G., Fernandes, F. P., Basso, R. L. O., & Hönnicke, M. G. (2022). Spectroscopy and in-situ X-ray diffraction analysis on the corrosion process at the interface Pb/H2SO4 using a low-cost electrochemical cell. *X-Ray Spectrometry*, *n/a*(n/a). https://doi.org/https://doi.org/10.1002/xrs.3300

***Acknowlegments*:** D.O.G. Espinola aknowledges CNPq/SEMPI/MCTI nº 021/2021 – Programa RHAE and PRPPG / UNILA (88/2019 and 30/2021) for the fellowship..

Prototipagem em impressão 3D de uma fenda cônica para detecção do padrão de difração do oxalato de cálcio duplamente hidratado

R. O. Benedet[a], P. R. dos Santos[a] C. Cusatis[b] M. E. Poletti[c] and M. G. Honnicke[a]

[a]*Instituto Latino-Americano de Ciencias da Vida e da Natureza, Universidade Federal da Integração Latino-Americana, Foz do Iguaçu, Brasil.*

[b]*Laboratório de Óptica de raios X e Instrumentação, Universidade Federal do Paraná, Curitiba, Brasil.*

[c]*Faculdade de Filosofia Ciências e Letras de Ribeirão Preto, Universidade de São Paulo, Ribeirão Preto, Brasil.*

A presença de microcalcificações (MCs) em uma mamografia é frequentemente considerado um sinal precoce de neoplasias mamárias benignas ou malignas. As MCs podem ser formadas por oxalato de cálcio duplamente hidratado (DHCO - fase de weddellite) [1] ou por fosfato de cálcio (CP - fase de hidroxiapatita) [1]. O DHCO é encontrado na forma cristalina [1,2] e está associado à calcificação secretora [3]. O CP pode ser encontrado em forma cristalina [1] e não cristalina [2]. Além disso, as MCs de DHCO estão mais relacionadas à doença benigna da mama do que as MCs de CP [1,2]. Desta forma, a identificação da composição química de uma MCs torna-se um marcador muito útil do tipo de neoplasia mamária.

Neste trabalho está sendo avaliada a eficácia do uso de uma fenda cônica prototipada em impressão 3D (Fig. 1a), para detecção de MCs de DHCO, visando medidas "in-vivo". Para isto, foi montado um fantoma simples que simule uma mama comprimida com espessura variável contendo microcalcificações de DHCO (que não é termodinamicamente estável) imersas em banha de porco comercial. Foi necessário desenvolver a síntese do DHCO. Testes iniciais de uma amostra sintetizada, utilizando a metodologia apresentada por LePage & Tawashi [3] mostram a formação de DHCO (Fig. 1b). Com o processo de síntese consolidado e o fantoma montado, os testes da fenda cônica estão sendo realizados com um equipamento de raios X com alvo de Mo, seguindo um procedimento já estabelecido [4] com vistas a demonstrar uma forma de detecção e identificação de MCs benignas da mama, sem a necessidade de realização de biópsia.

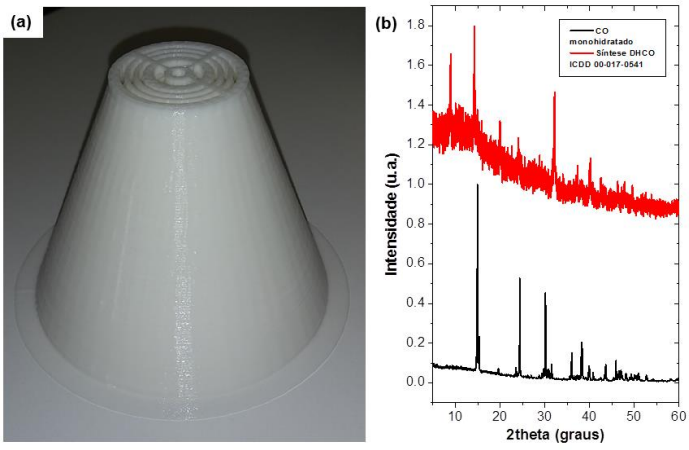

Figura 1: a)Fenda cônica prototipada e impressa a partir dos parâmetros dos cones de difração do DHCO, para ser utilizada com radiação MoKα (17,4 keV). b) Difratograma da amostra sintetizada de DHCO (em vermelho, indexada por ICDD 00-017-0541). Por comparação, é mostrado o difratograma da amostra de oxalato de cálcio (CO) monohidratada (em preto). Ambas as medidas foram realizadas com radiação CuKα

Referências:

1- L. Frappart, M. Boudeulle, J. Boumendil, H.C. Lin, I. Martinon, C. Palayer, Y. Malletguy, D. Raudrant, A. Bremond, Y. Rochet, J. Feroldi, Hum. Pathol. 15(1984) 880–889.

2- C.N. Chinyama, Benign Breast Diseases: Radiol.–Path.–Risk Assess., Springer-Verlag, New York, 2004

3- L. LePage and R. Tawashi, J. Pharm. Sci. 71 (1982) 1059-1062.

4- M. Fioreze, C. Cusatis, J.W. Keister , M.G. Hönnicke, Nucl. Instrum. Meth. A 867 (2017) 171–181.

Acknowlegments: PROBIC/UNILA (PIB3391-2023) and Universal / CNPq (436858/2018-5).

Investigation of structural changes on human hair induced by thermal and cosmetic treatments

A. C. C. Bandeira[a], C. R. R. C. Lima [a] , C. L. P. Oliveira[a].

[a] Institute of Physics, University of São Paulo, São Paulo - Brazil

Human hair has two major morphological regions well distinct: the cuticle and cortex. Between the cells of the cuticle and cortex, cell membrane complexes (CMCs) are present, consisting of lipid layers and bilayers. The main function of the cuticle, the outer structure, is to provide mechanical protection for the cortex [1], which contains a helical fraction comprising a crystalline phase (intermediate filaments - IFs) embedded in amorphous matrix filaments that is sensible to water [2], largely influenced by the relative humidity [1]. High temperatures can induce changes in the hair structure, and it is possible to investigate these variations using experimental methods like small-angle X-ray scattering (SAXS), differential scanning calorimetry (DSC), optical and electron microscopy (OM, EM), among other methods relate [3,4]. As a result, one can evaluate the changes in the IFs in the cortex, lipid molecules in the CMC and many other damages on the hair structure.

In this work a systematic investigation of the effects of dehydration and denaturation on human hair subjected to thermal and chemical treatments will be presented [4]. In situ SAXS measurements (from 30° Celsius to 300° Celsius) were performed and correlated with a number of other methods. As will be shown, important results on the thermal induced damages on the hair structure were obtained, as well as the effect of different cosmetic treatments.

References:

[1] C. R. Robbins. Comportamento químico e físico do cabelo humano (Springer-Verlag, Nova York, 2002), p. 42, 52, 260-272.
[2] Feughelman, M. A Two-Phase Structure for Keratin Fibers. Textile Research Journal 1959, 29 (3), 223-228. DOI: 10.1177/004051755902900305.
[3] Lima, C. R. R. C.; de Couto, R. A. A.; Freire, T. B.; Goshiyama, A. M.; Baby, A. R.; Velasco, M. V. R.; Constantino, V. R. L.; Matos, J. D. Heat-damaged evaluation of virgin hair. Journal of Cosmetic Dermatology 2019, 18 (6), 1885-1892. DOI: 10.1111/jocd.12892.
[4] C. R. R. C. Lima; R. J. S. Lima; A. C. C. Bandeira; R. A. A. Couto; M. V. R. Velasco; H. N. Bordallo; C. L. P. Oliveira (2023) - Alterations promoted by acid straightening and/or bleaching in hair microstructures. J. Appl. Cryst. 56:1002-1014. doi: 10.1107/S1600576723005599.

Acknowlegments: CNPq, FAPESP, INCT-FCx e SOLVAY Group

Structural characterization of conjugated polymer obtained by the oxidative synthesis of *p*-anisidine monomer

D. C. Menezes[a], E. A. Sanches[b] , Y. P. Mascarenhas[c].

[a]*São Carlos Engineering School, University of São Paulo, São Paulo, Brazil.*
[b]*Physics Department, Federal University of Amazonas, Manaus, Brazil.*
[c]*São Carlos Physics Institute, University of São Paulo, São Paulo, Brazil.*

Standard chemical oxidative polymerization of p-anisidine was performed. Solution I was prepared by solubilizing 2.0 g of p-anisidine monomer in HCl 1M, and Solution II was obtained by adding 4.0 g of ammonium persulfate also in HCl 1M. Solution II was incorporated dropwise to Solution I under constant stirring. After 3 hours, the dark powder was vacuum filtered, washed, and kept in a desiccator until constant weight to obtain poly(*p*-anisidine) (PPA).

X-ray powder diffraction was obtained with CuKα radiation, 40 kV, and 20 mA. The scan mode was performed with 0.02°/s step, velocity of 5°/min, in the 2θ = 3 – 73° interval. The XRD pattern of PPA showed a broad halo, between 2θ = 15° and 34°, and centered at 2θ = 24.5°, due to the polymer amorphous phase, a strong peak at 2θ = 5.2° and some small, superimposed peaks indicated some crystallinity [1].

A tridimensional model for the molecular structure of the repeating unit was suggested and hoping that the packaging of the molecules would be similar in the semi-crystalline phase of the polymer, several tentative unit cell parameters were obtained from a search of similar molecular structures reported in the Cambridge Crystallographic Data Center (CCDC). The better fitting of the XRD pattern of PPA was obtained from the crystalline structure of end-capped polyaniline single crystals, corresponding to Space Group P-1.Taking in consideration that the repeating unit in the polymer crystal should contain more than one monomer, that unit cell had to be adapted for a tetrameric model and a repeating unit with 2 tetramers per asymmetric unit, cell dimensions equal to a=10.000 Å, b=20.000 Å, c=20.000 Å, alpha=84.00°, beta= 92.00° and gamma= 94.00°. This choice of unit cell also yields good agreement with average value of polymer density. The software package FullProf was then used to perform the Whole Powder Pattern Decomposition (WPPD) and the least squares refinement of the initial cell parameters using the Le Bail method resulting in final agreement indices of a=10.043 Å, b=20.160 Å, c=17.205 Å, alpha=85.16°, beta= 92.34° and gamma= 95.49°.

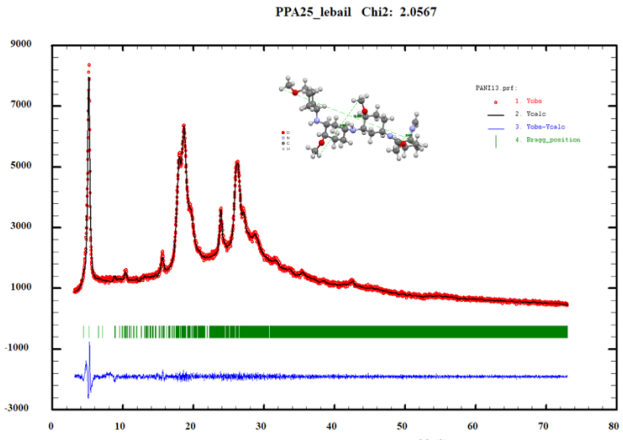

Figure 1: Le Bail fit of PPA.

References:
1- L. Rodrigues de Oliveira et al., “Head-to-Tail and Head-to-Head Molecular Chains of Poly(p-Anisidine): Combined Experimental and Theoretical Evaluation,” 2022, doi: 10.3390/molecules27196326.

Acknowlegments: Multiuser Laboratory of Structural Crystallography (LaMuCrEs).

Difração de raios X por micropó para a identificação de espécies minerais preservadas em museus

A. A. A. Exposito De Queiroz[a], P. H. O. Santiago[a], J. Ellena[a], M. B. Andrade[a,b].

[a]*Instituto de Física de São Carlos,Universidade de São Paulo, São Carlos, Brasil.*

[b]*Departamento de Física , Universidade Federal de Ouro Preto, Ouro Preto, Brasil.*

As rochas são um dos itens mais comuns encontrados em museus de Ciências Naturais ao redor do mundo. Elas podem ser usadas para pesquisas sobre a história da Terra e outros planetas, para ensinar sobre os diferentes tipos que podem ocorrer e como elas são formadas, assim como para mostrar os diferentes processos físico-químicos pelos quais elas passam ao longo do tempo. A goethita é um hidróxido de ferro (FeO(OH)) bastante frequente em minérios de importância econômica e é importante em vários contextos geológicos e ambientais, foram encontradas evidências de sua utilização no período paleolítico em amostras de pigmentos amarelo-ocre de tintas retiradas das cavernas de Lascaux, na França.[1] A técnica de difração de raios X por pó (DRX-pó) tem restringido os estudos de caracterização mineral de amostras de museus, uma vez que a conservação das amostras de rochas tem sido priorizada acima de qualquer informação que possa ser obtida, impossibilitando a utilização de uma quantidade de amostra que geralmente é necessária para a técnica de DRX-pó.

Este trabalho descreve a aplicação da difração de raios X por pó em um difratômetro de monocristal como uma técnica para a identificação de espécies minerais em rochas preservadas em museus, uma vez que são utilizadas pequenas quantidades das amostras com dimensões da ordem de algumas dezenas de micrômetros. O equipamento utilizado foi um difratômetro de raios X de monocristal Rigaku XtaLAB Synergy-S do laboratório multiusuário de cristalografia estrutural (LaMuCrEs) do IFSC-USP, equipado com um goniômetro de quatro círculos com geometria Kappa e gerador de raios X de fonte dupla (fontes de raios X microfocais de cobre e molibdênio) e um detector HyPix-6000HE. Neste trabalho foi usada a fonte de molibdênio (λ=0.71073Å). O estudo foi conduzido em amostras do Museu de Geociências da USP.

Os resultados obtidos indicam uma espécie mineral com estrutura cristalina do tipo (hcp), com os íons de oxigênio ocupando sítios sob as formas de hidroxila e óxido formando planos paralelos à direção [001], e com Fe^{3+} apresentando coordenação octaédrica, com dimensões de célula unitária de a = 9.9536(5); b = 3.02075(14) e c = 4.6101(3) Å. Estes resultados confirmam a presença de goethita, que são compatíveis com análises conduzidas por espectroscopia Raman, que é outra técnica não destrutiva utilizada no LaMuCrEs.

A técnica de difração de raios X de micropó possibilitou a caracterização dos materiais geológicos com resolução microespacial de forma não destrutiva permitindo caracterizar com precisão a distribuição da goethita formadora da rocha. Na literatura, este é um dos poucos artigos que analisa a goethita presente em rochas do acervo de museus de Ciências Naturais brasileiros em uma escala tão pequena, e os resultados devem ser valiosos na caracterização de rochas metamórficas, ígneas e sedimentares e poderá contribuir para a proteção do património geológico dos museus de Geociências.

Referências:

1- Chalmin E, Farges F, Vignaud C, *et al*. Discovery of Unusual Minerals in Paleolithic Black Pigments from Lascaux (France) and Ekain (Spain). *AIP Conference Proceedings* 882, 220-222 (2007). https://doi.org/10.1063/1.2644480.

Agradecimentos:

Os autores agradecem a Miriam Della Posta de Azevedo, Chefe Técnica do Museu de Geociências da USP, pelo acesso às amostras de goethita usadas neste trabalho.

Efeito da inserção de hidróxidos duplos lamelares na cinética de hidratação do cimento

A.C.L Rosa, C. C. dos Santos, C.V. Santilli, S.H. Pulcinelli

[a]*Instituto de Química, UNESP, Brasil*

A alta demanda para a construção de novas infraestruturas civis, assim como a manutenção das já existentes, tornou o cimento Portland o material mais manufaturado do mundo. Em consequência, a indústria cimentícia elevou a produção de gases responsáveis pelo efeito estufa, acarretando a busca por materiais mais sustentáveis e eficientes para sua substituição [1]. Porém, as propriedades mecânicas e a versatilidade do cimento Portland fazem com que esta substituição seja dificultada, impulsionando a utilização de aditivos nano estruturados que elevem a sua durabilidade e propriedades mecânicas [2]. Recentemente, os hidróxidos duplos lamelares (HDL) vêm sendo utilizados para favorecer as propriedades mecânicas do concreto, seja pelo preenchimento de poros ou pelo sequestro aniônico de íons danosos. Além disso, a decomposição térmica do HDL leva à formação de óxidos mistos (OM), que possuem capacidade de regeneração da estrutura lamelar em contato com água e/ou solução aniônica, o chamado efeito memória [3]. Neste contexto, a influência da presença do HDL (1% m/m) na estrutura de compósitos de cimento aditivado foi avaliada durante seu envelhecimento (3-14 dias). Os monolitos foram caracterizados por difração (DRX) e espalhamento de raios-X a baixo (SAXS) e alto (WAXS) ângulo. A regeneração do HDL em diferentes soluções comprova que o OM regenera a sua estrutura lamelar, além de sequestrar, preferencialmente, os íons carbonato presentes na matriz cimentícia (distância interlamelar = 0,760 nm). O crescimento tridimensional das fases de hidratação do cimento, devido ao formato do monolito, não permitiu observar o espalhamento das nanopartículas, em especial a fase C-S-H que é o principal produto da hidratação do cimento, sendo responsável pelo endurecimento do concreto. Porém, observou-se o espalhamento a alto ângulo (difração) de produtos de hidratação maiores, como as fases Aft (etringita), C3S (Alita) e C2S (Belita), com leves deslocamentos de pico para ângulos maiores. Em relação ao envelhecimento das amostras, ligeiras modificações como a diminuição da intensidade dos picos atribuídos às fases de hidratação C3S e C2S com a adição do HDL, foram observadas principalmente entre os dias 3 e 7. Nas amostras de monolito aditivadas, há um ligeiro aumento na formação da fase etringita nos períodos iniciais de envelhecimento em relação ao monolito não aditivado. A semelhança cristalina entre o aditivo e a etringita (sistemas lamelares) indica que o HDL pode estar atuando como ponto de nucleação dessa fase, acelerando a sua formação. Ademais, há uma diminuição significativa das fases carbonatadas nos monolitos aditivados em comparação com os não aditivados, evidenciando o sequestro aniônico por parte do HDL durante sua reestruturação. Como o cimento hidratado apresenta em sua composição tanto fases cristalinas quanto fases amorfas, a quantificação por meio do método de Rietveld se torna imprecisa sendo necessário a utilização do método externo afim de quantificar corretamente todas as fases, inclusive a fase C-S-H, principal responsável pelo endurecimento da pasta. Portanto, novas formas de preparar as amostras são necessários para compreender os efeitos do aditivo no cimento, principalmente durante as primeiras horas de hidratação.

Referências:

1- Li, K. et al. *Journal of Cleaner Production* **34** (2018) 933-942.
2- Huntzinger, D. N.; Eatmon, T. D. *Journal of Cleaner Production* **17** (2009) 668-675.
3- Almeida, A. A. et al. *ACS Applied Nano Materials* **5** (2022) 7896–7907.

Agradecimentos: INCT CEMtec – Advanced Eco-eficient Cement Technologies, e agências de fomento brasileiras: CNPq, CAPES e FAPESP.

Avaliação da reações de hidratação de monolitos de cimento aditivados com Hidróxidos duplos lamelares

C.C. dos Santos[a], A. A. Almeida[a], S. H. Pulcinelli[a], C. V. Santilli[a].

[a]*Institute of Chemistry, UNESP, Brazil*

Produtos à base de cimento são os materiais sintéticos mais utilizados pela humanidade, porém, sua produção gera problemas ambientais associados às questões de aquecimento global[1]. A busca por materiais mais eficientes e sustentáveis tem impulsionado a utilização de aditivos nanoestruturados no cimento, visando melhorias em suas propriedades e durabilidade[2]. Recentemente, os hidróxidos duplos lamelares (HDL) têm sido utilizados para aumentar a durabilidade do concreto, seja pela diminuição dos poros do compósito ou pelo sequestro de ânions danosos[3]. A decomposição térmica do HDL leva à formação de óxidos mistos (OM), que podem regenerar a estrutura quando em contato com água e soluções aniônicas, através do efeito memória. Esta modifica as propriedades físicas e mecânicas da pasta de cimento aditivada[3]. Nesse contexto foi avaliada a influência da área especifica de superfície (AES) do HDL e sua contribuição na estrutura de compósitos de cimento aditivados na forma de monolitos de cimento com HDL (3 % m/m) em diferentes tempos de envelhecimento (3 – 28 dias), por difração de raios X. Os resultados indicam que a AES é aumentada com a decomposição térmica e faz com que o OM tenha uma AES superior à do HDL, também foi observado que o aumento é proporcional AES inicial do HDL. A regeneração do HDL em diferentes soluções comprova a recuperação da estrutura cristalina do HDL e sua capacidade de sequestro de aníons carbonato presentes (distância interlamelar de 0,77 nm). A AES elevada (220 m^2g^{-1}) e o efeito memória, permitem que o OM possa atuar como ponto de nucleação modificando a microestrutura e a cinética de hidratação dos monolitos. Para o monolito não aditivado as estruturas cristalinas são compostas principalmente pelas fases $Ca(OH)_2$, $CaCO_3$ e C3S. Ligeiras modificações são observadas em função do envelhecimento, entre as quais o aparecimento do pico a 9 graus característico da fase etringita (Aft) após 14 dias. Por outro lado, para o monolito aditivado, o pico a 9º aparece a partir dos 03 dias de envelhecimento, comprovando a modificação das reações iniciais da cinética de consolidação do cimento, sugerindo um aumento na reatividade que favorece principalmente a formação da fase etringita ($Ca_6Al_2(SO_4)_3(OH)_{12}\cdot 26H_2O$). A semelhança estrutural (sistema cristalino) do aditivo e da etringita, o alto SSA e o efeito memória podem potencializar as reações em materiais cimentícios. Enquanto a amostra não aditivada contém uma fase semelhante à HDL, com composição variando de 2% a 2,3% e leve variação ao longo do período avaliado, para a amostra aditivada esta composição mais que duplicou. Ademais foi observada uma redução significativa na quantidade de carbonatos, de até 11,5% para a amostra envelhecida por 28 dias em comparação com as não aditivadas. Assim, o aditivo acelera as fases de hidratação do cimento, e é observada uma redução significativa (~ 10% após 03 dias) no teor inicial de $Ca(OH)_2$. Com o avanço do tempo de envelhecimento, as amostras não aditivadas apresentaram uma diminuição (~ 5%) nesta fase e um aumento de (~ 6,7%) na de $Ca(CO_3)$. Em contrapartida, a amostra aditivada apresentou um aumento (~ 3%) em $Ca(OH)_2$ e apenas 1,6% em $Ca(CO_3)$. Porém, a compreensão dos mecanismos de formação dos produtos de hidratação permanece complexa, pois os processos envolvidos podem atuar concomitantemente. Portanto, mais estudos são necessários para compreender os efeitos do aditivo no cimento. Esse estudo lança luz sobre as promissoras oportunidades de otimização do desempenho e sustentabilidade de materiais a base de cimento por meio da utilização de aditivos nanoestruturados.

Referencias:

1- Obrist, M. D., Kannan, R., Schmidt, T. J. & Kober, T. J Clean Prod 288, 125413 (2021).

2- Sanchez, F. & Sobolev, K. Constr Build Mater 24, 2060–2071 (2010).

3- Almeida, A. A. et al. ACS Appl Nano Mater 5, 7896–7907 (2022).

Agradecimentos: As agências brasileiras de fomento CAPES, Finep, FAPESP (project 2015/126385), CNPq, and INCT CEMtec. INCT CEMtec – Advanced Eco-efcient Cement Technologies.

The relevance of lamellar double hydroxides memory effect in the formation of crystalline phases during cement hydration.

A. A. Almeida[a] , C. C. Dos Santos[a], R. M. M. Santos[a], E. Elkaim[b], A. Beauvois[b], V. Briois[b], S. H. Pulcinelli[a], C. V. Santilli[a].
[a]*UNESP, Instituto de Química, Araraquara, SP, Brazil.*
[b]*Synchrotron SOLEIL, Saint-Aubin, Gif-sur Yvette, France.*

Lamellar double hydroxides (LDH) are a class of multifunctional synthetic clays, that when added to cement paste, can contribute to the crystallization of the of hydrated cement phases[1]. The thermal decomposition of LDH at moderate temperatures (~ 400°C) leads to the formation of nanocrystalline mixed oxides (MO), which can regenerate the lamellar structure when put in contact with water solutions, through the memory effect. The regeneration of the LDH lamellar structure directly influences the rheological behavior, accelerating the of paste consolidation in the first hours. These changes in rheological properties are associated with the regeneration mechanism of the HDL structure concomitant with cement hydration[2]. Investigations using the time-resolved X-ray absorption spectroscopy (XAS) demonstrated that the recovery of the ZnGa–HDL nanostructure was driven by a mechanism of nucleation and aggregative growth. In simulated concrete pore solution (pH 14) the formation of the HDL phase was verified, followed by dissolution in oxides of the component metals (such as ZnO). The formation of the hydration phases was monitored during 4 h by X-ray diffraction for the cement paste containing ZnGa-LDH and the respective MO and the results demonstrated the acceleration of the hydration process, evidenced by the increase in the formation of the ettringite (AFt), especially for samples containing MO, indicating that regeneration of the LDH structure favors the kinetics for obtaining AFt. These results are interesting, since the AFt, formed in the first hours, is converted over time into hydrated calcium monosulfoaluminate (AFm), which has a layered structure similar to that observed in hydrotalcite-type compounds. This makes it possible to correlate the effect of OM addition particles in the hydration phases with the structural changes of the cement.

References:

1. Norhasri, M. S. M. *et al*. Constr. Build. Mater.,133(2017), 91.
2. Almeida, A. A. *et al.* ACS Appl Nano Mater 5, 7896–7907 (2022).

Acknowledgements:
This work had financial support of the INCT project CEMtec Advanced Eco-efficient Technologies in Cementitious Products (CNPq #465593/2014, FAPESP #2014/509483 and CAPES #88887.136401/2017). The authors would like to thank the Synchrotron SOLEIL (France) for allowing us to carry out the XRD experiments using the CRISTAL beamline.

Synthesis, crystal structure, and Raman spectroscopy characterization of 1-(2`-hidroxyphenyl)-3-hidroxy-3-(4-methoxyphenil)propan-1-one

H. R. Bitencourt[a], A. P. Ayala[b], S. G. Moreira[a], C. M. R. Remédios[a].

[a]*Departamento Ciências, UniversdadeI, Cidade, País.*

[a]*Instituto de Ciências Exatas e Naturais, Universidade Federal do Pará, Belém-PA, Brazil.*

[b]*Departamento de Física, Universidade Federal do Ceará, P.O. Box 6030, Fortaleza-CE, 60455-900, Brazil.*

Single crystal of 1-(2′-hidroxyphenyl)-3-hidroxy-3-(4-methoxyphenil)-propan-1-one compound was obtained in our laboratory where 20 mL of methanol, 3g of 2-hydroxy acetophenone, 10 ml of sodium hydroxide solution (10%), and 3ml of p-anisaldehyde were added. The reaction mixture was kept under stirring at 80°C for 4h. Fig. 1 shows the representation of the chemical reaction. Then its crystalline structure was identified by X-ray diffraction. The title compound was crystallized on centrosymmetric space group P21/c. These crystals were dissolved in methanol and recrystallized by slow evaporation, producing prism-shaped and colorless crystals. The geometric parameters and supramolecular arrangement for the structures obtained from single-crystal X-ray diffraction data were analyzed. A suitable crystal 0.44×0.19×0.10 mm^3 was selected and measured on a Bruker D8 VENTURE Kappa Duo PHOTON II CPAD diffractometer. The crystal was kept at a room temperature during data collection. The structure was solved with the XT [1] structure solution program using the Intrinsic Phasing solution method using **Olex2** [2, 3] as the graphical interface. The model was refined with version 2018/3 of **XL** [1] using Least Squares minimization. All non-hydrogen atoms were refined anisotropically. Hydrogen atoms were located in difference Fourier maps and refined isotropically. Also, the vibrational spectroscopy investigation has been carried out by the Raman scattering technique. The experiment was performed in the backscattering geometry, and the scattered light was analyzed by using a spectrometer iHR 320, Horiba; width resolution 0.06 nm and detector Synapse, equipped with charge-coupled-device (CCD) detector. The assignments of vibrational modes and detailed synthesis information are presented.

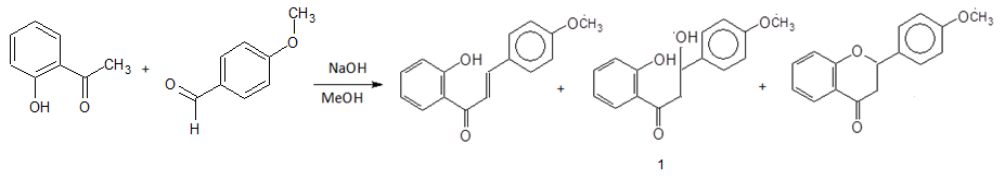

Figure 1: Representation of the Chemical reaction of the synthesis of the title compound.

.

References:

1- G.M. Sheldrick, *Acta Cryst.* A64 (2008) 339-341.

2- O.V. Dolomanov, L.J. Bourhis, R.J. Gildea, J.A.K. Howard, H. Puschmann, *J. Appl. Cryst.* 42 (2009) 339-341.

3 - Software for the Integration of CCD Detector System Bruker Analytical X-ray Systems, Bruker axs, Madison, WI (after 2013).

Acknowlegments: The authors acknowledge the financial support from the Brazilian agencies CNPq and CAPES

.

Superficial study of kaolin from Vitória do Jari, Amapá, Brazil by XRF, Raman Spectroscopy and 2D Micro-Powder XRD

G. A. C. Lopes[a,b], L. D. A. Sousa[c] , D. Atencio[d], J. Ellena[b], M. B. Andrade[e]

[a]*Laboratory of Physics, Amapá State University, Macapá, Amapá, Brazil.*
[b]*São Carlos Institute of Physics, University of São Paulo, São Carlos, São Paulo, Brazil.*
[c]*Mineral Processing Department, Federal Institute of Education, Science, and Technology of Amapá, Macapá, Amapá, Brazil.*
[d]*Institute of Geosciences, University of São Paulo, São Paulo, São Paulo, Brazil.*
[e]*Physics Department, Federal University of Ouro Preto, Ouro Preto, Minas Gerais, Brazil.*

Kaolin is an important resource widely used for the process of paper whitening and coating [1]. This ore is mainly composed of kaolinite, but other kaolinite-subgroup minerals may be present. Common impurities found in kaolin are minerals containing Fe and Ti ions. Quartz also often occurs as accessory mineral [2]. These ions alter the color and optical properties of kaolin and impact in its use in paper industry, so its detection and removal are important [3].

Some superficial purple modifications were observed in kaolin from Morro do Felipe Mine, Vitória do Jari municipality, Amapá State, in the North Region of Brazil, a locality where kaolin has been long explored and is currently administered by Kamin-Cadam company. Some pieces of the ore had already been provided by the company to the Mineral Processing Department of Federal Institute of Education, Science, and Technology of Amapá, but further study was not then possible due to the small amount of chemically modified superficial material (~10mg).

In this study, the technique of In-house bidimensional (2D) micro-powder XRD was performed to study the superficial material, using a Synergy-S single-crystal X-ray diffraction (XRD) equipment with microfocus high-brilliance X-ray sources (Mo kα 0.71Å) and a HyPix-6000HE hybrid photon counting x-ray detector. Good quality 1D powder diffraction patterns were obtained from the 2D data images collected. To access elemental composition, X-ray fluorescence (XRF) was performed and confirmed the dominance Si and Al, typical for clay minerals, and indicated presence of Fe and Ti in both, white and purple portions of the sample, with majority of Fe in the purple portion (~1,9% and ~6,5%, respectively). Raman spectroscopy allowed to access the presence of impurities and ancillary minerals and confirmed the presence of Fe and Ti in the crystalline phases of hematite and anatase. Quartz was also detected. Rietveld refinement on the white portion (Rwp=7,83%) indicated 86% of kaolinite and 14% of quartz. In the purple portion, the refinement (Rwp=13,13%) indicated 86,7% of kaolinite, 10,8% of hematite and 2,4% of anatase.

The purple color is attributed to the optical effect of the many small hematite dots disseminated on the sample, with minor contribution of quartz and stained anatase crystals. The density of red hematite dots varies in the surface, so that it changes from pink (light) to violet (dark) as the density increases. The chemical determination is useful for the mining process, allowing the optimal use of the mining resource and, furtherly, its residue.

References:

1- MONTES, C. R. *et al*. Genesis, mineralogy and geochemistry of kaolin deposits of the Jari River, Amapá State, Brazil. *Clays and Clay Minerals*, v.50, p.494-503, 2002.
2- KLOPROGGE, J. T. *Spectroscopic methods in the study of kaolin minerals and their modifications*. New York, NY: Springer, 2019.
3- SABEDOT, S; PETTER, C. O.; SAMPAIO, C. H. Mineral contaminants of the sedimentary kaolin ore from Ipixuna mine, Brazil. *Revista de Ciências Ambientais*, v.11, n.3, p.07-17, 2017.

Acknowlegments: Amapá State University (UEAP) for the PhD license and São Paulo Research Support Foundation (FAPESP) for funding, grant numbers 2013/03487-8 and 2019/23498-0.

Investigação da Estrutura Cristalina e de Interações Não-Covalentes de um Novo Complexo de Níquel(II) com Tiossemicarbazida

G. J. Lima[a], C. C. Gatto[a]

[a]*LASIC - Laboratório de Síntese Inorgânica e Cristalografia, Universidade de Brasília – Instituto de Química (IQ-UnB), Brasília-DF, Brasil*

Pesquisas com tiossemicarbazidas têm demonstrado o grande potencial desses compostos como agentes antimicrobianos, antifungicidas e antitumorais.[1,2] Alguns medicamentos como triapina, amitiozona e marboran são exemplos de compostos que pertencem a classe das tiossemicarbazidas e têm evidenciado eficiência comprovada contra diversas doenças.[3] Essa classe de ligantes orgânicos vêm se destacando em pesquisas na química bioinorgânica devido à sua capacidade quelante podendo se coordenar a diferentes metais de transição.[4] O níquel desempenha um papel importante na biologia de microrganismos e macroorganismo. Os complexos de Ni(II) com tiossemicarbazidas têm recebido atenção devido à identificação de um ambiente de coordenação rico em enxofre em centros biológicos de níquel, como os sítios ativos de certas ureases e hidrogenases.

Nesse sentido, este trabalho relata o estudo por meio da análise de difração de raios X de monocristal de um novo complexo de Ni(II) com uma tiossemicarbazida, $[Ni(tsc)_3]Cl_2{\cdot}2H_2O(DMF)$. Observa-se na estrutura molecular a presença de três moléculas de tiossemicarbazida coordenadas de forma bidentada através dos átomos doadores *NS* ao centro metálico resultando em um complexo com geometria octaédrica distorcida, Figura 1 (a). A estrutura cristalina do complexo é estabilizada por interações não-covalentes que geram a formação de uma estrutura supramolecular. As interações intermoleculares foram analisadas quantitativamente pela análise da superfície 3D de Hirshfeld e gráficos de impressão digital 2D associados, Figura 1 (b).

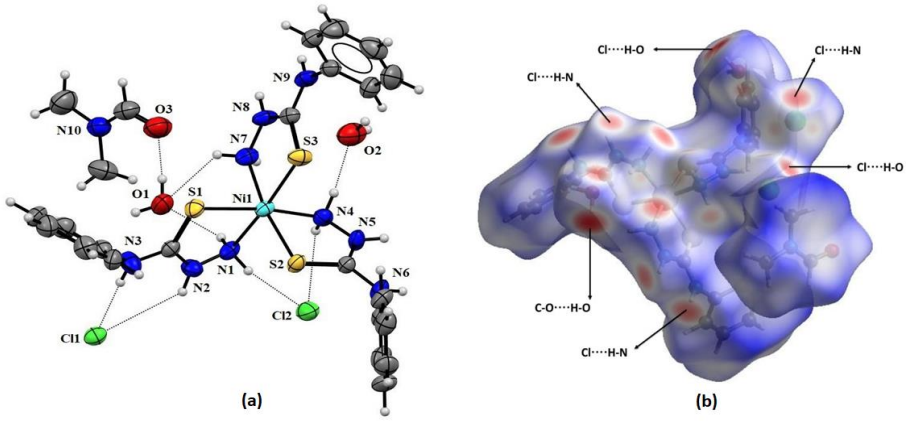

Figura 1. (a) Representação da estrutura molecular do complexo $[Ni(tsc)_3]Cl_2{\cdot}2H_2O(DMF)$ e suas interações intermoleculares (linhas pontilhadas). (b) Superfície de Hirshfeld mapeada com a função d_{norm} do complexo $[Ni(tsc)_3]Cl_2{\cdot}2H_2O(DMF)$.

Referências:

1. Popovici, C.; Pavel, C.-M.; Sunel, V.; Cheptea, C.; Dimitriu, D. G.; Dorohoi, D. O.; David, D.; Closca, V.; Popa, M.; *Int. J. Mol. Sci.* **2021**, *22*.
2. Aly, A. A.; Abdallah, E. M.; Ahmed, S. A.; Rabee, M. M.; Bräse, S.; *Molecules* **2023**, *28*.
3. Safiarian, M. S.; Watson, R. A.; Lieberman, R. L.; Barry, B. A.; Offenbacher, A. R.; *J. Phys. Chem. Lett.* **2021**, *12*, 9020.
4. Zhang, X.; Lei, P.; Sun, T.; Jin, X.; Yang, X.; Ling, Y.; *Molecules* **2017**, *22*.

Agradecimentos: CNPq, FAPDF e UnB.

SYNTHESIS AND CHARACTERIZATION OF A POSSIBLE BISTABLE COMPLEXES OF Co, Zn, Fe AND NAPHTHOQUINONE SERIES

Lucas Olímpio Michel Machado[a] and Carlos Basílio Pinheiro[a]

[a] *Departamento de Física - Instituto de Ciências Exatas, Universidade Federal de Minas Gerais.*
Av. Antônio Carlos, 6627, CEP 31270-901. Belo Horizonte Minas Gerais – Brasil

Functional materials, also known as intelligent solid-state materials, exhibit the ability to switch between two distinct states when subjected to external stimuli. The synthesis of such materials represents a significant challenge to modern materials science. These versatile materials find applications in a series of situations, including their use as sensors, signal processors, and information storage devices[1,2].

Promising categories of functional materials exhibit characteristics such as mixed valence, spin-crossover, or valence tautomerism[7,8]. An illustrative example of valence tautomerism involves coordination compounds featuring cobalt in combination with the o-dioxolene 3,5-di-t-butylsemiquinonate ($SQ^{\bullet-}$) and/or the 3,5-di-t-butylcatecholate (Cat^{2-}), both of which serve as redox-active ligands, alongside ancillary amine ligands[3]. Within these complexes, tautomeric interconversion between hs-Co^{2+} (hs-high spin) and ls-Co^{3+} (ls-low spin) interconvert through intramolecular charge transfer mediated by various external stimuli[4]. The precise mechanism that explains tautomeric interconversion within the solid state, as well as the factors influencing this phenomenon, remain subjects of ongoing research and exploration. Numerous studies have been dedicated to producing valence tautomers employing diverse combinations of metal ions and ligands[5]. In this context, it is noteworthy that Lawsone-cobalt complexes exhibit molecular geometry and crystal packing similar to valence tautomer complexes formed with o-dioxolene-cobalt complexes. However, these Lawsone-cobalt complexes lack both structural and electronic evidence of valence tautomeric interconversion[6].

In this work, we are engineering and synthesizing a series of complexes using 2,2'-Methylenebis(3-hidroxi-1,4-naphtoquinone) (MBHN) as redox-active ligand, Co, Zn and Fe as metallic ions and phenanthroline and bipyridine as ancillary ligand. MBHN presents similar geometrical and electrochemical properties of the *o*-dioxolene molecules used to build valence tautomers. The presence of valence tautomerism in such materials has been investigated using both varying temperature X-ray diffraction experiments (XRD) that provides structural information.

References:

1- Sato O. Nature Chem. 2016. *8*, .644–656
2- Manrique-Juárez, M. D.*, et. al. Coordination Chemistry Reviews*. 2016, 308, 395–408.
3- SHULTZ, David A.. Valence Tautomerism in Dioxolene Complexes of Cobalt. **Magnetism**: Molecules to Materials II, [S.L.], p. 281-306, 12 jul. 2001.
4- Hendrickson, D.N., Pierpont, C.G. Valence Tautomeric Transition Metal Complexes. In: Spin Crossover in Transition Metal Compounds II. Topics in Current Chemistry, vol 234. Springer, Berlin, Heidelberg.
5- TEZGEREVSKA, Tina; ALLEY, Kerwyn G.; BOSKOVIC, Colette. Valence tautomerism in metal complexes: stimulated and reversible intramolecular electron transfer between metal centers and organic ligands. **Coordination Chemistry** Reviews,
6- RIBEIRO, Marcos A.; STASIW, Daniel E.; PATTISON, Philip; RAITHBY, Paul R.; SHULTZ, David A.; PINHEIRO, Carlos B.. Toward Controlling the Solid State Valence Tautomeric Interconversion Character by Solvation. Crystal Growth & Design
7- WANG, Min; LI, Zhao-Yang; ISHIKAWA, Ryuta; YAMASHITA, Masahiro. Spin crossover and valence tautomerism conductors. Coordination Chemistry Reviews, [S.L.], v. 435, p. 213819, maio 2021. Elsevier BV. http://dx.doi.org/10.1016/j.ccr.2021.213819.
8- DRATH, Olga; BOSKOVIC, Colette. Switchable cobalt coordination polymers: spin crossover and valence tautomerism. Coordination Chemistry Reviews, [S.L.], v. 375, p. 256-266, nov. 2018. Elsevier BV. http://dx.doi.org/10.1016/j.ccr.2017.11.025.

Acknowlegments: CNPq; FAPEMIG.

Large pore silica adjuvant for oral vaccines

M.C.A. Fantini[a], D.A. Souza[a], L.C. Cides-da-Silva[a], P.L. Oseliero-Filho[a], O.A. Sant´Anna[b]

[a]*Physics Institute, University of São Paulo, Rua do Matão 1371, 05508-090, São Paulo, SP, Brazil,*

[b]*Butantan Institute, Av. Vital Brasil 1500, 05503-900, São Paulo, SP, Brazil*

Three different swelling agents (SA): 1,3,5 Tri-isopropyl-benzene (TIPB), toluene (TOL) e cyclohexane (CHEX) were used in the synthesis of mesoporous silica, named SBA-15, in order to obtain a mean pore size (<D>) of at least 16 nm, determined by gas desorption measurements. In the usual synthesis with $PEO_{70}PPO_{20}PEO_{70}$ (P123) template, without the SA, <D> attains ~10 nm, already tested in oral vaccines [1,2]. For example, larger mesopores can accommodate the tetanus anatoxin (larger dimension in the order of 14 nm), to be used in polyvaccines [3].

To attain this goal, four different concentration ratios (SA:P123, in mass) and isothermal heat treatments (HT) were tested (100°C or 130°C for 48 hours). The porous pattern is formed by removing the structure-directing compounds using solvent extraction and calcinating under nitrogen, which was afterward switched to air, and kept for 5 hours.

CHEX was used with 1:1 concentration in HT=100°C, while o TOL was used in two processes, first with 1:1 e 2:1 concentrations at TH=100°C and, second with 2:1 concentration at HT=130°C. The attained results were obtained by means of Nitrogen Adsorption Isotherm (NAI) and Small Angle X ray Scattering (SAXS) data. The results shown below report the data from the syntheses performed with 2:1 concentration at TH=100°C, because with these conditions the largest <D> were reached. Other checked conditions, such as ratios of 4:1 and HT=130°C showed no improvements in terms of pore enlargement. The synthesis with CHEX has shown, by NAI and SAXS, only 18% of <D> enlargement, while larger <D> values were attained with toluene. The SAXS results revealed that the introduction of the swelling agents promoted an increase in the correlation distance (TIPB e TOL) or lattice parameter (CHEX), forming a material with disordered pores.

Preliminary biological tests in vitro in acidic and basic solutions provided information on the release kinetics of the antigens from the silica matrix.

In conclusion, by comparing the synthesis with TOL and CHEX, keeping the other conditions identical, it was verified that TOL is a more efficient compound to increase mean mesopore diameter. Also, compared with TIPB, TOL promoted a larger pore entrance, besides it has the advantage to be six times less expensive. The resume proves that it is possible to produce a material with expanded pores, having a sponge-like mesoporous structure to be given as DT oral vaccine. Other advantages are less cost and a non-painful intramuscular injection collateral effect.

References:

1- Mariano-Neto, F. et al., (2014). J. Phys. D: Appl. Phys. 47, 425402.
2 - Fantini, M.C.A. et al., (2022). IUCrJ 9, 11.
3 - Rasmussen, M.K. et al., (2021). Microporous and Mesoporous Mater.312,110763.
4 - Trezena, A.G. et al., (2022). Biologicals 80, 18.

Acknowlegments: Thanks are due to the Brazilian financial agencies FAPESP(2017/17844-8, 2019/12301-1, 2019/07007-7, 2021/13055-4) and CNPq (308248/2021-0).

Refinement of the Crystal Structure of Low‑Carbon Polycrystalline AISI 420 Martensitic Steel (C = 0.27%)

Marcos Tadeu D´Azeredo Orlando[a], Vinicius Danilo Nonato Bezzon[b], Mariane Gonçalves de Miranda Salustre[a], Julia Boni Vaneli[a], , Elson Silva Galvão[a], Estéfano Aparecido Vieira[c], Alex Arbey Lopera Sepúlveda[d]

[a]*Universidade Federal do Espírito Santo, Vitória-ES, Brasil.*
[b]*Universidade Federal de Ouro Preto, Ouro Preto-MG, Brasil.*
[c]*Instituto Federal do Espírito Santo, Vitória-ES, Brasil.*
[d]*Universidade Nacional da Coombia, Valledupar-Cesar, Colombia.*

Although several works have proposed modeling the low-carbon steel lattice parameters considering their carbon content, no detailed information about the crystalline structure has been reported. Herein, the crystal structure of the polycrystalline martensitic steel with carbon content of 0.27% has been refined, giving details about the sites and occupancies for the iron and chromium atoms. The carbon content was determined by Optical Emission Spectrometer. The body-centered tetragonal crystal system with space group I4/mmm was considered for the refinement. The obtained results show that the refined occupancies for Fe and Cr (around 0.83 and 0.17, respectively) are close to the values reported in the technical references for this kind of steel. The final structure yields a well-adjusted refinement, with Rwp = 8.49%, gof = 1.70, and RBragg = 3.17%.

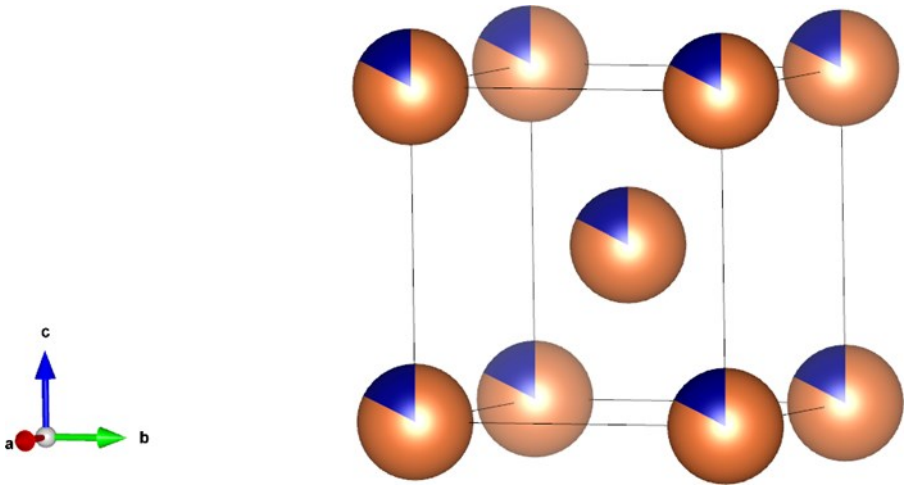

Figure 1: shows the unit cell generated from the refined crystal structure, with the representation of the atom's occupations represented by different colors (orange for Fe and blue for Cr) in their obtained proportions.

References:

1- Vinicius D N Bezzon, Mariane G de Miranda Salustre, Julia B. Vaneli1, Alex Arbey L Sepúlveda, Elson S Galvão, Marcos T D Orlando, Brazilian Journal of Physics (2023) 53:57, https://doi.org/10.1007/s13538-023-01269-x

Acknowlegments: The authors acknowledge the Universidade Federal do Espírito Santo, Fundação de Amparo à Pesquisa do Estado do Espírito Santo – FAPES (TO 1031/2022) EDITAL FAPES Nº 20/2022 CHAMADA DE APOIO A NÚCLEOS CAPIXABAS EMERGENTES EM PESQUISA, Acordo UFES (Brasil) UNAL (Colombia) 23068.032870/2019-87, and CNPQ.

Growth mechanism of platinum nanoparticles: SAXS and UV-Vis evaluation

Rodolfo Fini, Celso V. Santilli, Sandra H. Pulcinelli

Institute of Chemistry, UNESP, Brazil

Platinum nanocrystals play an important role in several applications, such as catalyst on CO and NO_x oxidation reactions, and hydrogenation reactions [1]. It is well established that size and shape can play important role in the nanoparticle (NP) materials properties, so that, unravelling the growth mechanism of such materials could enlighten the path for controlling such quality attributes. Here, we have studied the synthesis of platinum NP reduced with ascorbic acid (AA) [2,3] and stabilized with tetradecyltrimethyl-ammonium bromide (TTAB); the role of TTAB concentration (TTAB/Pt^{2+}molar ratio of 50, 100 and 150) in the particle size, kinetics and growth mechanisms was also focused on. The NP growth kinetics was evaluated using *in situ* SAXS (Small Angle X-Ray Scattering) and UV-Vis spectroscopy data, from which we could follow how NP number (N) and size evolved over time. NP images were obtained from transmission (TEM) and scanning (SEM) electron microscopy. The overall mechanism is displayed in Figure 1 and follows 4 steps: un incubation period, where $[PtCl_4]^{-2}$ is transformed into $[PtBr_4]^{-2}$, which is quickly reduced in Pt^0 nuclei; these nuclei readily aggregate into bigger Pt particle. The following growth period is characterized by concomitant size and number of particles growth (aggregative nucleation step), while in the next one Pt NP grows as their number stabilize. In fact, the growth mechanism is governed by aggregative process counter-balanced by attractive and repulsive driving forces. TTAB/Pt^{2+} plays an important role in the growth mechanism steps: the higher the content of TTAB the bigger the size of the aggregates, and the smaller the size, the narrower the particle distribution of primary nanoparticles. This behaviour influences directly the rate of NP formation as well as the number of dense aggregates.

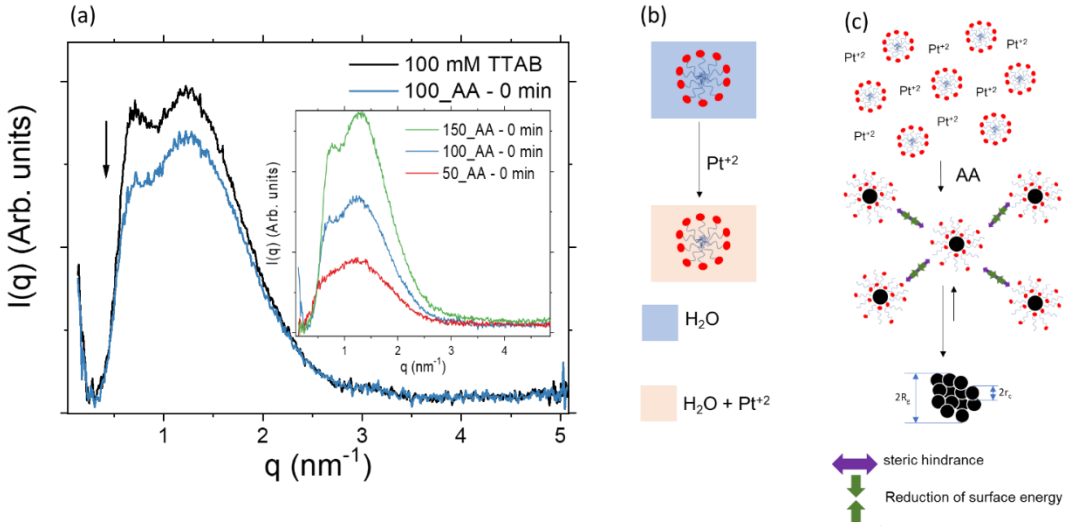

(a) SAXS curves of the 100 mM TTAB solution prior to the addition of Pt^{2+} solution and the AA (black), and after the addition of platinum salt and different amounts of AA; (b) schematic representation of the system prior and after the addition of the platinum salt and (c) the different steps occurring during the Pt NP synthesis mediated by TTAB.

Authors thank financial support from the Brazilian agencies FAPESP, CAPES and CNPq.

Engineering porous materials MOFs-Based - technological applications and dynamic crystals

Alisson Luiz Rocha Balbino[a], Priscilla J Zambiazi [a] , Giovanna Pereira Correia[a], Dagoberto O Silva[b], Liane Rossi[a]

[a]*Instituto de Química, Universidade de São Paulo, São Paulo, Brasil.*
[b]*MofTech, São Paulo, Brasil.*

The development of open structures composed of metal clusters connected by organic ligands has generated significant interest due to their versatile applications, including gas storage, separation, catalysis, and controlled nutrient delivery. These structures exhibit unique features, combining flexibility with stability, making them ideal hosts for reversible dynamic processes triggered by external stimuli. Some structures can intelligently adjust their porosities to accommodate guest molecules, expanding or shrinking as needed. These materials bridge the gap between rigid metal coordination structures and highly flexible self-assembled materials, offering the advantage of maintaining crystallinity after modification[1], enabling fine-tuning of properties, including magnetism, resulting in multifunctional materials.

Coordination polymers are a type of supramolecular material that utilizes intermolecular bonds for self-assembly, controlling the arrangement within crystalline solids to give them specific properties. This process is known as "crystal engineering"[2]. Coordination polymers with three-dimensional connectivity and microporosity are called MOFs (Metal-Organic Frameworks). MOFs consist of metal nodes forming one-dimensional structures called SBUs (Secondary Building Units). Organic linkers bridge these SBUs to increase the structural complexity in three dimensions. Most research on MOFs focuses on creating durable structures capable of maintaining their architecture even after removing solvent molecules, with the added feature of undergoing structural transformations in response to external stimuli.

The materials in this study were synthesized using hydrothermal methods with water as a solvent and characterized through single-crystal X-ray diffraction and Mössbauer spectroscopy, This aims to produce coordination polymers with useful properties, such as magnetism, high surface area, and adjustable porosity. For instance, current laboratory work involves Fe(II/III) complexes that are similar to those used for controlled nutrient release[3]. The resulting compounds find applications as “new materials” in the solid state, offering valuable properties suitable for advanced and innovative technologies.

References:

1- Rasheed T, Rizwan K, Bilal M, Iqbal HMN. Metal-Organic Framework-Based Engineered Materials-Fundamentals and Applications. Molecules. 2020 Mar 31;25(7):1598. doi: 10.3390/molecules25071598.

2- Mark D. Allendorf, Vitalie Stavila (2015) Crystal engineering, structure–function relationships, and the future of metal–organic frameworks CrystEngComm, 2015,17, 229-246. https://doi.org/10.1039/C4CE01693A

3- WU, Ke et al. Optimization of metal–organic (citric acid) frameworks for controlled release of nutrients. RSC advances, v. 9, n. 55, p. 32270-32277, 2019.

Acknowlegments: We gratefully acknowledge support of the RCGI – Research Centre for Gas Innovation, hosted by the University of São Paulo (USP) and sponsored by FAPESP – São Paulo Research Foundation (2014/50279-4 and 2020/15230-5) and Shell Brasil, and the strategic importance of the support given by ANP (Brazil’s National Oil, Natural Gas and Biofuels Agency) through the R&D levy regulation.

Structural and morphological characterization of Ni-MOF-74 films synthesized varying physical and chemical parameters

João. A. O. Neto, Juliana A. P. Figueiredo[a], Maximiliano J.M Zapata[b], Carlos B. Pinheiro[c].

[abc]*Departamento de Fìsica, Universidade Federal de Minas Gerais, Belo Horizonte, Brasil.*

Metal-organic frameworks (MOFs) are materials known for presenting several properties due to the careful selection of organic linkers and metallic building blocks, which lead to different arrangements with micro and mesoporosities [1]. Among these structures, MOF-74 stands out for its open hexagonal 1D infinity porous structure, which is suitable for applications in catalysis, generation and/or storage of clean energy [2, 3], as well as in the manufacturing of electronic devices [4-6] and gas sensors [7]. We are producing Ni-MOF-74 films using the solvothermal synthesis method [8], while varying physical and chemical parameters such as temperature, concentration, and preparation time. This is done to investigate the influence of these parameters on the crystal structure and morphology of the films. The Ni-MOF-74 films have been produced on a fluorine-doped tin oxide-coated glass substrate, with the aim of developing resistive sensors for detecting greenhouse gases such as CO2, CH4, among others. The structural characterization and particle morphology of the Ni-MOF-74 films have been investigated using grazing incidence X-ray diffraction (GIXRD) and scanning electron microscopy (SEM) techniques (Figure 1).

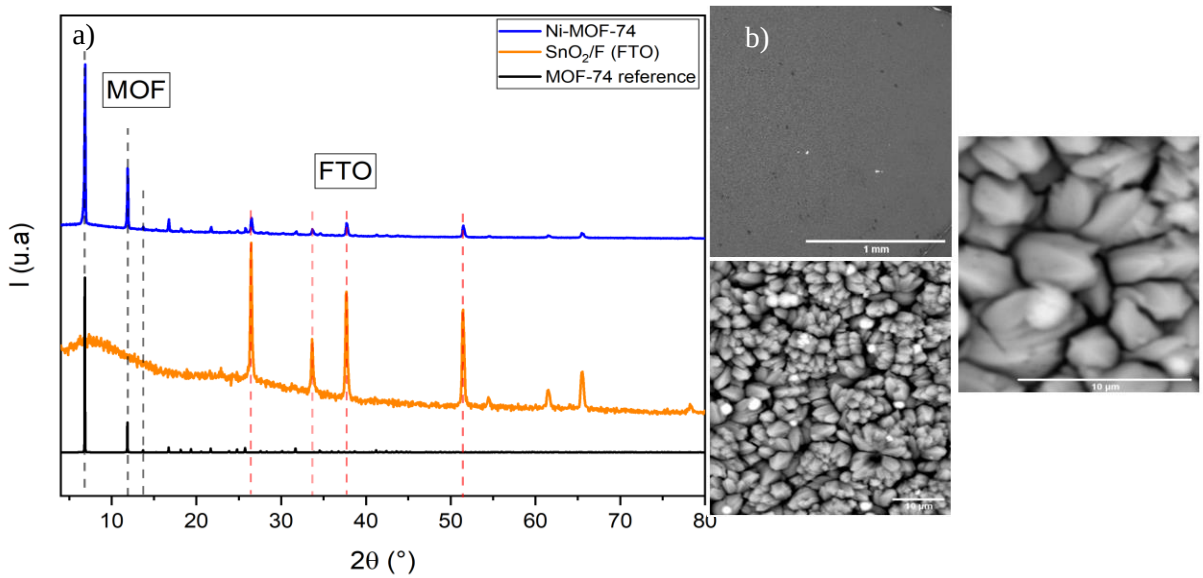

Figure 1: Illustration of Ni-MOF-74 synthetized film characterization by (a) X-ray Diffractogram and (b) SEM images.

References

[1] H. Deng, S. Grunder, O. M. Yaghi et. al, *Science*. **336**, 1018 (2012).

[2] S.-L. Li and Q. Xu, *Energy Environ. Sci*. **6(6)**, 1656–1683 (2013).

[3] A. H. Chughtai, et al., Chem. *Soc. Rev.* **44(19)**, 6804–6849 (2015).

[4] P. Falcaro, R. Ricco, C. M. Doherty, et al. *Chem. Soc. Rev*. **43(16)**, 5513–5560 (2014).

[5] M. R. Ryder and J. C. Tan, *Mater. Sci. Technol*. **30(13a)**, 1598–1612 (2014).

[6] I. Stassen, N. Burtch, A. Talin, et al. *Chem. Soc. Rev*. **46(11)**, 3185–3241 (2017).

[7] Ina Strauss, et al. *ACS Applied Materials & Interfaces* **2019**.

[8] Grant Glover, and Yaghi, O. *Chem. Eng. Sci.* **66**, 163–170. (2011).

Acknowlegdments: CNPq; Fundação de Amparo à Pesquisa FAPEMIG; CAPES, LabCri-UFMG.

A Novel 2D Nickel(II) MOF Containing Trimesic Acid as Ligand

João Manoel R. Gonçalves[a], Regina C. G. Frem[b], Augusto H. Piva[b], Pedro H. O. Santiago[c], Javier A. Ellena[c], Benedito S. Lima-Neto[a].

[a]*Instituto de Química de São Carlos, Universdade de São Paulo, São Carlos, Brasil.*
[b]*Instituto de Química, Universidade Estadual Paulista, Araraquara, Brasil.*
[c]*Instituto de Física de São Carlos, Universdade de São Paulo, São Carlos, Brasil.*

Metal-Organic Frameworks (MOFs) are a sub-class of coordination polymers consisting of a metallic ions or clusters linked to organic multitopic ligands, forming crystalline 2D or 3D metalorganic networks with permanent porosity[1]. The more common coordinating functional groups are usually carboxylates and imidazolates, among others[2]. There are several methods of synthesizing these compounds[3], such as microwave, mechanochemical or electrochemical routes; however, the direct method, which involves mixing a metallic salt with the organic ligand in a polar solvent, which are left under constant heating, usually for a few days, is what provides better quality products, often crystalline. Under this perspective, single crystal X-Ray diffraction is essential to elucidate these complex structures and it was helpful for the growth of the research involving MOFs. Because of the potentially empty cavities in the structure of the MOFs, these compounds have applications in many areas such as gas storage and separation, heterogeneous catalysis, drug delivery systems, photonics, among others. In this work, a new Ni(II) MOF illustrated in Figure 1, was synthesized using $NiCl_2 \cdot 6H_2O$ metal precursor, the ligand benzene-1,3,5-tricarboxilic acid (BTC or trimesic acid) and *N,N'*-Dimethylformamide (DMF) as solvent. The coordination polymer was hydrothermal synthesized in a stainless-steel reactor with Teflon chamber at 120 °C for 48 hours, yielding green crystals (also shown in the figure). As can be seen in Figure 1, in the MOF framework, the distorted octahedral coordinated Ni(II) ions are bridged by BTC ligands, which occupy the equatorial positions with two axial coordination sites occupied by DMF molecules.

The Ni^{2+} cation has a d^8 configuration and both the BTC and DMF are weak field ligands, so an octahedral environment is preferred for the metal center. As the BTC ligand is planar with three coordinating points in opposite positions, the coordination of this ligand through the equatorial positions enabled the formation of 2D layers for the MOF, which are intercalated by the DMF molecules in the axial positions of the coordination polyhedron

Figure 1. Green crystals (a), metal environment coordination (b), network viewed in the [010] direction (c) of Ni-BTC DMF MOF.

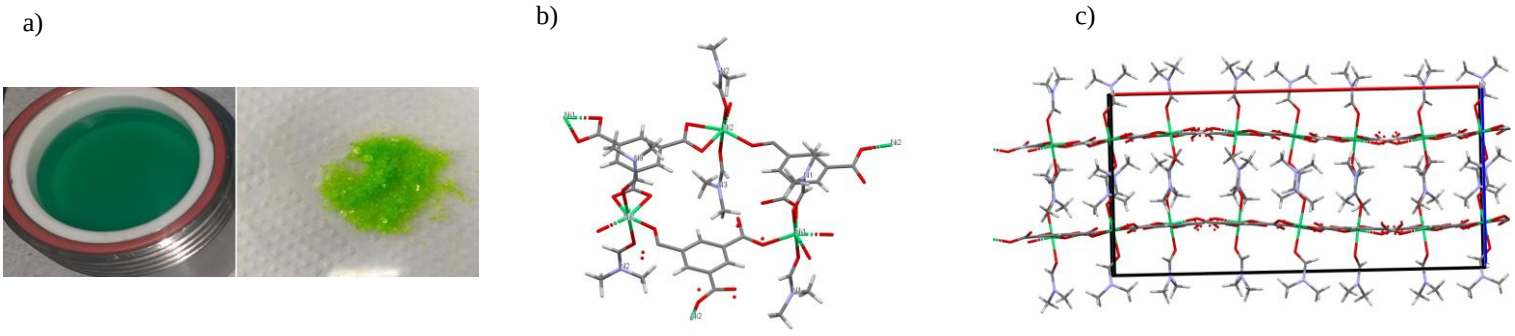

References:
1. Frem, R. C. G. *et al*. *Quim. Nova* **41**, 1178–1191 (2018).
2. Chai, L., Pan, J., Hu, Y., Qian, J. & Hong, M. **17**, 1–31 (2021).
3. Stock, N. & Biswas, S. S *Chem. Rev.* **112**, 933–969 (2012).

Acknowledgments:
To the Brazilian research funding agencies **CNPq**, **Capes** and **FAPESP**.

Structure determination of Ruthenium(II) complex containing cinnamic acid fluorine derivative

P. Sgarbiero[a], L. S. de Andrade[a], J. L. de Souza[a], C. C. Candido[a] , M. I. F. Barbosa[a], and A. C. Doriguetto[a].

[a]*Institute of Chemistry, Federal University of Alfenas, Alfenas-MG, Brazil.*

Many ruthenium complexes have been investigated for their biological activities, especially for antitumor purposes, due to their lower toxicity and higher selectivity than platinum-based drugs[1,2]. We have recently reported the synthesis and characterization of three ruthenium(II) complexes containing cinnamic acid derivatives as ligands as well as their cytotoxic profile against four melanoma cell lines (HT-144, SK-MEL-147, CHL-1, and WM1366)[3]. One of the complexes, [Ru(trans-4-(trifluoromethyl)cinnamic acid)(dppb)(bipy)]PF_6, called complex (2), was the most active compound, and it effectively inhibited proliferation and migration of CHL-1 melanoma cells at very low concentrations. In addition, complex (2) promoted reduction of the BAX/Bcl-2 ratio and induced apoptosis in CHL-1 cells. Taken together, our data suggest that ruthenium(II) complex (2) is a promising anti-melanoma metallodrug prototype to be considered for future ‘‘in vivo’’ studies[3]. Now, after several attempts, single-crystals of the complex (2) were successfully obtained enabling its crystal structure study. The crystal structure was determined in the P-1 space group, cell parameters 12.3047(1), 15.0297(1), 16.2447(2), 112.269(1)°, 105.459(1)°, and 93.888(1)°. Figure 1 is an ellipsoid view of the complex geometry. Indeed, this crystallographic study is ongoing as a disorder involving the hexafluorophosphate ions and solvent molecules occupying voids has been challenging. Additionally, attempts to obtain single crystal of the complexes (1) and (3) are underway.

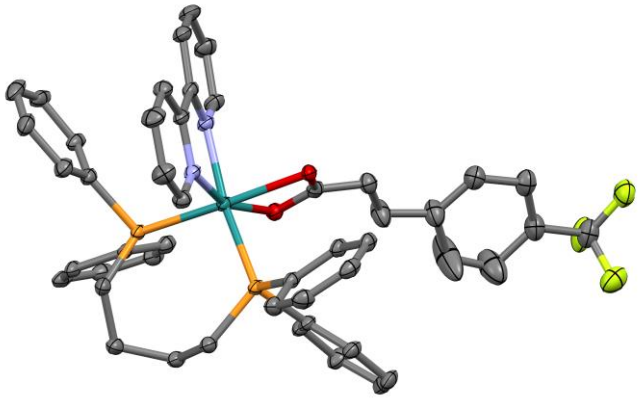

Figure 1: Crystal structure of the complex (2).

References:
1- K. Lin, *et al*., Front. Pharmacol., 9 (2018) 1323.
2- P. De, *et al*., Curr. Med. Chem., 18 (2011) 1672–1703.
3- A. A. Negreti, et al., New J. Chem., 46 (2022) 3325–3337

Acknowledgments: CAPES; CNPq; FAPEMIG; FINEP; PIBICT-UNIFAL-MG.

Síntese e caracterização de um polímero de coordenação de Nd(III) por difração de raios X por monocristal

V. F. M. Calisto[a], H. A. de Abreu[a], R. Diniz[a].

[a]*Departamento de Química, Universidade Federal de Minas Gerais, Belo Horizonte, Brasil.*

Os polímeros de coordenação (PCs) são compostos altamente desejados por possuírem estruturas rígidas e versáteis, apresentando, dessa forma, propriedades únicas e aplicações potenciais em uma variedade de campos da Química. Assim, tanto a estrutura, como as características físicas, químicas ou biológicas dos polímeros de coordenação são decorrentes da combinação de suas substâncias precursoras, ou seja, do(s) ligante(s) e do centro metálico [1]. Em relação às habilidades de luminescência e eletrônicas de PCs, a utilização de metais de terras raras para a composição do centro metálico pode contribuir com esse objetivo devido à ocorrência de transições bem definidas do tipo 4f → 4f, favorecidas pelo efeito antena provocado pela presença de ligantes detentores de alta conjugação π [2]. Dessa forma, sabe-se que o conhecimento da estrutura de um polímero de coordenação é essencial e indispensável, visto que ele possibilita o estudo das propriedades físico-químicas de tal composto e, consequentemente, de suas possíveis aplicações. Nessa perspectiva, foi sintetizado um polímero de coordenação, de Nd(III), com fórmula molecular $\{[Nd_4(H_2O)_{15}(INH)_4(PSB)_6].2H_2O\}_n$, em que a sigla INH se refere à isoniazida e a PSB, ao ácido 4-sulfobenzóico em sua forma desprotonada. Esse composto, indicado pela figura 1, é formado por um polímero de coordenação unidimensional interconectado a outro polímero de coordenação tridimensional poroso. A caracterização estrutural do material sintetizado foi feita por meio de difração de raios X por monocristal e a caracterização química ficou a cargo da espectroscopia de absorção no infravermelho e da análise elementar de carbono, hidrogênio e nitrogênio.

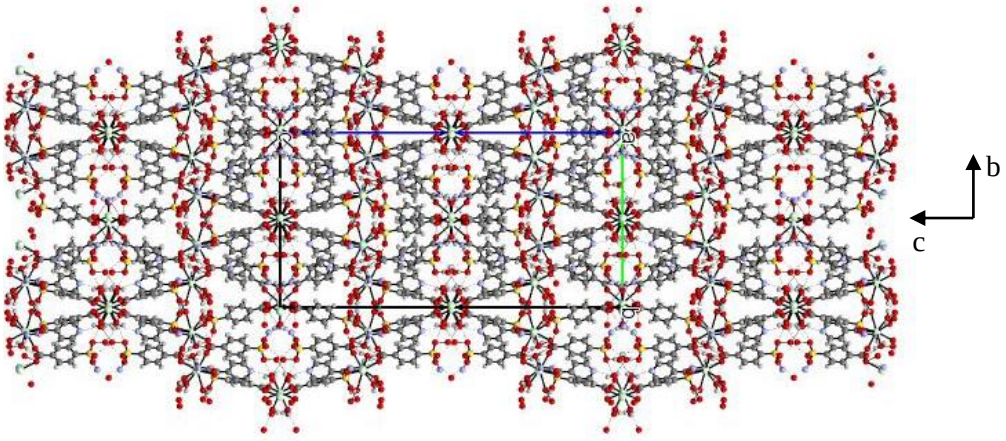

*Figura 1: Crescimento da estrutura polimérica ao longo do plano **bc**.*

Referências:

1- BATTEN, S. R.; NEVILLE, S. M.; TURNER, D. R. Coordination polymers: design, analysis and application. 1ª Ed. Cambridge: The Royal Society of Chemistry, 2019.

2- YOUNIS, S. A.; BHARDWAJ, N.; BHARDWAJ, S. K.; KIM, K. H.; DEEP, A. Rare earth metal–organic frameworks (RE-MOFs): Synthesis, properties, and biomedical applications. Coordination Chemistry Reviews, v. 429, p. 213620, 2020.

Agradecimentos: Agradecemos ao Departamento de Química e ao Laboratório de Cristalografia, LabCri, da Universidade Federal de Minas Gerais pelo espaço e infraestrutura cedidos. Além disso, agradecemos às agências de fomento, CAPES, CNPq e FAPEMIG, pelos recursos financeiros que subsidiam pesquisas científicas.

Evaluation of H-atom position in short intramolecular hydrogen bond through Hirshfeld Atom Refinement

Camila B. Pinto[a], Leonardo H. R. Dos Santos[a] , Bernardo L. Rodrigues[a].

[a]*Departamento de Química, Universidade Federal de Minas Gerais, Belo Horizonte, Brasil.*

The proper localization of H-atom positions represents one of the difficulties in X-ray structure elucidation, due to the fact that X-rays are mainly diffracted by electrons, and the only electron present in H atoms is participating in chemical bonds, and hence, the determination of the nuclear position of these atoms is hindered. Experimentally, neutron diffraction is the most accurate method for finding the position of H atoms; however, due to the difficulties in accessing facilities for this technique, approximations are made for the localization of H atoms using X-ray diffraction data. Usually, H atoms have their positions fixed in distance values obtained by neutron diffraction. However, a method recently proposed known as the Hirshfeld Atom Refinement (HAR)[1,2] has demonstrated to give H atom positions very close to those found through neutron diffraction[3].

In order to further evaluate the method, a series of transition-metal complexes presenting short intramolecular H-bond, namely tetraaquabis(hydrogenmaleato)metal(II) (with metal = nickel, manganese, cobalt and zinc) (Figure 1a), was synthesized and the single crystals obtained were subjected to the X-ray diffraction experiment (room temperature and maximum resolution of approximately 0.86 $Å^{-1}$). The geometric parameters for the short intramolecular H-bonds were evaluated.

The method demonstrated good accuracy when compared to the neutron data for the zinc compound[4] [D–H = 1.12(2)Å (HAR) *vs.* 1.097(7)Å (neutron); H···A = 1.31(2)Å (HAR) *vs.* 1.316(5)Å (neutron)]. In addition, the small differences in H atom position follow the expected pattern throughout the series as obtained by Ruggiero & Korter (2010)[5] *via* theoretical calculations, in which the Mn compound presents the most symmetric H-bond, and the Ni compound presents the least symmetric H-bond (Figure 1b). These results also indicate that the method can achieve good enough results even for data collected at conventional resolutions and room temperature.

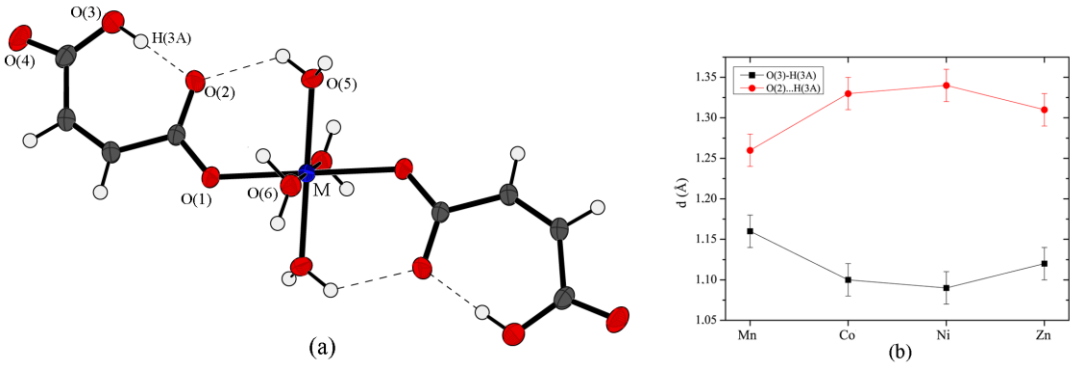

Figure 1: (a) Crystal structure (M = Mn, Co, Ni, Zn), (b) comparison of O–H distances for the H-bond throughout the series.

References:

1- Jayatilaka, D.; Dittrich, B. *Acta Cryst.*, A**64**, 383-393, 2008
2- Kleemiss, F. *et al*. *Chem. Sci.*, **12** 1675-1692, 2021
3- Woińska, M. *et al*. *Acta Cryst.*, A**70**, 483-498, 2014
4- Sequeira, A. *et al*. *Acta Cryst.*, C**48**, 1192-1197, 1992
5- Ruggiero, M. T.; Korter, T. M. *Phys. Chem. Chem. Phys.*, **18**, 5521-5528, 2016

Acknowlegments: Programa de Pós-Graduação em Química (UFMG), CAPES, CNPq and FINEP.

Experimental and theoretical study of the synthesis and morphological and microstructural properties of electrodeposited Cu_2O nanostructured thin films

Cristiane B. Gonçalves[a], Rafael T. Silva[a], Gustavo Dalenogare[b], Mateus M. Ferrer[b], Marcelo Assis[d], Elson Longo[c], Hugo B. Carvalho[a], Antônio C. Doriguetto[a].

[a] *Universidade Federal de Alfenas, Alfenas-MG, 37133-840, Brasil.*
[b] *Universidade Federal de Pelotas, Pelotas-RS, 96010-610, Brasil.*
[c] *Universidade Federal de São Carlos, São Carlos-SP, 13565-905, Brasil.*
[d] *Universitat Jaume I, Castelló, 12071, Espanha.*

We present a comprehensive analysis of the morphological and microstructural properties of Cu_2O thin films electrodeposited on SnO_2:F (FTO) substrates. The films were synthesized in the galvanostatic mode at different pH values (9 and 12) and temperatures (40, 45, 50, 55, 60 and 65°C) and characterized by scanning electron microscopy (FE-SEM) and X-ray diffraction (XRD). The obtained films show deposit uniformity, reproducibility, chemical stability, constitutional purity (only the Pn3m Cu_2O phase) and crystallinity. Additionally, a theoretical study based on Wulff's theorem[1] was carried out to investigate the influence of the synthesis environment on the growth process. The deposited films exhibited different morphologies (cubic and octahedral, truncated or not) with distinct exposed crystalline faces, and growth orientations [111 or 100][2]. The FE-SEM also reveal that the crystal size of the films increases with both increasing pH and temperature. we made a significant contribution to the exploration of multifunctional semiconductor materials for applications in photocatalysis, photovoltaic cells, photoelectrochemistry, and other advanced materials.

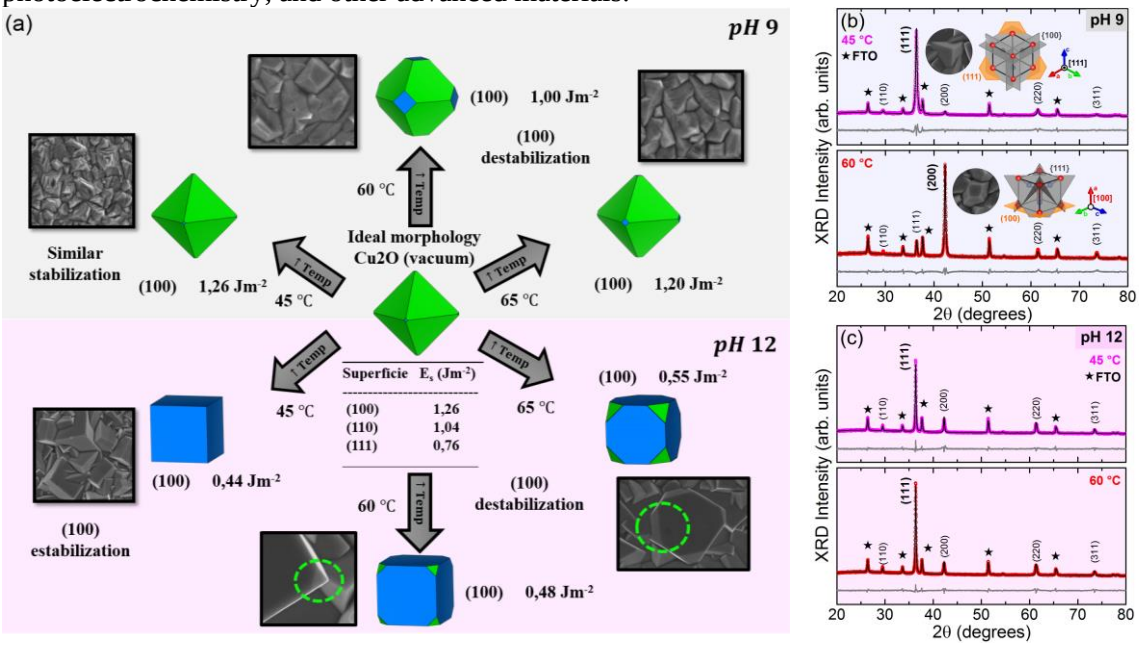

Figure 1:(a) Morphology diagrams starting from the ideal morphology by Wulff's construction method in a vacuum condition, and the change paths according to the surfaces stabilizations of the Cu_2O thin films deposited; (b) and (c) refined XRD profiles for the films deposited at different temperatures and pH. The insets in (b) show the difference in the crystal shape corresponding to growth direction ⟨111⟩ (upper panel for 45 °C) and ⟨100⟩ (upper panel for 60 °C).

References:

1- G. Wulff In Warschau, XXY. Zur Frage der Geschwindigkeit des Wachs-thums und der Auflösung der Krystallflächen, n.d.
2- Y. Zhou, J.A. Switzer, Electrochemical Deposition and Microstructure of Copper (I) oxide films, 1998.

Agradecimentos: CNPq, CAPES, FAPEMIG, FAPESP, FAPERGS, FINEP.

CARACTERIZAÇÃO DE ELEMENTOS QUÍMICOS EM AMOSTRAS DE SACHÊS DE AÇÚCAR E ADOÇANTES DE MESA

Hussein Abdul Karim Moussa[a], Diego Osmar Galeano Espinola[a], Sandy González Hernández[a], Marcelo G. Hönnicke[a].

[a]*Instituto Latino-Americano de Ciências da Vida e da Natureza, Universidade Federal da Integração Latino-Americana, Foz do Iguaçu, Brasil.*

Neste trabalho, foram analisadas química e estruturalmente 29 amostras de saches de açúcar e adoçantes de mesa (16 amostras de açúcar e 13 amostras adoçantes de baixa caloria ou zero caloria) coletadas, aleatoriamente, em diversas cafeterias no Brasil, Argentina e Paraguai. As técnicas de espectroscopia de infra-vermelho (FT-IR), microscopia eletrônica de varredura associada a espectroscopia por dispersão em energia (EDS/SEM) e difração de raios X (XRD) foram empregadas. Para as amostras de açúcar, a FT-IR detectou sacarose em todas as amostras. A sílica, usada como agente anti-humectante [1], foi identificada em cerca de 38% das amostras. Imagens SEM revelaram cristais monoclínicos em 88% das amostras (Fig. 1a). Os resultados de EDS confirmaram a presença de sacarose em todas as amostras. O XRD identificou estruturas cristalográficas consistentes com a sacarose em 100% das amostras (Figura 1b). Apenas duas amostras de açúcar foram consideradas relativamente seguras, uma vez que tanto sulfitos como agentes anti-humectantes não foram detectados nessas amostras. Além disso, aluminossilicatos, associados à doença de Alzheimer [2], foram detectados em uma amostra. Os adoçantes de baixa caloria e zero caloria apresentaram resultados mais complexos. O FT-IR identificou sacarose ou lactose em 92% dessas amostras. O EDS revelou sulfitos ou ciclamato de sódio em cerca de 85% das amostras e sílica em cerca de 70% das amostras. O XRD detectou sacarose ou lactose em 92% das amostras e aspartame, um potencial carcinógeno[3], em quase 50% das amostras.

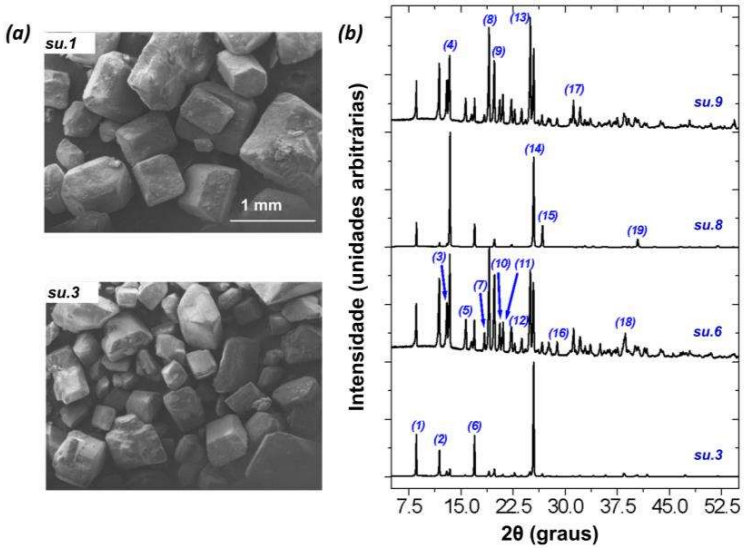

Figure 1: a) Microscopia eletrônica da amostra su.X (a que você escolher) mostrando a presença de monocristais com estrutura monoclínica. g) Medidas de difração de raios-X (XRD) realizadas com diferentes amostras de açúcar.

References:

1- A. M. Hollenbach, M. Peleg, R. Rufner, Food Science 1982, 47, 538-544.

2- J. D. Birchall, J. S. Chappell, Clin Chem. 1988, 34, 265-267.

3- E. Riboli, A. F. Beland, A. Frederick, D. W. Lachenmeier, M. M. Marques, D. H. Phillips, E. Schernhammer, et al., Lancet Oncol. 2023.

Agradecimentos: A P. M. M. Ramos pelas medições de FT-IR.

Structural Characterization of Virgin and Treated Caucasian hair Using Optical Microscopy Methods

J. P. P. Valadares[a], A. C. C. Bandeira[a], C. R. R. C. Lima[a], C. L. P. Oliveira[a]

[a]*Physics Institute, University of São Paulo, São Paulo - Brazil* .

Hair style, appearance, color, shape, etc, are very important features of human figure. An enormous number of treatments and cosmetic procedures can be used on human hair in order to promote different types of changes as coloring, bleaching, straightening, among many other procedures. Besides several types of investigations, a detailed visual inspection of the hair is certainly a very important point. Even though electron microscopy techniques (transmission EM, scanning EM etc) can provide high resolution information on the hair structure (down do nanometers sizes), these methods requires ultra-high vacuum or the use of chemical agents in order to enhance the detected signal. Optical microscopy (OM), on the other hand, can be performed in air, without any further preparation. The structural details can be close to micron our submicron range, depending on the setup used in the equipment. Also, OM allows dynamic investigation on the system upon temperature variation, environment (acid, basic, etc) and fluorescence or light polarization effects by the use polarizers for in the optical system. Several investigations on this way are shown in the literature, in several applications, in particular for forensic cases.

In this work initial tests on the use of OM methods are being performed in order to obtain detailed protocols for sample preparation, mounting and measurement procedures. Certified human hair samples (caucasian) either virgin (no treatment), bleached, straightened hair are being evaluated with the aim of comparing and characterizing certain conditions caused by determined chemical transformations in the hair fiber. As will be shown, interesting results could be already be obtained, indicating an enormous potential of the method for the investigation of human hair samples.

References:

1- Robbins, Clarence R. 2012. Chemical and physical behavior of human hair. 5th ed. ed. Heidelberg: Springer.

Acknowlegments: We thank IFUSP, USP, FAPESP, CNPq, CAPES and INCT-FCx for the support on our research.

Sub-micrometer X-ray imaging with a spherical multi-crystal Laue monochromator: a trial characterization with 3D printed parts

Rodolfo Javier Talavera[a], Raymond Conley[b] , Elina Kasman[b], XianRong Huang[b], Edson Massayuki Kakuno[a], and Marcelo G. Hönnicke[a].

[a]*Instituto de Ciencias da Vida e da Natureza, Universidade Federal da Integracao Latino-Americana, 2044, Foz do Iguacu, Parana 85867-970, Brazil,*

[b]*Advanced Photon Source, Argonne National Laboratory, 9700 South Cass Avenue, Argonne, Illinois 60439, USA.*

Hard X-ray imaging with single spherical Laue crystal has been studied either, theoretically[1] and experimentally[2]. Polymer-based substrates have been used for mounting cylindrical bent analyzer crystals[3] and multi-crystal spherical analyzers[4] for spectroscopy applications. In this work, we show the project and characterization of a short-working distance spherical multi-crystal Laue Si 220 monochromator (curvature radius of 62.5 mm) mounting on a 3D printed convex-concave substrate to work at 8.4 keV (WLα1) for sub-micrometer X-ray imaging purposes (Fig. 1). The characterization was carried out with a Microfocus X-ray source (Kevex PXS5-927) at 44 kV and 54 μA (X-ray source size with diameter of 5 μm) and includes multi-crystal misorientation and thickness requirements, thermo-mechanical stability, focus size and image acquisition. The use of such a device as focusing optics for coherent diffraction imaging purposes is envisaged.

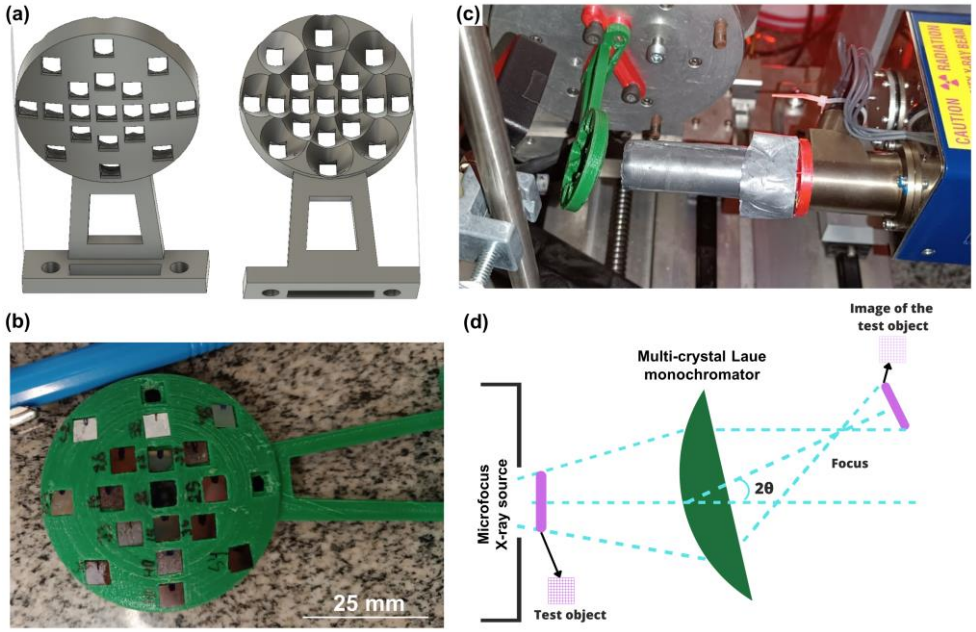

Figure 1: Fig. 1 (a) Convex-concave substrate design. (b) Mounting of the multi-crystal Laue Si 220 monochromator on the 3D printed convex-concave substrate. (c) Alignment procedure of the central crystal with the microfocus X-ray source and a collimator. (d) Schematic representation of the focus size and image acquisition characterization by using the microfocus X-ray source without the collimator.

References:

1- Sanchez del Rio M., et al., J. Phys. Conf. Series 425, 192021 (2013).
2- Faenov A. Ya., et al., Rev. Sci. Instrum. 74, 2224-2227 (2003).
3- Solovyev, M. A., et al., Rev. Sci. Instrum. 92, 073105 (2021)
4- Dickinson, B., et al., Rev. Sci. Instrum. 79, 123112 (2008).

Structural characterization of $CsPbX_3$ (X = Cl, Br, I) perovskites

R. S. Pinto, F. F. Ferreira

Centro de Ciências Naturais e Humanas, Universidade Federal do ABC (UFABC), Santo André, Brasil.

Quantum dots (QDs) are nanocrystalline semiconductors that exhibit excellent optical properties, the most notable of which is fluorescence. These semiconductors can be structured in the form of perovskites[1]. In this work, we synthesized and characterized QDs of the $CsPbX_3$ structure, with X being a halide (family 7A, Cl, Br, and I). The insertion of one of these elements – chlorine, bromine, or iodine – or the combination of two within a certain proportion allowed the semiconductor's fluorescence to cover the entire visible spectral range. For example, chlorine emits close to violet while green is produced by the compound bromine, and iodine emits in the opposite spectrum to red, indicating that this structure is ideal for light emission. Powder X-ray diffraction measurements carried out on a Stoe® STADI-P powder diffractometer with copper radiation showed the formation of the expected phases. Despite the intense Bragg peaks (Fig. 1), some diffuse scattering may be observed at the bottom of the peaks, which may indicate local distortions of the polyhedral. The amorphous contribution comes from the scotch tape used to deposit the sample. Ongoing work using pair distribution function analysis may shed light on such inferences.

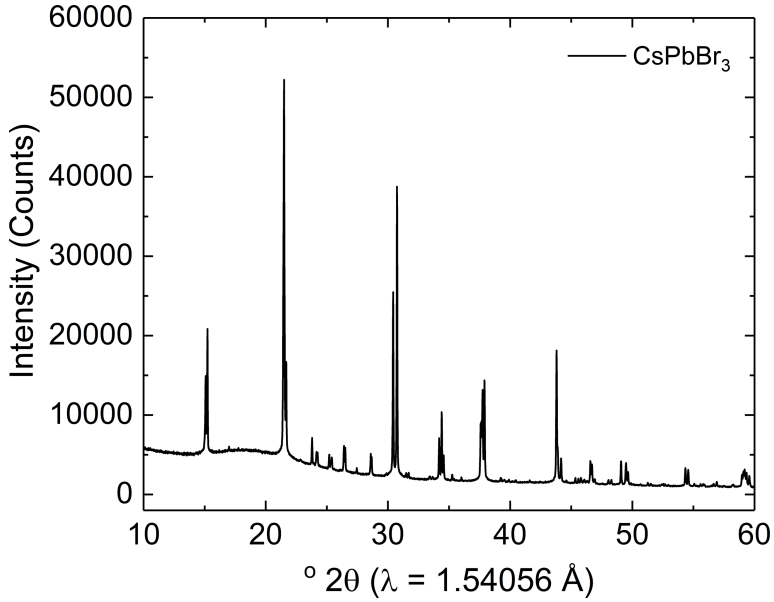

Figure 1. Powder X-ray diffractogram of $CsPb(Cl_{0.6}Br_{0.4})_3$.

References:

(1) Khan, M. Q.; Ahmad, K. Origin and Fundamentals of Perovskite Solar Cells. In *Recent advances in nanophotonics*; Kahrizi, M., Sohi, P. A., Eds.; IntechOpen: Rijeka, 2020. https://doi.org/10.5772/intechopen.94376.

Acknowledgments: The authors thank the financial support provided by FAPESP (proc. 2021/03640-7) and CAPES (finance code 001).

COMITÊ ORGANIZADOR:

Cristina Nonato (FCFRP-USP, Ribeirão Preto SP)
Alejandro Ayala (DF-UFC, Fortaleza CE)
Beatriz Guimarães (ICC-FIOCRUZ, Curitiba PR)
Cláudia Gatto (UnB, Brasília DF)
Cristiano de Oliveira (IF-USP, São Paulo SP)
Eduardo Granado Monteiro da Silva (UNICAMP, Campinas SP)
Fábio Furlan Ferreira (UFABC, Santo André SP)
Javier Ellena (IFSC-USP, São Carlos SP)
João Alexandre Barbosa (UnB, Brasília DF)
Márcia Fantini (IF-USP, São Paulo SP)
Narcizo Marques de Souza Neto (LNLS-CNPEM, Campinas SP)
Sandra Pulcinelli (UNESP, Araraquara SP)

PATROCINADORES:

CAPES

IUCr

Anton Paar

Essencis TECHNOLOGIES

Malvern Panalytical a spectris company

Rigaku Leading With Innovation

DAIRIX